Close-Range Remote Sensing of Forests

The state of the art, challenges, and opportunities for systems and data acquisitions

XINLIAN LIANG, ANTERO KUKKO, IVAN BALENOVIĆ, NINNI SAARINEN, SAMULI JUNTTILA, VILLE KANKARE, MARKUS HOLOPAINEN, MARTIN MOKROŠ, PETER SUROVÝ, HARRI KAARTINEN, LUKA JURJEVIĆ, EIJA HONKAVAARA, ROOPE NÄSI, JINGBIN LIU, MARKUS HOLLAUS, JIAOJIAO TIAN, XIAOWEI YU, JIE PAN, SHANGSHU CAI, JUHO-PEKKA VIRTANEN, YUNSHENG WANG, AND JUHA HYYPPÄ

xxxxx

Remote sensing-based forest investigation and monitoring have become more affordable and applicable in the past few decades. The current bottleneck limiting practical use of the vast volume of remote sensing data lies in the lack of affordable, reliable, and detailed field references, which are required for necessary calibrations of satellite and aerial data and calibrations of relevant allometric models. Conventional field investigations are mostly limited to a small scale, using a small quantity of observations. Rapid development in close-range remote sensing has been witnessed during the past two decades, i.e., in the constant decrease of the costs, size, and weight of sensors; steady improvements in the availability, mobility, and reliability of platforms; and progress in computational capacity and data science. These advances have paved the way for turning conventional expensive and inefficient manual forest in situ data collections into affordable and efficient autonomous observations.

Systems and operational protocols used in practices are the key factors affecting the quality of collected data and retrieved attributes. However, their roles and impacts have been insufficiently understood. This article aims to provide a comprehensive overview of state-of-the-art close-range remote sensing systems and commonly applied operational protocols to provide insightful understanding of the advantages, potentials, and challenges of the technologies and approaches in forest investigation. The characteristics of different platforms, i.e., static, mobile, terrestrial, and unmanned aerial, are briefly reviewed on the basis of their potential and recent developments. The performance of different sensors, i.e., active, passive, professional, and consumer level, are investigated in the context of practical applications. The strengths and limitations of hardware systems and operation protocols are studied through reported performance and benchmarking studies. Current challenges, new opportunities, and development trends are revealed through comparative and critical analyses.

It can be concluded that close-range remote sensing has fundamentally changed the landscape of forest in situ inventories. The most significant impact is that the technology has turned many previously impossible investigation scenarios into possible ones, reshaping the possibilities for future forest in situ observations by improving the automation, detail, accuracy, and comprehensiveness of data collection. The urgent problems to solve include the limited completeness and geometric accuracy of data as well as insufficient processing power, which limit advanced and practical applications and call for further studies. This review also provides practitioners useful guidance to select suitable systems and operational protocols when applying close-range remote sensing to collect tree and forest attributes at individual tree and plot levels.

Digital Object Identifier 10.1109/MGRS.2022.3168135
Date of current version: 15 June 2022

INTRODUCTION

Remote sensing-based forest observation detached from pure field surveys in the 1970s, when stereo photogrammetry began to be applied to stand-based forest inventories and with the launch of the first *Earth Resources Technology Satellite* (later known as *Landsat*). Since then, remote sensing forest observation and monitoring have experienced extensive

and progressive changes. Global and regional data coverage and their updates at different spatial and temporal resolutions have become widely accessible and affordable in the past 20 years through various satellite programs [1]–[6]. The *Landsat* and *Sentinel* series provide free global coverage data, e.g., at 15–120- and 10–60-m spatial resolutions and 16–18- and 10-day temporal resolutions, respectively. More frequent and flexible global data updates can be conducted by combining different satellite constellations, e.g., an average 2.9-day revisit interval through *Landsat 8*, *Sentinel-2A*, and *Sentinel-2B* [7]. High-spatial-resolution (≈1 m) satellite data products are also freely available across a broad range of ecoregions, e.g., in the United States and Mexico [6].

Country- and province-scale aerial imageries with higher resolutions at decimeter and centimeter levels are routinely captured in many regions of the world. Notably, airborne laser scanning (ALS), also known as *lidar*, began to be used in forest observations in the 2000s [8]–[11] and has evolved into a global operative forest inventory technology. Area-based inventories [8] have been operational since 2008. The pulse repetition frequency (PRF) increased about 1,000 times during the past 25 years. Today, it is easy to reach pulse densities needed in individual tree inventories [12]. Meanwhile, point cloud generation from overlapped images [13], [14] and improved radiometry from digital photogrammetry [15] were soon applied in forest observations. These data provide adequate supplies for various services, such as forest extent and change monitoring, forest type and property estimation, risk management, and soil protection.

Nevertheless, a bottleneck limiting effective use of such a vast volume of remote sensing data lies in the lack of affordable and detailed field references for necessary calibrations of satellite and aerial data. Another limitation is the applied allometric models that often introduce estimation errors due to spatial, temporal, and budget limitations [16]. Such a lack of accurate and up-to-date field references limits the reliability of global and regional observations because of error propagation in upscaling. In current workflows, field references are primarily collected through in situ forest investigations in sample plots. Sample plots of selected shape, number, and size are distributed throughout the area of interest according to a particular design [17], [18]. Individual tree attributes are measured within each sample plot and used to estimate plot-level forest attributes. Conventional field inventories are widely understood as time-consuming, labor-intensive, and costly. Yet, they are regarded as the most practical and reliable reference data source [19], [20]. Recent studies, however, found more evidence to question their reliability [21]–[23] and bias levels [19], [24], [25] in acquiring tree attributes that are not straightforward to measure.

Close-range remote sensing observes targets through a noncontact pattern and at a target-to-sensor distance ranging from very short lengths to several hundred meters and even longer. Such an automated and close-to-target observation pattern opens the door for improving the efficiency of in situ investigations, especially for observing parts of trees that are not reachable from the ground within traditional, nondestructive field measurements. The application of close-range remote sensing in forest observations has a long history. Film cameras have been used to measure tree dimensions and canopy characteristics since the 1950s. Hyperspectral (HS) and ultrasonic sensors have been used to estimate leaf biochemical parameters and canopy volumes since the 1980s [26]. In recent decades, close-range remote sensing experienced rapid development. Its application landscape has changed dramatically due to the constant decrease in the cost, size, and weight of sensors; steady advances in the availability, mobility, and reliability of platforms; and progress in communication capacity and data science. The technology was boosted in the late 1990s by the emergence of automated field data collection solutions, e.g., terrestrial LS (TLS), followed by the rapid miniaturization of sensors and advances in platforms and computing sciences in the 2000s.

Today, the available data sources that have the potential to match the requirements of field observations are proliferating at an unprecedented speed, and their applicable sensors range from survey-level instruments for professionals to ordinary consumer-level tools for citizens. The development of close-range remote sensing is on the way to turning conventional expensive, slow, and manual forest in situ field data collection into affordable, rapid, and autonomous observations. Furthermore, with a high level of mobility and automation, close-range remote sensing has the potential to push the boundary of in situ forest observations from a plot level to a transect, stand, and even a regional level and improve the level of detail (LoD) from the plot level to individual trees and, possibly, branches [27].

Based on this steady and rapid progress, close-range remote sensing has become one of the most active research areas in forest science and remote sensing. Its advances can be seen from different perspectives. Considering the broad scope of the topic and limited space, this review is dedicated to providing insightful information about and understanding of the current system, data, and commonly applied operational protocols. Among all factors, the system documents the physical world as digital representations, laying the foundation for all processing and applications. The protocols take specific designs to collect data to meet particular requirements that link the hardware, interpretation, and practices. Thus, the system and data acquisition protocol jointly determine the effectiveness of forest field observations through close-range remote sensing and jointly define what information can be acquired, to what scale and extent, and at what accuracy.

While recent benchmarking showed that processing algorithms directly decide the performance of remote sensing [28]–[32], little attention has been given to the role and impact of the system and protocol until now. Automated algorithms have been capable of retrieving primary information recorded in data [16]. The current limiting factors relate to data quality, i.e., what is recorded and at what LoD, according

to recent benchmarking studies of in situ forest attribute estimations [16]. Thus, the status, potential, and limitations of applied systems and protocols require more thorough understanding to clarify their roles and impacts in various processing and applications. Meanwhile, this review points out challenges that close-range remote sensing faces as well as development trends and new opportunities. In addition, it helps those interested in applying close-range remote sensing to their research and application tasks to find suitable systems and define appropriate operational plans. It also supports those who are developing methods for data processing by providing deeper understanding of various technological backgrounds of the data they are dealing with. Figure 1 illustrates the application scenario of the close-range, airborne, and satellite remote sensing, and the overview of the remote sensing of forests.

FOREST CLOSE-RANGE REMOTE SENSING IN THE LITERATURE

A literature study was made in November 2021. The analysis focused on eight different forest close-range remote sensing technologies. Three were ground based, i.e., TLS, terrestrial photogrammetry, and mobile LS (MLS), including handheld-, backpack- and personal-based LS, and five were unmanned aerial vehicle (UAV) based, i.e., UAV photogrammetry, multispectral (MS), LS, HS and synthetic aperture radar (SAR) imagery. Together with keywords for technologies, two keywords were used for targets,

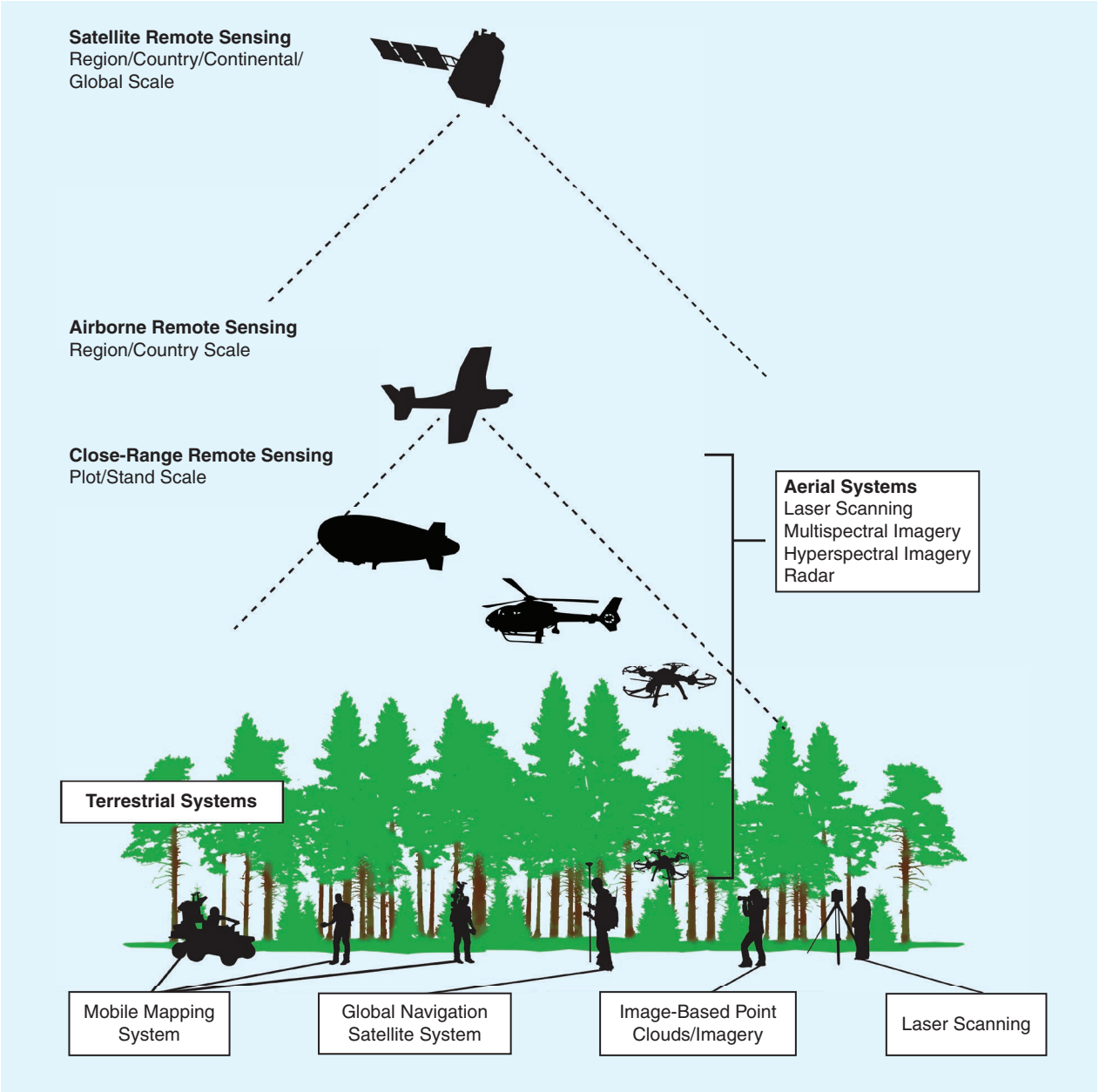

FIGURE 1. The overview of the remote sensing of forests and the application scenario of close-range, airborne, and satellite remote sensing.

i.e., "forest*" and "tree*," with an asterisk to include their plurals. The Web of Science database and core collection were employed to search the literature by using the platform's advanced search module. Altogether, 2,638 papers were found. The highest and lowest numbers of papers related to TLS, i.e., 1,176, and UAV-based SAR, i.e., four.

Figure 2 shows the number of papers published until 2021. The total papers published before 2010 is reported as a sum and listed in the category "Prior to 2010." The number of papers published in 2021 was reported but was not final since the period did not cover the whole year. Synonyms used for each topic are listed in Table 1. The number of published papers is reported in Table 2. TLS and terrestrial photogrammetry had the highest number of papers in 2018. The total increased by 41 and 333% in comparison with what it was the previous year, 2017, respectively. The technical aspects of these sensors have become stable to some extent. MLS also had the highest number of papers in 2018. The number is expected to grow since mobile laser scanners are proliferating and their performance is advancing. UAV-based SAR had the least research work in the literature, i.e., only four papers, which indicates that UAV SAR is at a very early stage of forest application.

CURRENT FIELD MEASUREMENT METHODS

Tree species, diameter at breast height (DBH), and height are the most commonly measured individual attributes in conventional plot-wise forest inventories. Alone and in combination, and with the application of species-specific equations, i.e., allometric models, tree attributes are used to calculate and estimate various tree-, plot- and stand-level characteristics, e.g., basal area, volume, biomass, carbon stock, and so on. Also, these attributes are commonly used to estimate the growth and productivity of forest stands as well as the site quality (index). Other tree attributes of interest are much less frequently measured in terms of spatial and temporal scales, usually because of limited resources, including time, tools, and budgets. Those features cover a broad spectrum of trees and forest attributes, depending on the application. They range from parts of an individual leaf to a plot and from biochemistries to spatial features, which include but are not limited to position, the first living branch height, the crown area and length, tree health, and wood quality. The DBH is the essential tree attribute collected during forest field inventories. It strongly correlates with tree volume and biomass and is directly used for basal area calculation [18], [33].

The impacts of individual tree attributes on a particular tree/forest parameter estimation can be notably different. Errors in tree height estimates have been found to have a more substantial influence on tree volume estimates than tree species misidentification [34]. Tree heights have also been recognized as an essential allometric factor in forest biomass estimates, and they must be included, although with extreme care, as measurement uncertainties may produce biased estimates of the carbon stock and biomass [35], [36]. In general, manual field mensuration can collect a wide range of forest attributes. However, the problem is that significant resources are required in most cases, which practically limits the amount, scale, and frequency of the practice.

SENSORS

Calipers and diameter tapes are the most commonly used instruments for DBH measurement, while Biltmore sticks and Bitterlich sector forks can be used with less precision [18]. In operational forest inventory, when many sample plots and trees have to be measured, calipers are preferred since they are easy and efficient to use [20], [37]. Tree height is defined as the vertical distance between the top of the crown and the base of a tree stem. Estimating individual tree heights is not a straightforward task, due to limited visibility of treetops and stem bases because of occlusion effects. The accuracy of tree height measurements has always been the focus of forest investigation and practice [38] since it can significantly influence the estimation and prediction precision of other important tree and forest attributes (such as volume and biomass) that are not directly measured in the field [24], [35].

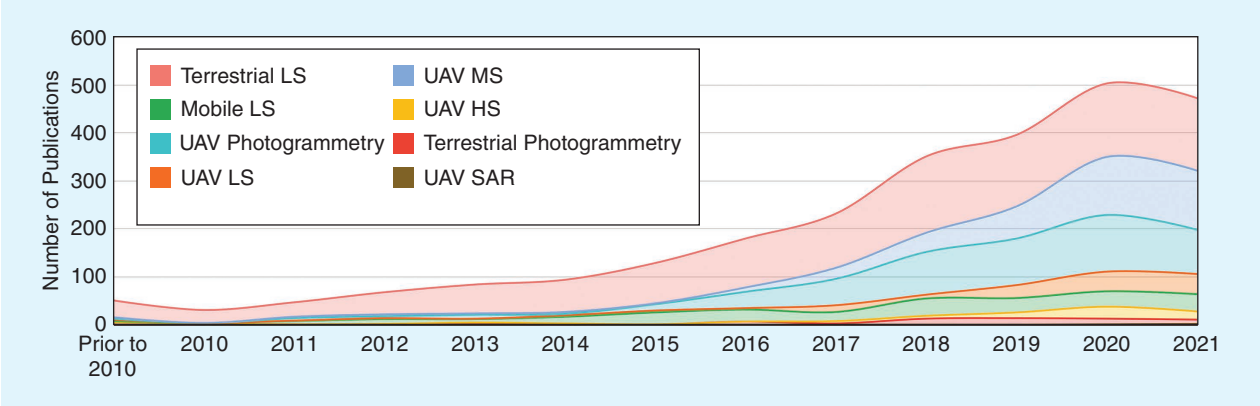

FIGURE 2. The area graph represents the number of papers for each considered close-range remote sensing technology from 2010 to 2021. Papers published before 2010 are reported using a cumulative number in the category "Prior to 2010."

Tree heights can be measured directly or indirectly in the field. Many techniques have been developed during the past decades to facilitate measuring procedures and provide more reliable tree height estimates. Tape measurements of felled trees offer the most accurate results [39], [40], but this is destructive and rarely applicable. The height of standing trees can be directly measured using telescopic height poles for small trees, usually up to 10 [41], 15 [17], and 21 m [18]. Similarly, direct tree height measurement can be conducted by climbing trees [35], [41], [42].

Indirect methods employ ultrasonic and laser-based hypsometers and trigonometric principles [38], [41]. In the tangent method, tree height is calculated based on the tangent function by using a measured vertical angle between the tree base and treetop and a slope distance to the tree stem. In the sine method, tree height is calculated based on the sine function via the measured slope distance to the treetop and base and a vertical angle between the tree base and top. Applying tangent and sine indirect approaches requires clear visibility to the tree base and treetop, which can be limited in complex and dense forest structures. The tangent method, in particular, can produce errors in tree height measurement when trees are leaning, while the sine technique is much more resistant to errors. In general,

TABLE 1. THE TERMS USED IN THE WEB OF SCIENCE ADVANCED SEARCH.

TECHNOLOGY	SEARCH CODE	NUMBER OF PAPERS
Terrestrial laser scanning (TLS)	TS=("terrestrial laser scann*" OR "terrestrial lidar") AND TS=(forest* OR tree*)	1,176
Unmanned aerial vehicle (UAV) photogrammetry	TS=(UAV OR UAS OR drone* OR RPA OR RPAS OR "Unmanned Aerial Vehicle*" OR "Unmanned Aircraft System*" OR "Remotely Piloted Aircraft") AND TS=(photogrammetry OR "Structure from Motion" OR sfm) AND TS=(forest* OR tree*)	522
UAV multispectral (MS)	TS=(UAV OR UAS OR drone* OR RPA OR RPAS OR "Unmanned Aerial Vehicle*" OR "Unmanned Aircraft System*" OR "Remotely Piloted Aircraft") AND TS=(multispectral) AND TS=(forest* OR tree*)	402
Mobile LS	TS=("Mobile laser scann*" OR "Handheld laser scann*" OR "Personal laser scann*" OR "Backpack laser scann*" OR "Mobile lidar" OR "Handheld lidar" OR "Personal lidar" OR "Backpack lidar") AND TS=(forest* OR tree*)	249
UAV LS (ULS)	TS=(ULS OR "Unmanned laser scann*" OR "UAS borne laser scann*" OR "UAV borne laser scann*" OR "Drone borne laser scann*" OR "UAS based laser scann*" OR "UAV based laser scann*" OR "Drone based laser scann*" OR "UAS Laser Scanning" OR "UAV Laser Scanning" OR "Drone Laser Scanning" OR "UAV lidar" OR "UAS lidar" OR "Drone lidar") AND TS=(forest* OR tree*)	152
Terrestrial photogrammetry	TS=("terrestrial photogrammetry" OR "close range photogrammetry" OR "terrestrial structure from motion" OR "close range structure from motion" OR "terrestrial sfm" OR "close range sfm") AND TS=(forest* OR tree*)	80
UAV hyperspectral (HS)	TS=("UAS borne hyperspectral*" OR "UAV borne hyperspectral" OR "Drone borne hyperspectral" OR "UAS based hyperspectral" OR "UAV based hyperspectral" OR "Drone based hyperspectral" OR "UAS hyperspectral" OR "UAV hyperspectral" OR "Drone hyperspectral") AND TS=(forest* OR tree*)	66
UAV synthetic aperture radar (SAR)	TS=("UAS borne SAR*" OR "UAV borne SAR" OR "Drone borne SAR" OR "UAS based SAR" OR "UAV based SAR" OR "Drone based SAR" OR "UAS SAR" OR "UAV SAR" OR "Drone SAR" OR "UAS borne synthetic aperture radar*" OR "UAV borne synthetic aperture radar" OR "Drone borne synthetic aperture radar" OR "UAS based synthetic aperture radar" OR "UAV based synthetic aperture radar" OR "Drone based synthetic aperture radar" OR "UAS synthetic aperture radar" OR "UAV synthetic aperture radar" OR "Drone synthetic aperture radar") AND TS=(forest* OR tree*)	4

TABLE 2. THE NUMBER OF PAPERS PUBLISHED UNTIL 2021 FOR EACH FOREST CLOSE-RANGE REMOTE SENSING TECHNOLOGY.

	PRIOR TO 2010	2010	2011	2012	2013	2014	2015	2016	2017	2018	2019	2020	2021
TLS	35	27	30	46	60	67	84	102	113	159	149	153	151
UAV MS	3	0	3	4	3	4	2	9	23	40	67	121	123
UAV photogrammetry	5	1	5	4	8	3	13	34	55	89	97	118	92
UAV LS	2	3	1	2	1	3	4	3	14	8	27	41	42
Mobile LS	3	3	7	10	7	14	25	25	19	36	30	32	36
UAV HS	3	0	0	0	1	0	0	0	5	6	12	25	17
Terrestrial photogrammetry	0	5	1	2	4	2	1	7	3	13	14	12	9
UAV SAR	0	0	0	0	0	1	0	0	0	0	0	1	2

Papers published before 2010 are reported as a sum in the category "Prior to 2010."

there is a tendency to overestimate tree heights through the tangent approach and underestimate them via the sine method [18], [41].

Other length and height measurements typically use the same sensors as tree height estimation, e.g., the first branch height and the crown size. Absolute positions in forests are commonly collected by a GNSS device or the combination of a GNSS device and total station. Relative locations with respect to known positions, e.g., within a plot, are measured by, e.g., a range finder and a bearing compass.

DATA ACQUISITION

The DBH is usually measured in sample plots for all trees above a specified minimum threshold (e.g., 5, 7.5, or 10 cm, depending on the regulations) and for sample trees selected through the angle gauge method. Since trees do not have a circular form, the DBH is usually measured with calipers from two perpendicular directions (i.e., cross measurement). The average (arithmetic) value is calculated. The work in [20] demonstrated that cross measurements considerably improved precision compared to single measurements. Diameter tapes measure circumference and give the DBH by recalculation, assuming a circular shape for the cross section. They are efficient when large trees (e.g., DBH >60 cm) are measured in dense forest structures [18] and when repeated and consistent measurements in permanent plots are needed [33]. DBH measurement using calipers and diameter tapes may seem straightforward but includes many potential sources of errors, such as the nonperpendicular orientation of devices with respect to the vertical axis of the stem, branches and other deformities of stems at breast height, steep slopes, leaning trees, limited operator experience and expertise, and so on [20]. Approaches for solving these issues can be found in forest inventory manuals and books, e.g., [17] and [18]. Several studies compared DBH measurements using different devices, and all reported no significant differences in accuracy between calipers and diameter tapes for operational use [33], [43]–[45].

Individual tree height estimates typically have lower accuracy and precision than DBH measurements [20]. With commonly used hypsometers, errors in individual tree height estimates can be 1–5 m and more [19], [24], [46], [47], mainly due to the limited visibility of treetops, especially in more complex forest environments with dense canopy layers. Tree heights are the costliest data to collect in a practical forest inventory [48]. To reduce the expense, field tree height measurements are often conducted only on a selected number of trees within sample plots (a representative subsample), a considerably lower number than what is involved in DBH estimation. For trees without actual measurements, the height is usually estimated using local species-specific DBH–height models [17], [18]. Further statistical modeling is also required to obtain unmeasurable parameters (e.g., volume, biomass, and carbon stock) at plot, stand, and national levels. However, error propagation is expected but often not considered in practice [16].

All three direct tree height measurements are relatively slow and thus are not suitable for measuring a large number of trees in a practical forest inventory [41]. Compared to direct methods, indirect approaches using hypsometers (ultrasonic and laser based) are more effective for larger samples, and therefore they are commonly used in practical forest inventories [19], [20], [49]. Regardless of the instrument and indirect method, tree height measurements are influenced by various factors, such as forest structure and complexity, tree species and crown shape, tree height, tree shape (e.g., leaning), topography, measuring distance, and human operators [16], [19], [25], [38], [46], [50], [51].

The importance and influence of various factors on the accuracy of field tree height measurements were investigated in [19], including measurement-related, topography-related, stand-related, and biometric characteristics of individual trees. The research included 2,388 trees of important European tree species [*Pinus sylvestris* L., *Picea abies* (L.) H. Karst., *Larix decidua* Mill., *Abies alba* Mill., *Quercus robur* L., *Fagus sylvatica* L., *Alnus glutinosa* Gaertn., and *Betula pendula* Roth]. Indirect tree height measurements using several standard instruments, i.e., clinometers, hypsometers, and range finders, were validated with measured lengths of felled trees. While the type of instrument showed a negligible impact on the accuracy of tree height measurements, biometric (tree length, species, and age) and topographic (terrain slope and altitude) factors were found to induce the most significant error. Heights of all species were underestimated, with relative error (RE) values ranging from –0.19 to –1.69% except for *Q. robur*, for which a systematic overestimation of 2.52% was observed. Overall, [19] obtained higher tree height measurement accuracy for coniferous than deciduous species, with an RE ranging from –0.19 to 1.23% and –1.25 to 2.52%, respectively. The tendency to underestimate tree height was also reported in [47] by comparing indirect measurements via Vertex IV hypsometer and direct measurements of the lengths of 15 felled *Pseudotsuga menziesii* (Mirb.) Franco trees. Indirect measures resulted in a mean error of –0.66 m and a root-mean-square error (RMSE) of 1.02 m.

Tree positions are usually determined using one or several reference positions and the relative distances and angles to the plot reference point (e.g., the plot center). The plot center coordinate is collected in circular plots by a GNSS device. The relative stem location within the plot is measured by, e.g., a range finder and bearing compass. The accuracy of stem positions depends mainly on the accuracy of the GNSS used for measuring plot centers and corners. The first branch height is usually measured in the same manner as the total tree height, i.e., using hypsometers and range finders, and is commonly known as *crown base height*. It is used to define commercial stem height, i.e., the length of the stem from the stump to the height of the stem at the point of the first living stem fork (branch) or the smallest merchantable diameter, i.e., the minimum stem diameter that can to be used as timber.

Crown dimensions (such as the crown length and crown radius) have various important applications in forestry practice and forest science, such as modeling tree growth and biomass, planning thinning operations and determining fertilizer trials, and so on [17], [52]. Crown length is calculated as the difference between the total tree height and crown base height. Crown radii are measured in four or eight cardinal directions from ground projections of the crown edge to stem center. Field measurements of tree crown dimensions are challenging, uncertain, and time-consuming and therefore not a part of extensive forest inventories [52]. The importance of proper training before indirect measurement was emphasized in [53]. Experienced surveyors do not introduce systematic error in measurements [19], which is in line with findings in [20], where no statistically significant differences were found in the precision of tree height measurements by four trained operators who used the same instrument (a Vertex IV hypsometer).

TERRESTRIAL SYSTEMS

The static TLS system has the highest geometric data quality among all sensors and platforms at the plot level. The data acquisition itself is pretty fast if transportation and registration issues are not of concern. TLS has led recent development and set standards for all solutions to study forest spatial characteristics. Mobile and portable systems significantly improve data collection efficiency and have the potential to be accepted as next-generation operational tools once they achieve geometric accuracy comparable to the TLS system. Terrestrial image-based point clouds can be collected using a wide variety of available professional and nonprofessional imaging sensors, thus providing a low-cost yet often less accurate alternative data acquisition solution to laser sensors. While point clouds have shown advantages in studying forest spatial properties in the past two decades, imageries are still a convenient tool in forest in situ observations.

LASER SCANNING

TLS and its applications in various forest measurement tasks have been immensely studied during the past 20 years. Theoretically, TLS measurements can cover an area of interest at random sizes by combining individual scans through data registration. Due to the static data acquisition pattern, i.e., measuring on a tripod at a single location, TLS is suitable for collecting data from small areas (e.g., sample plots) and individual trees at LoD 3 [27], i.e., suborder branches. Therefore, its most prominent application in forest sciences is acquiring auxiliary information, e.g., stem tapering and quality attributes [31], and detailed references for modeling that are costly to measure with traditional means or require destructive sampling [27], [54]–[56]. This section focuses on the most recent developments on plot and tree levels after 2016, when a TLS-specific review was published, e.g., [27]. While early studies demonstrated the feasibility of applying TLS in forest in situ observations, these latest advances have begun to investigate the next steps toward best practices.

SENSORS

TLS, as, in general, any LS application, provides the amplitude of a backscattered signal and other signal properties (e.g., the reflectance and waveform) characterizing target surfaces. It measures an environment with dense 3D point clouds, e.g., thousands or more returns (x, y, z) per square meter at a 10-m distance from the scanning position. Two common measurement types, i.e., phase shift and time of flight, exist in commercial systems, and the measurement principle seems to affect the incidence angle effect on intensity. Time-of-flight scanners are less affected by the incidence angle than phase-shift scanners, and they produce point clouds with less noise [57], [58].

Commercial TLS systems are under steady improvement. Their size, weight, and cost decrease rapidly, while their measurement speed, accuracy, and practical operability constantly increase. The most notable hardware advance is the introduction of MS and HS TLS. MS TLS simultaneously pulses a laser at several wavelengths, which combines accurate 3D coordinate and spectral information. Two up-to-date dual-wavelength systems are the dual-wavelength Echidna lidar (DWEL) [59] and Salford advanced laser canopy analyzer (SALCA) [60]. Both have full-waveform digitization capacity. They have weights similar to first-generation commercial TLS devices, e.g., 19 kg without batteries for DWEL and 15 kg for SALCA.

While a commercial MS TLS instrument has not become available, researchers combined two TLSs operating at different wavelengths to combine spatial and spectral information in postprocessing [57], [61], [62]. The multisensor approach has the advantage of high measurement efficiency. Commercial TLS devices measure at high speed, e.g., ~1 million points/s, have high range accuracy, and are eye safe to use in field operations. Their disadvantage is a time lag between consecutive scans, resulting in different point cloud geometries due to the wind effect and requiring additional work during postprocessing, e.g., finding linked points from different scanners.

HS TLS prototypes are being developed in laboratories. The first HS TLS utilized a supercontinuum laser [63]. The laser spectrum is spread across a spectral range of 480–2,200 nm, enabling the tuning of specific channels recorded by an avalanche photodiode array module that is sensitive to a spectrum of 400–1,000 nm. This instrument can be used in a laboratory [64] and in outdoor conditions to monitor the spectral variance through time of natural and human-made objects to separate artificial targets from natural ones [65].

A smaller, portable version was recently developed to measure rock surfaces to nondestructively reveal different rock types [66]. It weighs 15 kg and operates in the 400–1,000-nm wavelength range. A similar HS TLS with 32 channels was created using a supercontinuum laser [67]. A recent prototype demonstrated that an HS TLS could also employ longer wavelengths, expanding the spectrum to the short-wave infrared region [68]. A recently designed

acousto-optic tunable filter (AOTF)-based HS lidar (HSL) was with an improved spectral resolution at 10 nm [69]. Table 3 summarizes the specifications of MS/HS TLS devices used in previous literature.

DATA ACQUISITION

TLS point clouds can be collected from one or multiple positions through single, multisingle, and multiple scan strategies [27]. Each approach has strengths and weaknesses. Data acquisition at a single viewpoint is easy, fast, and less expensive. Given clear plot visibility, it can record most trees, e.g., even in high-density forest plots [71]. The application of multiple viewpoints can reduce the number of visibility gaps. Still, it is more labor/cost intensive in the field and more computationally expensive in postprocessing, due to the need for mutual matching/registration. Multiple scans are combined either at a data level, i.e., the multiscan method, which requires coregistration of the matched point clouds at millimeter-level accuracy, or at feature and decision levels, i.e., the multisingle scan approach, without building a merged data set. The multisingle scan technique has considerably lower computational costs in comparison with the multiscan approach.

The most significant advantage of the multisingle scan technique comes from the ability to link data sets from diverse sources, e.g., lasers and imagery, and at various points in time, when merging multiple data sets at the data level is difficult due to different point distribution patterns and changes among points in time. Until now, multiple scans from one plot or stand required artificial reference targets to combine multiple point clouds to one that covered the entire area of interest [27], [55]. Marker-free automated registration has been studied in recent years [72]–[75], aiming at improving the usability of TLS in forest conditions. The results showed that the methods do not reach the reliability of traditional approaches, where artificial reference targets were used. Lately, scanner manufacturers have released products with automatic registration of separate point clouds. Those solutions are either hardware dependent or not yet verified for processing in varying forest conditions.

From the tree modeling perspective, the TLS data acquisition design significantly impacts the point cloud quality, i.e., how comprehensively and accurately each tree is digitized through point clouds. This is especially important when data acquisition is carried out at the plot level and essential at the individual tree level. There has been increasing interest in obtaining the most detailed information from trees that is possible. The authors of [76] investigated the impacts of scan setups on the estimation of the stem volume of individual trees. They concluded that two scans from opposite sides of a tree at a distance of no longer than 50% of the tree height produced the most reliable stem volume estimates. For calibrating existing taper curve equations and estimating the stem volume for Scots pines, the work in [77] studied the effect the sample size had and found that a relatively small sample size of tens of Scots pines with a DBH of 5–40 cm is enough for consistent local volume estimates in southern boreal forests dominated by such trees.

The effects of the plot size, tree size, and scan pattern on tree detection were discussed in [31], [78], and [79]. The authors of [31] studied the impact of forest structures, e.g., the growing stage, species, and structural distribution, on tree detection and attribute estimates and found that structures have significant effects on the attribute estimates. The authors of [78] compared scan patterns and numbers in a temperate forest. Five scan patterns (i.e., diagonal, rectangle, triangle, and hexagon) and seven scan numbers (i.e., varying between one and seven) were investigated using a phase shift-based Faro Focus3D X330. Twenty-three circular plots with a radius of 20 m were dominated by either Norway spruce [*Picea abies* (L.) H. Karst.] or European beech (*Fagus sylvatica* L.) or were a mixture of Norway spruce, European beech, Scots pine (*Pinus sylvestris* L.), and fir [*Abies* sp. (Mill.)]. The stem density varied from 280 to 5,000 trees/hectare. They reported that seven scanning locations at the

TABLE 3. THE MS/HS TLS SPECIFICATIONS USED IN PREVIOUS LITERATURE.

SENSOR	NUMBER OF CHANNELS	SPECTRAL RANGE OR WAVELENGTH (NM)	BEAM DIVERGENCE (MRAD)	RESOLUTION (MRAD)	WEIGHT (KG)	MEASUREMENT TYPE
DWEL [59]	2	1,064, 1,548	1.25	1	19	Time of flight
SALCA [60]	2	1,063, 1,545	0.56	1.05	15	Time of flight
FGI HSL [63], [66]	8 tunable	400–1,000	–	–	–	Time of flight
HSL [70]	32 tunable	400–1,000	<5	0.17	–	Time of flight
HSL VIS-SWIR [68]	8	540–1,460	–	–	–	Time of flight
AOTF-HSL [69]	51	430–1,450	0.4	–	–	Time of flight
Faro X330 and S120 [62]	2	905, 1,550	0.16, 0.19	0.16	–	Phase shift
Leica P40 and P20 [57]	2	808, 1,550	0.23, 0.2	0.08	–	Time of flight

FGI: Finnish Geodetic Institute; SWIR: short-wave infrared range; VIS: visual.

vertices of a hexagon and the center of a plot produced the highest tree stem detection rate, at 82.4%.

The authors of [79] tested the effect of the sample plot size and tree size distribution (a proxy for plot heterogeneity) on tree detection in southern boreal forest conditions. They found that a five-scan pattern minimized occlusion and provided favorable scanning geometry in plots of 11-m radius. Four scans were placed approximately evenly on the circumference of the sample plot and one at the plot center. Additionally, the researchers reported that larger trees were more reliably detected and that plot heterogeneity affected the number of stems and basal area per hectare. In general, smaller plot sizes and lower stem densities increased the detection rate [31], [71], [78], but individual plots might not follow this general conclusion, as shown in [71].

In [55], the authors reported the time-of-flight performance of the Riegl VZ-400 scanner. They compared 27 TLS campaigns conducted mainly in tropical forests, collected in 10- (i.e., 10×10), 20-, and 30-m grids, concluding that the 10-m grid produced uniform data regarding density, which is required for characterizing LoD 3, i.e., suborder branches, toward the top of the canopy. The same study mentioned that fewer scan locations suffice if, for example, tree stems are of interest. The work in [80], on the other hand, reported that the number of automatically detected branches decreased as the distance between the scanner and Scots pine crown increased, especially above the base height of the live crown, using a Faro Focus3D X 330 phase-shift scanner. Despite a few recent studies, best practices for collecting TLS data are still unclear, especially in various forest environments and for different application purposes.

IMAGE-BASED POINT CLOUDS

Image-based point clouds for forest parameter acquisition recently gained widespread interest among researchers. The basic idea is to acquire forest structural parameters for quick, low-cost assessments of forest resources, such as tree positions and diameters, which can be used either as inventory data for decision making and planning or utilized as calibration and verification data for satellite and airborne remotely sensed data. The systems used in acquiring image-based point clouds are typically lightweight, low-cost, and easy-access camera types of sensors. Thanks to enormously increased computational power and software readiness, the data acquisition protocol and processing are easy to implement.

SENSORS

The principle behind image-based point clouds is to reconstruct 3D point clouds from highly overlapping 2D images by using a dense image matching algorithm. The quality of the 3D point cloud is mainly affected by lens selection, camera settings, and sensor calibration. The performance of different lenses in the single-tree approach was investigated in [81] and [82]. In [81], images were taken around a tree at 1–3-m distances and with an automatic shutter speed and light sensitivity (ISO) setting. The 25-mm focal length was found suitable to produce point clouds of individual trees. Both 35 and 50 mm failed to produce dense point clouds; the narrower field of view (FOV) of both lenses was assumed to cause low overlaps and consequently the failure. The authors of [82] compared fisheye and nonfisheye types of lenses that had a 15- and 35-mm focus length. Point clouds were reconstructed in both cases, and the results were not significantly different. Data acquisition using a fisheye lens was more efficient due to the large FOV.

The optimal camera settings are application dependent. In general, a large image size, small pixel size on the image array, low ISO, deep focus length, and high shutter speed are preferred: a large image size results in a high resolution, a small pixel size leads to a small ground sampling distance (GSD) at the same distance compared to a large pixel size, a low ISO reduces noise, a deep focus length achieves a large depth of field (so that objects both near and far from photographing positions can be clearly imaged), and a fast shutter speed helps avoid blurry images. For example, the image size is suggested to be at least 5 megapixels and preferably 12 megapixels, achieved using, e.g., commercial software [83].

However, meeting all these requirements in practice could be challenging; e.g., a low ISO and a fast shutter speed can hardly be simultaneously achieved within dense forests with limited sunlight, which easily leads to blurry images. The influence of different blur levels in images was investigated in laboratory conditions [84]. The number of successfully detected targets was affected by even a small level of blur. Camera calibration is an indispensable prerequisite for using modern, mostly consumer-grade, digital cameras. Fortunately, it has been widely available in commercial software. Yet, there is always room for additional research to enhance the models and processes employed with the many camera systems [85].

Alternatively, point clouds can be obtained with depth sensors. Research in forest conditions has only just begun, and the main systems that are employed are Tango, by Google [86]–[88], and Azure Kinect, by Microsoft [86], [89]. They use optical and depth sensors to reconstruct the surrounding environment in point clouds. For DBH estimation in forests, the reported RMSE is mainly around 1–2 cm when using Tango, e.g., between 1.61 and 2.1 cm across three plots [87], 0.73 cm over 80 trees [86], and 1.26 cm across nine plots [88]. Azure Kinect was reported to get an 8.43-cm RMSE over 51 urban trees [89]. Similar projects have been introduced, such as ARKit, by Apple, and ARCore, by Google. Unlike Tango, they do not require depth sensors, thus enabling a greater number of devices to use them. On the other hand, their accuracy is worse than Tango's. The problem with this type of technique is that direct sunlight causes failures in data acquisition, primarily for infrared sensors. Therefore, dense forest with full coverage is beneficial for the acquisition [87], which

reduces the number of cases where a camera is exposed to direct sunlight.

The short functional distance is also a significant limitation. The authors of [89] suggested that the distance between target trees and Azure Kinect be less than 3 m. The newest version of ARKit supports lidar, implemented on iPad Pro 2020 and iPhone 12 Pro and Pro Max. Lidar directly gives depth information and thus may solve the short functional distance problem. Currently, the lidar in these devices works up to 5 m. The performance and accuracy have not been studied. The systems' practical advantage is that an operator can see a resulting point cloud right away in the field and then adapt the data acquisition approach for the environmental conditions. In addition to handheld cameras, images can be simultaneously taken through a multicamera system, e.g., [90] and [91]. Multicamera systems are typically stable and precalibrated, and they have sufficient overlaps among individual cameras, which, in principle, produces better image quality than single cameras. Specially designed imaging systems target mainly professional users and have some cost accessibility limitations.

DATA ACQUISITION AND GENERATION

Two popular methods for acquiring image-based point clouds are the stop-and-go and mobile/kinematic approaches. In the stop-and-go method, images are captured at stop positions. The operator moves from one imaging position to the next, with relatively small steps, to achieve the required photography baseline and overlap among consecutive images. Alternatively, successive images can be captured at selected positions within a plot [92] through the camera movement, e.g., vertical movement on a telescopic pole [92]–[94]. The stop-and-go technique enables the operator to adjust the imaging settings to collect sequences with specific characteristics, e.g., camera positions and image overlaps. The stable camera position also makes it possible to use a slow shutter speed, low ISO, and high aperture, e.g., in dark environments. A camera mounted on top of a tripod, e.g., as in [95], provides the most stable imaging condition.

The camera continuously captures images along the operator's movement in the mobile method, controlled by either a time or traverse interval [96], [97]. However, the fixed camera settings and constant operator movements may result in blurry images (motion blur) if the shutter speed is relatively slow, leading to point cloud reconstruction failures [82]. Instead of holding the camera by hand, the authors of [96] mounted a camera on a 4-m-long pole to capture oblique images in the mobile data collection mode. However, using sticks in forests may be challenging when there is a dense canopy and understory, which causes collisions with branches and thus results in lower-quality images with little overlap between consecutive images and a failure in image acquisition, as shown in [98]. Different results in [96] and [98] were most likely the result of a tree density that was almost four times higher (155 versus 547 stems/hectare).

Path selection in image collection is of particular importance. Studies have used paths from outside/inside the plot or both. The work in [99] and [98] compared the results of DBH estimation from different paths. The applied method used inside and outside paths and was found to be more accurate in both studies. The DBH RMSE was 5.04 versus 3.84 cm in [99] and 5.01 versus 4.41 cm in [98]. An example of an image-based point cloud produced using the stop-and-go method and the combination of outside and inside paths is given in Figure 3, which is the most accurate point cloud within the experiment in [82]. Other point clouds from the study can be interactively seen on https://mapy.tuzvo.sk/CRPmethods.

The point cloud generated from overlapped images is in a coordinate system defined by the image registration. To set the scale of an image-based point cloud requires at least one pair of points with a known distance in the field and their correspondences in the point cloud data. In principle, any known distances in the physical and data spaces can scale the data. Artificial targets, e.g., sticks with a known length, have been commonly used. Distances between trees were applied in [100]. Surveying level measurements from total stations was applied to improve accuracy in [95] and [96]. When a multicamera system is employed at fixed positions, mutual camera positions can be used to scale the point clouds [90], [101]. The authors of [101] confirmed that point clouds scaled by mutual camera positions have high accuracy. High-accuracy point clouds can be harnessed to obtain tree diameters and volumes with accuracy equivalent to conventional inventory techniques.

Camera orientation influences which objects are recorded and what information can be extracted. A horizontal camera orientation increases image overlaps and potentially improves image registration qualities. A vertical camera orientation increases coverage in the tree height direction but has a lower overlap rate if the same baseline is used as the horizontal orientation. The authors of [99] compared landscape and portrait orientations by using the outside path and achieved higher accuracy than the data set, where

FIGURE 3. An example of an image-based point cloud from the stop-and-go method and the combination of the outside and inside paths.

images from outside and inside were merged with a portrait orientation. The combination of horizontal and vertical camera orientations is applied in [92] to ensure that most plot areas can be seen from a limited number of images. The images were collected from a horizontal camera orientation at the plot center and locations about 6 and 12 m from the plot center in eight cardinal directions. Meanwhile, the images were taken at each location by using a vertical camera orientation, including heights of about 2, 3, and 5 m.

Other factors impacting image/point cloud quality include the target distance, baseline length, ray intersection angle, to name a few, which should also be considered during the planning phase. The quality of a generated point cloud is limited by the operational range of a camera, even if the camera is set to a deep focus mode to achieve a large depth of field for the collected images. In [99], the authors compared stem point clouds generated from 5- and 20-m operational ranges. The stem points from the 5-m operational range were dense and accurate. In comparison, the stem points from the 20-m range were sparse and noisy, and such low-quality stem point clouds cannot be accurately modeled for further stem parameter estimation. The baseline length consequently influences the image matching and point cloud quality. Stem detection accuracy is lower using point clouds generated in wide-baseline situations than small-baseline situations (72 versus 84%) [99]. The work in [92] found that the main factors affecting the estimation of tree location are the tree size, tree species, and stem density, while the primary factors affecting the assessment of DBH include the tree size and distance from a tree to the camera.

Compared with TLS, the strength of image-based methods is that they can automatically connect to other images, given proper overlap and sufficient matches. Camera orientations are automatically reconstructed, enabling full horizontal coverage of irregular objects, such as stems. On the contrary, TLS can rarely fully "hit" all parts of the horizontal cross section unless a very high number of scanner positions is used, which is impossible in a way similar to that of photogrammetry. Meanwhile, the strength of image-based methods also becomes its weakness because a single pair of consequent images with ill conditions, e.g., insufficient overlapping, can result in a completely incorrect image block. Therefore, the accumulated errors may be so large that the detection and mensuration of targets become impossible.

Reported times needed for data acquisition [95], [96], [98], [99], [102] and image postprocessing [95], [99], [102] are summarized in Table 4. The time required to capture images highly depends on the data acquisition method. The mobile approach requires the shortest time for data acquisition, e.g., 0.5 s/image [96]. On the other hand, the stop-and-go mode with a tripod in dense forests takes much longer, e.g., 14 s/image, on average [95]. The image processing time to a dense point cloud is difficult to compare. It mainly depends on computer configurations together with the software that is and its version. Additionally, different settings for image matching and dense point cloud generation are used in postprocessing workflows, which highly impacts postprocessing time. It is worth noting that postprocessing time is not a period where the operator actively works with the software. In most postprocessing, the operator is required only to start the process and evaluate the results.

The proportional time needed to capture one tree in the field when the plot-based approach is used varies among studies. To calculate the time, the number of trees that were successfully detected on a plot was used. The time needed varied from 0.1 to 2.7 min. For single-tree studies, the average time required to capture a single tree was 2 min when a fisheye lens was used and the DBH RMSE was no higher than 0.5 cm [82]. Concerning the software, Agisoft Metashape (formerly Agisoft Photoscan) was mostly used across the reviewed studies, whereas a few studies employed Pix4D. This could be because of cost: Pix4D is more expensive.

TABLE 4. THE DATA ACQUISITION AND POSTPROCESSING TIME REPORTED IN THE PLOT-BASED APPROACH.

STUDY	NUMBER OF IMAGES	DATA ACQUISITION TIME (MIN)	DATA ACQUISITION TIME PER DETECTED TREE (MIN)	PROCESSING TIME (H)
[99]	97–1,070	13–49	0.8–2.7	0.2–39
[102]	804–862	13–15	0.9–1	5.8–8.1
[96]	1,774	15	0.1	–
[98]	440–1,552	9–40	0.4–1.2	–
[95]	338–775	30–120	0.7–2.2	17–50.8

IMAGERY

Besides the recent popularity of point cloud data, various terrestrial imagery-type sensors have a long history in forest in situ observations. Earlier studies using film cameras to measure tree diameters date to the 1950s, and many systems were proposed in the following years [121]. For terrestrial imaging systems, key technical issues include camera calibration, feature extraction, scaling, and protocols. In particular, determining the scale among objects in an image and the field is challenging, and a wide range of solutions exists.

CONSUMER-GRADE CAMERAS

Individual trees can be measured at close to a professional level by using a digital camera with supporting equipment and particular protocols. The authors of [122] tested a laser camera under typical boreal forest conditions, which integrated a Canon EOS 400D digital reflex camera with a Mitsubishi ML101J27 laser line generator. The laser camera measured the diameters of trees from the center of a sample plot without visiting individual trees. The method semiautomatically processed the images and achieved accuracies of 6 and 2.5 mm in terms of the standard error

and bias of diameter measurements, respectively [123]. An imaging system was developed to determine the stem curve of individual Scots pines in one image [124]. It consisted of a calibrated camera, laser distance measurement device, and calibration stick. Stem curves were determined by stem diameters from an image and a tapering model. Two [125] and four [121] photos were taken in orthogonal directions to derive the stem curve. Measurement settings (i.e., the inclination angle of the camera, viewing angle, and distance measurements) were also recorded in the field for data interpretation in [125].

PANORAMA IMAGES

Panorama images have been used to determine stem locations in forest plots [126]. The positions were determined by field-measured DBHs together with angle and DBH measurements of each tree in an image; 85% of the measured trees were within 0.5 m of the field-measured tree locations. Lately, smartphones have been used in in situ observations, following ideas similar to the studies mentioned in the preceding. More discussion is in the "Operations" section.

HEMISPHERICAL IMAGERY

Hemispherical, or fisheye, photography has been used in forest research since the 1950s [127]. It is the most widely used ground-based method for describing canopy characteristics and forest light regimes [128]. Since digital cameras and computer processes became available, it has been increasingly employed to indirectly obtain foliation and canopy architecture. Hemispherical imagery is an indirect method to study light transmittance. It does not inherently vary with time and cloud cover, though the associated error level can occasionally be substantial [129]. The light transmittance of the canopy can be described by the percentage of the incident solar radiation at a given site compared to the total incident solar radiation in the open through the same period [130], which requires gap positions and site geographical locations so that the sun track can be superimposed onto the hemisphere.

Hemispherical imageries are also used to estimate other plant canopy properties, e.g., to invert the leaf area index (LAI). Hemispherical photography is markedly cheaper than the alternatives [131]. However, the derived effective plant area index may be significantly affected by the exposure of the photographs, and the determination of the declination angle of plant elements may be substantially different from that derived from a canopy analyzer, as demonstrated in [132]. For canopy structures, original images are typically converted to black and white, and a threshold is used to determine, e.g., the canopy cover and openness. One of the main problems in applying hemispherical photography to determine the LAI is the selection of an optimal bright threshold to distinguish leaves from the sky [131].

The image quality also affects the features that are estimated; e.g., overexposure may lead to overestimating the sky fraction. In addition, the determination of the clumping index was also suggested to be part of plant area index measurements derived using optical and radiation methods [132] since clumping seems to be one of the main factors causing errors in LAI estimation [131]. Similarly, hemispherical photography from smartphones has been used as a cheap and fast alternative to conventional hemispherical imageries. It was found that smartphone images provide results comparable to traditional cameras for describing forest canopies and light regimes [133].

HYPERSPECTRAL INSTRUMENTS

HS instruments have been widely used in terrestrial observations since HS remote sensing technology was developed in the 1980s [134], [135]. The first portable field reflectance spectrometer, from the Jet Propulsion Laboratory, produced spectra between 400 and 2,500 nm at a speed of at least 60 s and promoted the development of more advanced and easily carried instruments [136]. As one of the most widely used field spectrometers, the Analytical Spectral Devices instrument can cover the intact and contiguous spectral range from 350 to 2,500 nm for determining vegetation spectrum [134] demand, and it takes no longer than 100 ms to obtain a full spectrum.

In situ HS measurements have conventionally provided test and calibration information for airborne and spaceborne observations. Lately, more and more studies have begun to focus on surveys of individual trees and small forest stands. Leaf-level measurements take leaf samples into laboratories to obtain spectra, physiological, and biochemical parameters, such as leaf thickness, area, water content, chlorophyll, nitrogen levels, and so on. Statistical analyses indicate correlations between spectral indices and leaf biochemical components, and their quantified results have been applied in rapid and nondestructive instruments for field measurements. For example, the SPAD-502, of Konica Minolta, a widely used leaf chlorophyll meter, uses spectral traits of two bands at 650 and 940 nm to measure leaf relative chlorophyll content [138].

Canopy-level measurements are always labor and cost consuming when using traditional ways of placing spectrometer probes vertically above the forest canopy. Imaging spectrometers may address the problem via their multiangle scanning on the ground. Although most imaging spectrometers are air- and spaceborne, in situ measurements take advantage of designing specific experiments to gain elaborate data sets, which significantly contribute to the establishment of models, such as PROSPECT, LIBERTY, and 5-SCALE. As more and more lightweight and easily carried spectrometers came into use in recent years, UAV platforms increasingly became popular alternatives to in situ canopy-level measurements. Besides, the combination of ground-level HS features with other characteristics has the potential to solve more challenges in forest monitoring. For example, HS features have been combined with lidar metrics to improve tree species recognition at the individual tree level [139], [140].

MOBILE MAPPING SYSTEMS

Terrestrial mobile mapping systems (MMSs) offer benefits that eclipse stationary systems by providing movable observation positions along trajectories, or measurement paths, that require multiple passes to cover objects of interest from different directions, thus increasing work efficiency and the completeness of the data.

SENSORS AND SYSTEMS

MMSs integrate positioning and data collection sensors on a kinematic platform. Early MMSs for forest observations were generally based on all-terrain vehicles (ATVs), which later evolved into portable systems that were either carried or held by a person. ATVs can be complemented with other vehicles, such as unmanned ground vehicles [103] and harvesters. There is ongoing development of harvester-installed, real-time systems to monitor surroundings during operations. Here, vehicle-based systems are considered MLS, and systems carried by a person are viewed as personal LS (PLS). PLS can be further grouped into subcategories according to how a system is mounted, such as backpack and hand-held systems. Figure 4 illustrates an operational MLS mounted on an ATV and a backpack/handheld PLS (PLS_{hh}).

The most prominent MMS sensors have been cameras and laser scanners [104], [105] since the advent of the technology about 15–20 years ago. GNSS receivers and inertial measurement units (IMUs) are typically tightly coupled and form the basis for positioning subsystems [104] to collect platform movements and sensor orientation data. The system position and sensor orientation at any given time, to a discrete sampling time interval according to system specifications, are used for direct georeferencing of collected data [106].

LS sensors on MMSs collect 3D point clouds up to thousands of points per square meter or more at short ranges. A high point density is provided by the high pulse rate and scan frequency, and high data quality is achieved by the narrow beam divergence angle and millimeter-level ranging precision. A GNSS IMU system determines the accuracy of an MLS point cloud. Errors vary through time because of system dynamics, scene characteristics, satellite visibility, and the GNSS/IMU grade. When GNSS signals are sufficient for positioning, i.e., there are enough satellites and there is acceptable instantaneous constellation geometry, 1–3-cm of position accuracy can be achieved with high-end MLS systems supported by trajectory postprocessing and by using real-time kinematic (RTK) positioning in urban and semiurban environments [107]. However, 1–3 cm of uncertainty can introduce multiple copies of objects (e.g., tree stems, branches, and so on) in multipass data, with centimeters that differ from one another.

Recent studies showed that 0.2–0.7 m of absolute accuracy could be achieved with postprocessed positioning using a tactical-grade GNSS IMU [108], [109] in boreal forests. However, the accuracy can degrade to several meters [110]. In general, subcentimeter data cannot be achieved with low-cost IMUs, due to the high rate of positional drift in low GNSS visibility conditions and more significant angular uncertainty that increases the spatial point error for long-range measurements. Low-cost IMU solutions are usually coupled with simultaneous location and mapping (SLAM) to cope with the drift and provide real-time data.

PLS is very similar to MLS concerning the type of sensors used. The main difference is that all sensors are carried by a person with PLS, thus achieving high operability and efficiency even in rugged and soft terrain, confined spaces among/in trees, vegetation, and channels. Assuming that they are passable with an ATV, such environments take significant efforts to plan and collect data. In many cases, PLS has a higher level of mobility in comparison with MLS, offering flexibility in the data collection path to minimize object occlusion and maximize data coverage in areas with structural complexity. Such flexibility is mainly preferred

(a) (b) (c)

FIGURE 4. Examples of mobile scanning: (a) ATV-mounted MLS, (b) backpack-borne MLS, and (c) handheld PLS.

in forest observations, due to complex forest environments with rugged terrain and high stem density [111].

Initial PLS was conceived as a backpack LS [112] and soon applied to forest in situ observations [113]. Rapid development of sensors and batteries led to the fast growth of lightweight PLS systems. Today, similar performance has been achieved in point measurement and scanning rates, as the first 22-kg PLS [112] can be realized using a 1.55-kg LS (RIEGL miniVUX-1UAV) with, however, a lower ranging accuracy. PLS systems often use SLAM-type approaches to solve the system pose and improve trajectory accuracy, making them suitable for areas with weak and absent GNSS signals.

A prominent result of sensor miniaturization is the PLS_{hh}, which appeared in the early 2010s. PLS_{hh} mainly uses low-cost laser sensors because of their lighter weights. However, the collected data are consequently less accurate and noisier. Low-cost sensors also typically have a considerable beam divergence and therefore reduce the laser's penetration through dense understories with moving leaves [81], [114]. The range may also be limited, as shown in recent studies [114]–[118], limiting applicability in forested areas. For example, ZEB1 and ZEB-REVO-RT had a declared a range of 30 and 15–20 m indoors and outdoors, respectively. Due to limited scanning ranges, the height estimation of taller trees is hindered or completely disabled. The agreement on height estimates between TLS and PLS_{hh} was found to be high for trees shorter than 20 m (RMSE: 1.34 m), and low for trees taller than 20 m (RMSE: 9.44 m) [116]. PLS_{hh} was also found to considerably underestimate tree heights when trees surpassed a certain height, in comparison to TLS-based estimates. Namely, the RMSE was 0.74 m for trees shorter than 10 m, whereas the RMSE was 3.79 m for an entire sample that included all trees. This revealed that the underestimation of tree heights above a certain height threshold (10 m) from certain PLS_{hh} is even more significant than for TLS, where TLS was also confirmed to underestimate tree heights above 15 m [24].

The authors of [116] found that the height threshold, above which PLS_{hh} estimations fail, depends on the maximum scanning range of the instrument and the illumination conditions. Namely, measurements of trees taller than 15 m are not recommended with instruments that have a limited scanning range (e.g., ZEB1 and ZEB-REVO) in unfavorable conditions (sunny days). Similar measurement range limitations were also reported in [117], in a Mediterranean forest with an average tree height of 12.5 m and a standard deviation of 3.9 m. Compared to field reference data, PLS_{hh} tree heights were underestimated, with a bias of –4.61 m and an RMSE of 2.15 m. New sensors are solving such hardware limitations. The work in [25] reported reliable tree height measurement using a new version of PLS_{hh} that had an approximately 100-m measurement range. Lately, consumer-grade laser sensors have been added to smartphones. These low-cost sensors are expected to multiply in the future, providing more PLS_{hh} that is easy to use [91].

DATA ACQUISITION AND GENERATION

The application of MMSs in forest environments largely depends on the point cloud data quality, which primarily depends on the success of the strip adjustment and SLAM algorithms. Up to now, the performance of those algorithms has not been satisfactory in complex forest conditions. Ghost trees and tree parts exist around the actual positions; e.g., clusters from the same object scanned from several positions do not align correctly. For stem curve and volume estimations, a recent publication presents methods to overcome this spatial inaccuracy by using SLAM and inclination angle correction [119].

According to [114], the automatic coregistration procedure of presented PLS_{hh} systems (ZEB-REVO-RT) is sensitive to stem density in forest plots, especially in the case of a dense understory with moving leaves. Low stem densities hindered object recognition in the SLAM algorithm. In contrast, high stem densities and a dense understory resulted in slight offsets of the points at stems and the appearance of double stems in the point cloud. In [120], the coregistration failed for two out of 10 scanned plots because of the low and high stem densities. The relatively short measurement distance of the laser sensor could be a reason for the failed data correction.

For forest inventories, the GNSS IMU trajectory of an MLS was adjusted for reducing positional and attitude drift in postmission processing by adapting graph SLAM [109]. Features extracted from the point cloud were used to find correspondences among overlapping data measured at different times during mapping. The method was evaluated on three boreal forest test plots of 64×64 m in a square. The results showed that the technique could improve point cloud quality. The internal consistency of tree stem locations was reduced from 10–20 cm to a millimeter level in terms of the distance residual standard deviation. The ability to correct absolute coordinates was found slightly weaker.

The quality of PLS_{hh} point clouds, and consequently tree detection and DBH estimation, are also directly related to the walking scheme, scan path density, and field conditions. Three walking scan paths were tested in [118]. It was found that walking around each tree improved the detection rate for small trees (DBH < 10 cm). The path back and forth along straight lines and around each tree provided similar results, and the 10-m distance solution balanced the accuracy, cost and time. However, choosing a walking path that suits data processing is not straightforward. Obstacles, such as stones and branches, often block the operator's way in field data collection [111]. In addition, path selection is also limited by time and cost considerations. There has been very limited knowledge of the best practices for data collection using MMSs.

GNSS

The GNSS receiver is another common sensor used in environmental observations, such as in forests [141] and when testing soil moisture [142]. GNSS positioning is widely known to be problematic under forest canopy, e.g., [108], [142], and

[143]. The denser the canopy is, the less accurate the positioning solution [144], [145]. However, GNSS signals can be used as an informative indicator to measure some physical properties of forests, e.g., according to signal degeneration due to the mass of biomass. High correlations between the statistical features of GNSS signals and plot-level forest attributes were found in boreal forest conditions, including the mean tree height, mean DBH, basal area, stem volume, and tree biomass. Prediction accuracies were evaluated using a reference data set of 292 sample plots. The relative RMSEs were 14.77–20.98% for the mean tree height, 15.76–22.49% for the mean DBH, 15.76 and 33.95% for basal areas, and 27.76–40.55% and 26.21–37.92% for the plot-based stem volume and aboveground biomass, respectively, when different combinations of receivers and constellations were used [141].

The GNSS-derived predictions were shown to be as accurate as results derived from imaging spectrometry and aerial photographs, which were the best 2D remote sensing techniques and far more precise than satellite-based 2D techniques in terms of the correlation coefficients and RMSE. Although 3D techniques achieved more accurate predictions in most cases, GNSS-based predictions evidently cost less. The correlation coefficients were higher when observables of several GNSS constellations were combined than when the coefficients of a single constellation were used, such as GPS and the GNSS. The combination of multiple GNSS constellations is expected to provide more accurate statistical features. It will thus further improve predictions of forest attributes as the European Galileo and Chinese BeiDou systems come into full operation [141].

PERFORMANCE

Different systems record forests with varying efficiency, LoD, and quality. Figure 5 illustrates point clouds of one tree that were derived through TLS and PLS_{hh}, representing geometrical qualities and point distributions. In general, TLS provides the most accurate terrestrial point clouds at the millimeter level. The performance of state-of-the-art TLS for tree and forest attribute estimation was evaluated in an international benchmarking study [31]. The evaluation was conducted on tree and plot levels by using single- and multiscan TLS data within diverse sample plot conditions in boreal forests. Altogether, 18 research groups participated, contributing their algorithms to the benchmarking, which revealed that the quality of a point cloud (i.e., its comprehensiveness) substantially influences the results of tree detection and the accuracy of forest attribute estimates. In general, the tree attribute estimates are accurate as long as the objects (i.e., the trees) are comprehensively and precisely recorded in the data. Inaccurate tree and forest estimates typically happen at places where the quality of a point cloud is low.

The comprehensiveness of a point cloud is mainly affected by the data acquisition design (e.g., single or multiple scans) and forest structure (e.g., species, density, development stages, and terrain). The delineation of all trees within a sample plot when using TLS becomes considerably more difficult as the number of observation positions decreases and the plot's structural heterogeneity increases. The completeness of tree detection decreased from ~90% in easy plots (600 stems/hectare, with a 20-cm mean DBH) and medium plots (1,000 stems/hectare, with a 15-cm mean DBH) to ~66% in complicated plots (2,000 stems/hectare and a 10-cm mean DBH) with the multiscan approach. While the completeness decreases sharply in complex stand conditions, the correctness of the algorithms appears stable, i.e., commonly above 90% in all three complexity categories, indicating that the detecting algorithms are mostly reliable. With single-scan data, most recent algorithms have approximately 75, 60, and 30% completeness in easy, medium, and complex plots, respectively, and the correctness stays at roughly 90%.

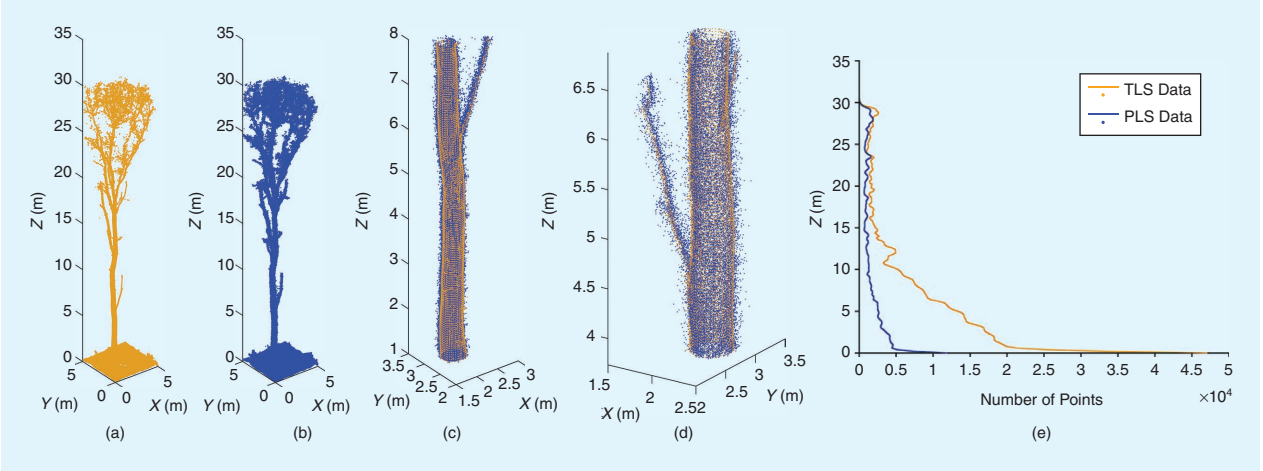

FIGURE 5. A tree shown in TLS and PLS_{hh} point clouds. (a) and (b) The TLS and PLS_{hh} point clouds of the whole tree. (c) The stem section, where the TLS data are in yellow and the PLS_{hh} data are in blue. (d) The upper section of the stem as illustrated in (c), giving more detail about the point cloud data. (e) The point distribution according to the height.

The DBH estimations remained stable across three stand complexity categories for many algorithms. Robust algorithms had an RMSE range of 2–4 cm and RMSE of 8–20% when using a single-scan approach. Multiscans reduced the RMSE to less than 2 cm and the RMSE to a range of 5–10% for easy and medium stands and 10–15% for difficult forest stands. Current algorithms can estimate the DBH with a close-to-zero bias and bias percentage for the easy and medium complexity categories when utilizing multiscan data. When a single-scan is applied, the bias and bias percentage are close to zero in all three stand complexity categories when employing conservative and robust algorithms.

The stem curve estimation was relatively stable in terms of stand conditions, i.e., a mean RMSE 1.3–6 cm from single-scan data and 0.9–5 cm from multiscan data for all three stand complexity categories. The impact of the stand complexity on the percentage of the tree height covered (PHC) was greater than that of the RMSE. A higher PHC is expected more from multiscan data than from single-scan data. An interesting finding in the benchmarking is that the DBH and stem curve estimates had similar accuracy for a few algorithms in terms of the RMSE percentage for single and multiple scans and across the three complexity categories. These results indicate that automated algorithms can have similar capacity in estimating the DBH and stem curve, and stem curves can be used as a tree attribute similar to DBH in future inventories. The RMSE percentages of the stem volume values in three complexity categories were 35.1, 60.4, and 81%, respectively, with single-scan data and 28.3, 47.3, and 77.1%, respectively, with multiscan data. A strong correlation between the RMSEs of the stem curve and stem volume estimates exist, indicating that the stem curve has a more determining role than the tree height.

At the plot level, the best current automated algorithms gave volume estimates similar to reference data from multiscan data, i.e., 107, 107, and 94% trunk volume ratios for easy, medium, and difficult plots, respectively. Despite the high level of omission errors in medium and difficult forests, the estimated total stem volumes in plots were close to the reference values, indicating that the omitted trees were mainly small ones with a minor role in plot-level estimation. The plot-level trunk volume ratios were 94, 87, and 43%, respectively, for single-scan data. The biomass was predicted as a function of the DBH and tree height. The accuracy of DBH estimates had a stronger correlation with the biomass accuracy than with the tree height but was not the determining factor. The average RMSE percentage values of a few representative algorithms were 23.9, 43.2, and 53.2% for easy, medium, and difficult plots, respectively, with single-scan data and 15.9, 27.2, and 39.3%, respectively, with multiscan data. At the plot level, when an algorithm was capable of providing accurate estimates of the DBH and tree height while maintaining the completeness and correctness of the stem detection, the biomass ratio reached 86.1, 81.2, and 40.2% for easy, medium, and difficult plots, respectively, with single-scan data and 98.9, 95.8, and 80%, respectively, with multiscan data.

The authors of [111] benchmarked TLS and MMSs, e.g., MLS and PLS, and evaluated the applicability of MMSs in various forest conditions as the TLS benchmark. Point cloud data were processed through the same chain, and thus the results indicated the capacities of TLS and MMSs in forest digitization. The evaluation showed that an MMS can assess homogeneous forests as well as static observations but cannot handle heterogeneous forest conditions. The major challenge is the data quality, i.e., data coverage and accuracy. MLS showed some limitations in mobility in challenging forest and terrain conditions. The results indicated that future research into robust registration techniques between strips is required, especially in complex forest conditions.

Terrestrial point clouds from imagery, TLS, and MMSs were benchmarked in [99] in a boreal forest. The study indicated that photographic measurement is easy and relatively fast. The state-of-the-art dense matching algorithm is robust. Point clouds can be generated in dim light conditions, e.g., after sunset in winter. Meanwhile, the data collection has a direct and significant impact on the quality of the generated point cloud. The tree detection accuracies were between 60 and 84%, and the RMSEs of the estimated DBH were between 2.98 and 6.79 cm among five data collection methods. The accuracy of the tree attribute estimates was lower than that achieved with the LS techniques but close to an acceptable level for forest field inventories. On the other hand, TLS and PLS showed a close to 100% detection accuracy, and the DBH estimate RMSEs were 2.38 and 2.92 cm. PLS had superior speed, i.e., 5 min, over terrestrial imaging, i.e., 13–43 min. Terrestrial point clouds from imagery and TLS were benchmarked in [32]. Altogether, 15 algorithms were used to detect individual trees and estimate the DBH. TLS was confirmed to provide more reliable data, where the completeness and RMSE of DBH estimates were higher and more accurate across the research plots and algorithms.

AERIAL SYSTEMS

Low-altitude airships have undergone fast development in the past two decades, accompanied by a recent boom in applications, driven by the rapid evolution of the platforms, onboard sensors, batteries, navigation, processing algorithms, computing power, and affordability. The most popular aerial systems in close-range remote sensing are UAVs, also known as *drones*; unmanned aerial systems; and remotely piloted aircraft systems. Helicopter, hybrid airship, and similar systems are also employed when low-altitude observations are made.

Low-altitude airships are suitable for quick data acquisition at high spatial resolution in small areas where the application of airborne systems is too expensive, in remote areas inaccessible by other solutions, and in dangerous scenarios

where close-to-target sensing should be avoided. They have LoDs comparable to terrestrial remote sensing [146], and they outperform terrestrial systems in efficiency in terms of data collection speed and area covered, e.g., hectares to square kilometers in several tens of minutes, as their movement is free of ground obstacles [147]. They were quickly recognized as cost-effective platforms in many environmental applications, such as agriculture [148]–[150], geosciences [151], [152], and forests [153]–[156]. In addition, they provide a link between airborne and terrestrial observations and may profoundly change field observations. This section reviews current platforms and operations and then discusses passive and active onboard sensors. Performance is evaluated in the "Performance" section.

PLATFORMS

UAVs are currently the dominant platform among low-altitude airships. UAVs have variable sizes, ranges, and avionics. The most popular ones in current research and forest applications are powered by electricity. Fixed-wing platforms are similar to conventional airplanes and consist of rigid frames with airfoils and propulsion systems. Rotary-wing platforms use one or multiple rotors for vertical lift and flight. Forward motion is not required to produce airflow to generate lift, which gives rotary-wing platforms the advantage of vertical takeoffs and landings and operation through small openings. Fixed-wing platforms are superior in endurance and flight speed, including coverage, cost, and efficiency. However, they must maintain a minimum flight speed to stay in the air, limiting the spatial resolution in a single flight when given the same sensor configuration. They also need space and time to turn to follow flight plans, especially during area mapping.

Rotary-wing platforms enable slow flight, which contributes significantly to high spatial resolutions. Their agile maneuvering also opens a wide range of new possibilities that require sophisticated flight trajectories, e.g., vertical, circular, and 3D flight, and maintaining observations of a single target for a period of time. Vertical takeoff and landing provide easy operation and support more flexible flight planning in comparison with fixed-wing systems. According to a recent study [157], rotary-wing UAVs are more frequently used than fixed-wing platforms in forest studies, i.e., 71 versus 29%. Hybrid platforms have notable advantages, such as vertical takeoff and long-endurance flight. Despite these, only a few studies based on hybrid platforms have been reported [158], which may be due to immature technology and high prices.

In electrically powered systems, batteries usually make for a large part of the takeoff weight; hence, efficient battery technology is appreciated. Lithium polymer batteries are the most common. Solid-state lithium batteries are expected to double the energy capacity of lithium polymer variants and are safer to use and easier to maintain. Their main drawback is a high price, making it an open question whether their use will be financially justified. Clear advances in UAV flight control have been achieved in recent years [150]. Control algorithms are under development, e.g., in open source communities, such as Ardupilot, that support various frames. Swarm technology is being intensively developed.

UAV platform sensors are similar to those commonly used on mobile mapping platforms. The navigation system is composed of a GNSS receiver and an IMU. A variety of sensors have roles in specified tasks, e.g., passive sensors, such as visual spectral [red–green–blue (RGB)], MS, HS, and thermal (TIR) cameras, and active sensors, including lidar and radar. Multiple sensors are commonly used simultaneously, and their various combinations provide the possibility to investigate targets from different perspectives. Lidar and RGB cameras provide geometric and color information, respectively [147]; RGB and TIR cameras obtain high-quality TIR point clouds through filtering based on a fixed distance filter and RGB cloud [159]; and RGB and MS cameras acquire geometric and spectral data for aboveground biomass estimation [160].

Until recently, the maximum payload of popular UAVs was low, e.g., a few kilograms. The combination of multiple sensors is mainly limited by the payload and, consequently, efficiency; hence, sensors are rarely redundant and almost exclusively complementary. The payload also limits the mounting of heavy and high-power-consumption systems on UAVs, e.g., radar. More sensor details are provided in the following sections. Helicopters are another popular platform that has much larger payloads than small UAVs. High-grade yet typically heavier sensors are convenient to install on helicopters. A hybrid airship combines aerodynamic lift from lighter-than-air and heavier-than-air components. Hybrid airships typically have long-endurance flights, which suit long-term observations with a bird's eye view.

OPERATIONS

UAVs operate above and below canopies and in seamless modes. Similar platforms are used, though undercanopy UAVs typically have a smaller frame size to help maintain safe distances from surrounding objects. Up to now, flying above the canopy has been the most common protocol [161]. Early demonstrations of undercanopy flight can be found in [162]–[164], using laser sensors [165], [166] and imageries [167], [168]. An above/below-canopy pattern in a single flight was reported in [166]. It was shown to acquire highly complete imagery of upper canopies from above the treetops and of stems from a terrestrial perspective. It represented a step forward to achieve a fully autonomous in situ forest inventory by combining the advantages of terrestrial static, mobile, and above-canopy UAV observations [166].

Registration and georeferencing are fundamental to providing high-quality UAV data. They can produce large geometric errors [166], [169]–[171], especially in complex forest environments and undercanopy flights, and require more thorough investigation. Ground control points (GCPs) are

commonly used to georeference UAV data to a predefined coordinate system. However, setting up and measuring GCPs is time-consuming and challenging due to a lack of open areas. Depending on the UAV campaign, the time needed varies from tens of minutes to a couple of hours. The area of interest is typically large when a fixed-wing UAV is used, e.g., several hundred hectares, requires at least a couple of hours to collect GCP information. In addition, placing GCPs at positions visible in UAV-captured data is not always easy, e.g., in dense forests. Lately, dual-frequency GNSS receivers mounted on UAVs are becoming more affordable. An RTK/postprocessing kinematic (PPK) solution typically has a 1–3 cm of positional accuracy and can add coordinates to images, thus providing a GCP-independent georeferencing solution.

GCPs' influences on positional accuracy were studied in [171] by using a fixed-wing UAV and 40 validation points. A solution purely based on RTK/PPK was found to provide comparable results to the conventional solution that depends on GCPs, with potentially better accuracy. In addition, image processing, e.g., to generate point clouds, was found to be more reliable when using image positions from RTK/PPK. Image matching with known positions is supposed to be more robust than with images without coordinates, especially in leaf-off seasons, when forests and images are more homogeneous.

Besides technical issues, UAV operations have to meet legal requirements according to local regulations. Flights in forests are almost exclusively beyond the visual line of sight (BVLOS), which legally differs from VLOS operations, depending on the national aviation authority rules. BVLOS operations are considered increased risk operations, even in unpopulated areas, such as forests. This issue is recognized and acknowledged by the European Union Aviation Safety Agency as a "standard scenario," and officials plan to authorize such operations through legislation.

LASER SCANNING

UAV-based LS (ULS) combines near-ground aerial perspectives for observations from drones and the canopy penetration capacity of LS sensors. It avoids access constraints on the ground and the degradation of GNSS signals beneath canopies. It provides point cloud data at an LoD comparable to terrestrial observations. Thus, ULS diminishes the boundary between airborne and terrestrial observations [147]. Early studies [172]–[174] explored the possibility of delineating individual trees and soon became a hot topic in environment studies.

SYSTEMS AND SENSORS

High-end and low-cost ULS systems are available on the market. High-end ones typically provide more accurate point clouds through a professional body, navigation unit, and sensors, with obviously significant expense. Low-cost platforms often use inexpensive sensors and are more affordable to many users. They can achieve a point density similar to that of high-end systems, but the data quality, i.e., the geometric accuracy and spatial coverage, is typically lower.

A good example of a high-end system is the Riegl RiCOPTER with a VUX-1UAV laser sensor. The scanner has a beam divergence of 0.5 mrad, providing 2.5- and 5-cm footprints at 50 and 100 m, respectively. The navigation system has an Applanix AP20 GNSS inertial system, which gives a position measurement accuracy better than 0.1 and 0.2 m in horizontal and vertical directions, respectively. The roll/pitch and heading measurement accuracy exceeds 0.015 and 0.035°, respectively. Points at the nadir and far end of the FOV at 50 m above the ground are measured at an accuracy superior to 3.6 and 7.1 cm, respectively, without considering positioning and ranging errors. So far, high-end ULS system geometrical accuracy has not reached the level of TLS point clouds and what is required in practical applications [147].

High-end ULS system performance was investigated in three complex forest categories [147]. The average RMSE of the ULS-based stem position estimates was between 6 and 15 cm, considering the stand complexity, i.e., about two times as much as TLS-based results. ULS overestimated the DBH in automated and manual estimations, and the overestimation was more significant than that of MLS. The tree attribute estimation, in general, can achieve results comparable to TLS only in easy forest conditions. These results indicate that hardware improvement is urgent to provide accurate enough point cloud data from UAV platforms.

Low-cost solutions often use sensors such as those from Velodyne. The beam divergence of the Puck VLP-16 is 3 mrad, which provides 15- and 30-cm footprints at 50 and 100 m from the scanner, respectively. The systems also typically include lower-grade GNSS receivers and IMUs, resulting in less accurate position and orientation estimates. Their data quality has significant variance due to differences in sensor configurations. Instead of directly measuring tree attributes from a point cloud, e.g., [175], researchers also investigate the use of indirect methods, i.e., statistical models, to derive estimates.

In [161], the authors compared these approaches for the calculation of tree height and the DBH. The test plot was 64×64 m and dominated by Scots pine and Norway spruce, with a mean height of 18.1 m and a mean DBH of 21.6 cm. Altogether, 201 trees were measured using a low-cost ULS with 800 points per square meter. The results showed that the difference between indirect and direct tree height measurements was small when using low-cost solutions. On the other hand, the DBH estimate from the direct approach was less accurate than the indirect method based on point cloud metrics and regression. This indicates that low-cost ULS data have significant measurement errors.

It seems that low-cost systems are suitable for collecting tree heights and crown diameters in open forest conditions. Tree height estimates from a low-cost ULS were more reliable than conventional field observations in a deciduous

forest [25]. The performance of low-cost ULSs was identified as comparable to high-end systems for tree height and crown diameter measurement [177], with a high correlation of $R^2 = 0.998$ and $R^2 = 0.806$, respectively. However, low and complex trees were delineated with poor quality by inexpensive UAV solutions, due to insufficient point density. A clear difference between hardware exists. The authors of [175] compared two scanners from the same company to evaluate stem parameter estimation, i.e., the RIEGL VUX-1UAV and RIEGL miniVUX-1DL. Both scanners belong to the high-end category, but the VUX-1UAV clearly has better accuracy than the miniVUX-1DL. The study confirmed that the accuracy of the equipment itself has significant influences on data accuracy. Namely, a high-quality scanner has better accuracy.

Studies also reported differences in the point density between high-end and low-cost systems, i.e., 12–1,500 points/m^2 in low-cost systems at an average altitude of 65 m above ground flight height and 200–18,000 points/m^2 in high-end systems at an average altitude above the ground of 84 m (references). The authors of [177] compared low-cost and high-end ULS systems (a Velodyne VLP-16 and Riegl VUX) in 12 plots of dawn redwood and poplar on a plantation and three plots of seedlings on nursery land. The point densities of low-cost and high-end systems were 12 and 224 points/m^2, respectively. The point density of the high-end solution was much better than that of the low-cost version, even though the altitude was greater (140 versus 70 m). Also, huge differences exist in the range resolution and multiecho properties of low-cost and high-end sensors, which especially impacts forest applications.

DATA ACQUISITION

Data acquisition is a tradeoff among practical issues and needs a careful design. A lower flight height and a larger overlap between strips increase the possibility of completely capturing a tree but reduce the area covered during the same amount of data acquisition time. Elements considered typically include 1) the needs of a particular application, e.g., point density, point and model accuracy, coverage area, and repeatability, and often neglected traceability in terms of standards, quality, and reliability of data and measurements; 2) practical implementation; and 3) costs and budgets. Typical flight speeds and durations in recent studies are approximately 5 m/s and 20 min, respectively. Current studies primarily focus on field sample plots, e.g., with a 10–20-m radius in a circle or 32×32 m in a square, and thus practically limit the flight speed. The flight height varies depending on the application and laser sensor. If less accurate or range sensors are selected, the altitude has to be kept low, which means more time spent, more battery consumed, and possibly higher cost. A practical issue that is worth keeping in mind is the downdraft from rotary-wing UAVs. It may move the top of the canopy when a UAV flies close to treetops, but the effects are mostly minor when the distance between the platform and treetops is a couple of tens of meters.

A typical ULS flight pattern appears in Figure 6. The IMU is typically responsible for the precise trajectory

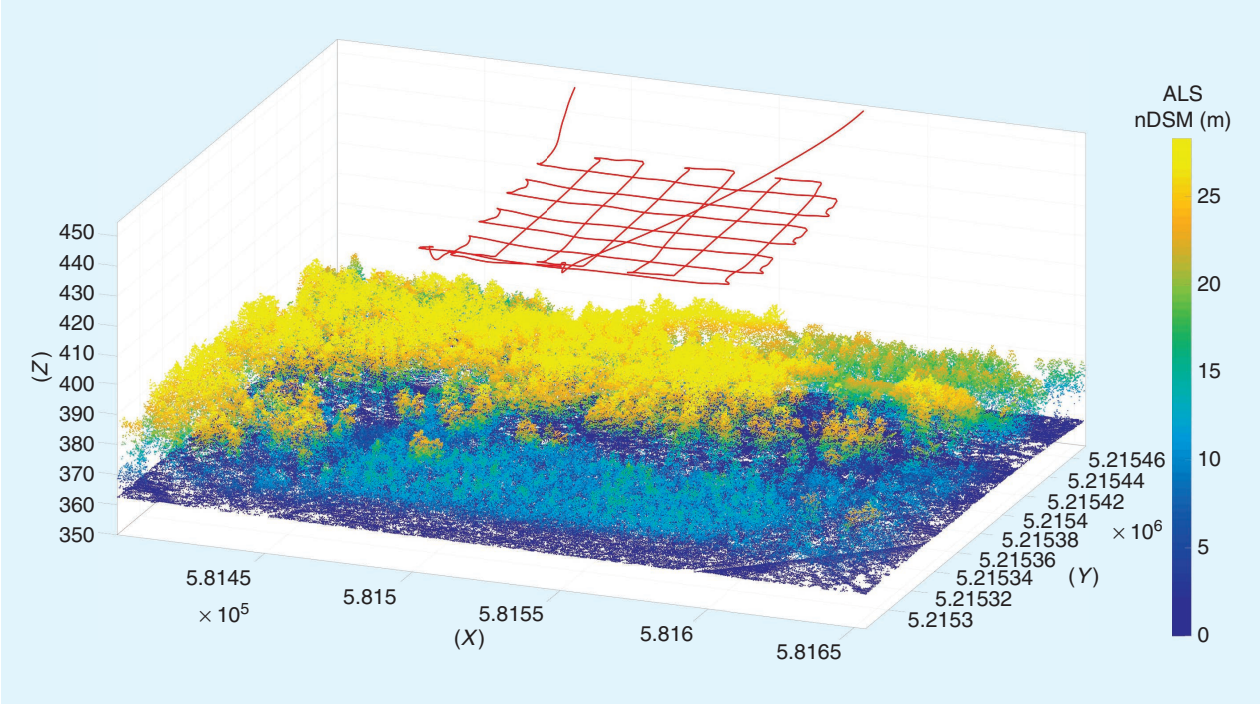

FIGURE 6. A 3D view of a ULS campaign's flight paths. An ALS point cloud is shown in the background, colored with the normalized canopy heights. nDSM: normalized digital surface model.

calculation. Complicated flying patterns with curves and rotations may or may not have a negative impact on the final data, depending on the IMU accuracy. The design of the flight pattern is mainly linked to particular applications. The authors of [175] evaluated acquisition characteristics for stem parameter estimation and found that as long as half of a stem is covered with points, neither the data density nor the completeness across the stem has significant influences. This finding indicated that sparse flight lines are enough for capturing stems.

One particularly important issue that must be considered in the implementation design is the completeness of a forest in collected ULS data. Complete coverage of an individual tree from the stump to the top can be achieved if the viewing geometry is ideal, but in most cases, it is challenging. UAV platforms suffer from occlusion effects that are similar to those of terrestrial systems. While mainly induced by bushes, small trees, and lower parts of trees in terrestrial point clouds, occlusion effects in ULS point clouds are primarily caused by the upper parts of canopies, as shown in Figure 7. Leaf-off season mitigates occlusion in deciduous forests but cannot solve the problem in coniferous ones [147].

In addition, occlusion effects become significant when a large scan angle and small overlap rate between scan lines are selected, e.g., to cover the area of interest in a short time and when budgets are small. Thus, objects near the ground, e.g., the lower part of a tree stem, may be fully, partially, or barely recorded in ULS data, due to occlusion from canopies and nearby trees, depending on the scanning geometry, species, and forest stand conditions. ULS data showed a steady declining trend in the completeness of stem mapping when stand conditions became more complicated [147]. Forest digitization is still limited, especially in complex conditions.

MULTISPECTRAL IMAGERY

UAV image-based techniques have attracted increasing interest in recent years [154], [178]–[180] and have become a preferred option for high-quality aerial mapping in local areas. MS cameras have proliferated because of their lower prices and fewer barriers to the process.

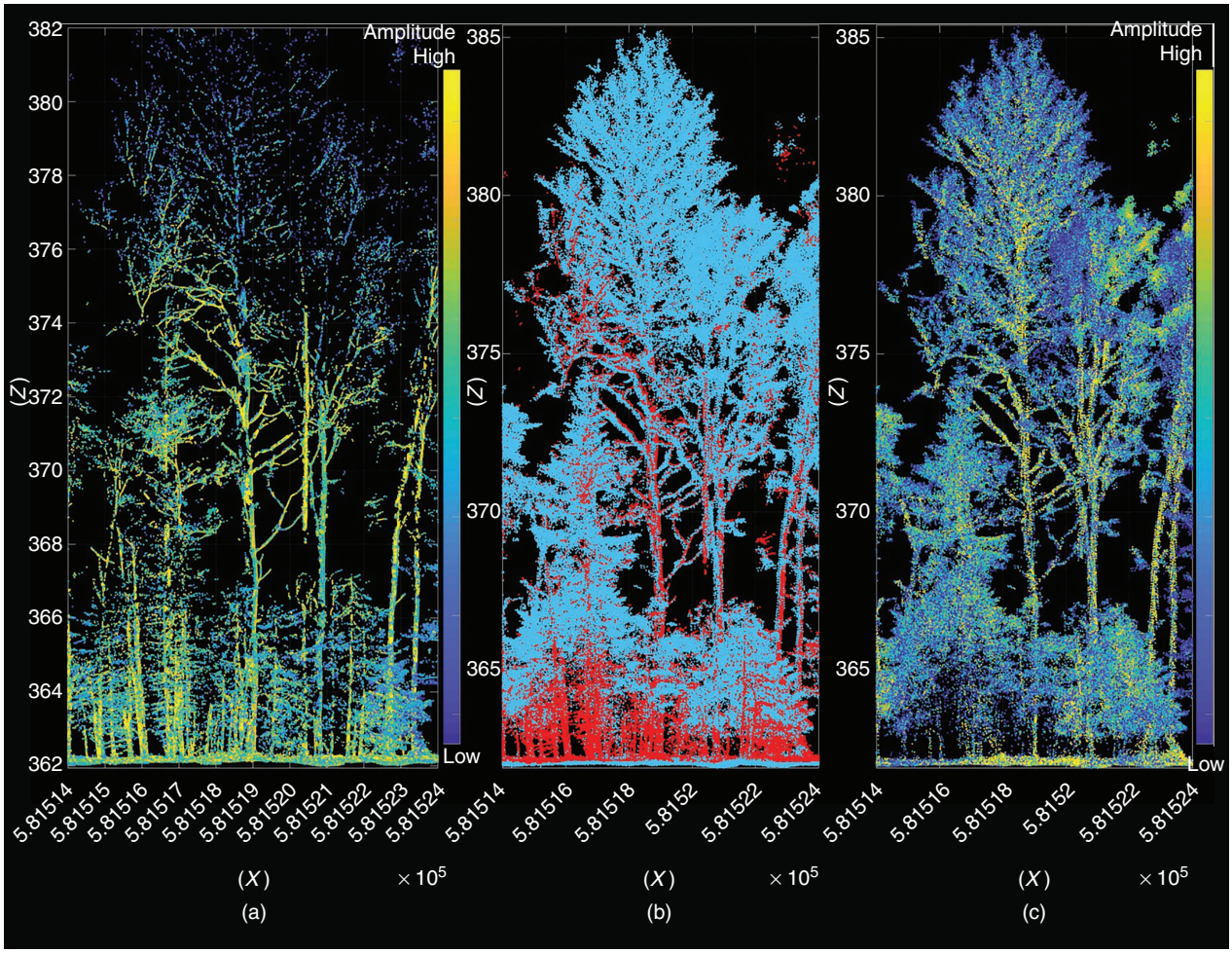

FIGURE 7. The difference between TLS and ULS point clouds. (a) The TLS points colored with the amplitude. (b) The TLS (red) and ULS (blue) points. (c) The ULS points colored with the amplitude values. The TLS data were obtained using a Riegl VZ-2000, and the ULS data were acquired with a Riegl RiCopter and Riegl VUX-1LR scanner.

SENSORS

MS cameras acquire spectral responses of subjects within specific wavelength ranges (typically 3–10 nm) optimized to certain spectral regions, e.g., up to 15 bands, typically in the wavelength range from ultraviolet to near-infrared spectra, such as blue, green, red, red edge, and near infrared. Each distinct band is commonly sensed with a separate sensor and optical system, and MS information is captured through a few registered and synchronized cameras. Examples of popular MS sensors include the Sequoia, MiniMCA6, and RedEdge/Altum. Consumer-grade RGB sensors and modified color infrared sensors can also collect spectral data and are the most common UAV onboard sensors. However, such systems often come with wider and less optimized spectral bands.

Modern digital cameras are mostly equipped with CMOS and charge-coupled device (CCD) sensors. Most consumer-grade cameras use CMOS sensors, and CCD types are used in medium- and large-format aerial cameras. CMOS sensors have a lower manufacturing cost, power consumption, and readout time, while their drawback is a rolling shutter effect when cameras and scenes are in motion. The rolling shutter effecting can be modeled [181], [182] and mitigated if a global shutter CMOS sensor is used. CCD sensors have a higher dynamic range and low noise, with the drawback of high power consumption and a slow readout time.

TIR cameras provide scene temperatures by detecting emitted, reflected, and transmitted TIR energy. They are significantly more expensive than MS cameras, due to construction complexity, i.e., the need for special lens material. Cooled and uncooled TIR cameras are used. Uncooled cameras are cheaper, lighter, and less power hungry than cooled ones. Cooled cameras provide superior data quality and resolution, but they are unsuitable for common UAV platforms due to their weight and size. Interest in TIR cameras on UAVs can be seen in recent studies [159], [183], [184]. Sensor optical systems simultaneously influence images' geometric and radiometric properties. Therefore, they need to be modeled through bundle adjustment and laboratory calibration.

DATA ACQUISITION

The data acquisition parameters in UAV imagery applications are a tradeoff between quality, e.g., the detail and precision of reconstructions, and efficiency, e.g., flight and image processing time. A series of operational issues are optimized and compromised to achieve satisfying results, including sensor parameters, e.g., the pixel resolution, FOV, shutter speed, ISO, aperture, frame rate, and storage write speed, and flight parameters, e.g., the altitude, speed, and overlap in flight and side directions. These parameters affect the GSD and number of required images per area, which are key parameters to achieve the best reconstruction quality without decreasing efficiency [185].

Factors linked to high-quality UAV images have been discussed in the geoscience context [186]. Despite great interest in applying UAV image-based techniques in forests, the best data acquisition protocol has been discussed in only a few studies [185], [187]–[189], e.g., the altitude, overlap, and GSD. Nevertheless, the studies all concluded that flight line direction overlaps and GSD and their relation play a central role in point cloud reconstruction over forests. As expected, more flight line direction overlap is favorable, while a very fine GSD can introduce noise due to small wind-induced movements and gaps when there is insufficient overlap. MS cameras are often georeferenced, utilizing structure-from-motion (SfM)-based solutions and multisensory calibration [190]. Additional discussion is provided in the "Image-Based Point Clouds" section.

Uncontrollable external influences, e.g., illumination and wind, may pose significant challenges for data acquisition and processing. Reports on the impact of external factors have been mixed. Wind and illumination variation influences on canopy metric calculation were reported as negligible in [187]. More studies recommend avoiding image acquisition during windy weather [188]. Repetitive patterns from aerial images [191] and moving branches [185], [192] were reported to hinder feature and dense matching processes. Thorough radiometric equalization in the case of variable illumination is also recommended [193], [194]. For TIR cameras, environmental properties, such as humidity, distance, and attitude relative to the scene, and other sources of reflected TIR radiation should be considered in the data acquisition design.

HYPERSPECTRAL IMAGERY

HS sensors aim at reconstructing the object reflectance spectrum by using multiple, e.g., more than 20, narrow spectral bands of less than 10 nm of the full width of the half maximum (FWHM). HS sensors are expected to improve the automation potential and sensitivity of object analysis. The concepts of UAV MS and HS imageries, i.e., the spectra over leaves when using UAV MS and HS sensors, are illustrated in Figure 8. Yet, HS sensors have been relatively less frequently used because they are quite expensive and challenging to operate, especially in forested environments.

SENSORS

HS sensors differ based on the arrangement, range, and number and widths of bands as well as the mechanism to achieve spatial and spectral discrimination [180]. According to the operating principle and the resulting data type, sensors can be grouped into point, line, and area technologies. Imaging spectrometers based online and area sensors provide spatially continuous spectral images, whereas point spectrometers provide spectral data at the distinct projected footprint of the sensor.

Line array-based push broom scanning is the most common technical implementation of HS cameras. This type of sensor captures an object line by line, resulting in carpet-type images. State-of-the-art, commercially available push broom cameras include those operated in the visible and near-infrared range (400–1,000 nm, with an approximately

2–6-nm FWHM), e.g., the Mjolnir V, micro/nano-hyperspec, AFX10, and Resonon Pika, and those operated in the short-wave infrared range (SWIR), at 900–2,500 nm, with a roughly 5–10-nm FWHM, e.g., OCIF SWIR, Mjolnir S, and AFX17. The first studies with miniaturized UAV-based HS push broom scanners can be found in [195]–[198], and more were recently presented, e.g., [199] and [200].

Examples of area-based sensors include the HSI, which operates on the time sequential spectral scanning principle; filter-on-chip sensors, e.g., Focus cameras that have Imec snapshot mosaics with a 4×4 pixel pattern (470–620 nm, with a 15-nm FWHM) and a 4×4 pixel pattern (600–975 nm, with a 15-nm FWHM); and the light field with a variable bandpass filter ULTIRS 20. Area-based imagers can capture stereoscopic images, enabling HS 3D reconstruction of objects [201], [202]. There has been interests in point spectrometers because of their ability to capture spectral data at a very high spectral resolution, which enables, for example, studies of sun-induced fluorescence [203].

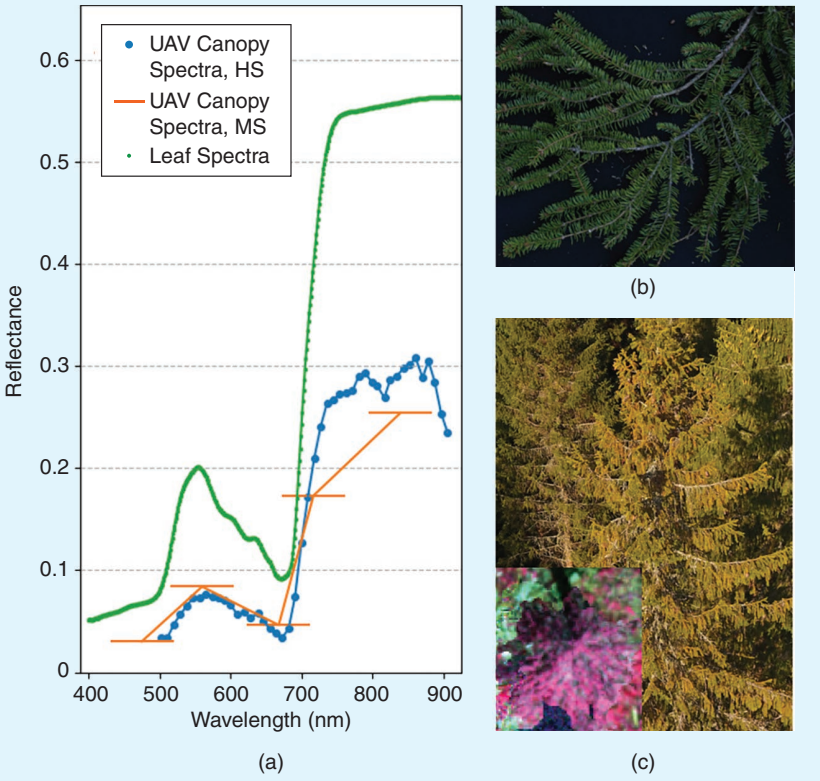

FIGURE 8. The concept of UAV MS and HS imageries over tree canopies. (a) The spectra over leaves and the hyperspectral and multispectral responses using UAV sensors. (b) and (c) Examples of leaves in imageries at different scales and at different times.

DATA ACQUISITION

UAV HS sensors have data acquisition concerns similar to MS camera systems. In particular, they require careful calibration and georeferencing to acquire object spectral responses. HS cameras are typically calibrated and characterized in a laboratory to determine lens fall-off corrections, temperature effects, absolute radiometric calibration coefficients, and the spectral response [180], [204]. The essential steps in the calibration process include corrections based on sensor calibration, compensation of illumination-related effects, atmospheric correction, object anisotropy correction, so-called bidirectional reflectance distribution (BRDF) correction, and topography correction [180].

Solutions for atmospheric correction are mostly empirical line-based calibration methods. In these, two or more panels with a known reflectance are installed in the area of interest. A linear transformation is estimated between the image gray values and object reflectance of the panels. Direct calibration technologies utilize onboard irradiance observations to transform image radiances to reflectance [205], [206]. The advantage is that reflectance targets are not needed on the ground, which is particularly useful in forested environments, where suitable places for installing panels might not exist. Furthermore, irradiance sensors provide valuable information about changes in illumination when data sets are captured under varying conditions [180], [201].

Alternative and supplementary solutions for radiometric calibration are software based for atmospheric correction. These can be based on estimating irradiance by using atmospheric radiative transfer models [180], [195]. When utilizing blocks of images, it is also possible to develop block adjustment-based approaches for radiometric correction. These techniques determine correction functions, for example, utilizing radiometric tie points in overlapping image areas, reflectance panels, and irradiance observations, depending on availability. BRDF modeling can be integrated into the process. These methods are thus capable of producing radiometrically homogeneous sets of images, optimally adjusting external irradiance data and image block data to compensate for varying illumination conditions [207].

The georeferencing solution depends on the sensor type. 2D spectral images can be georeferenced utilizing well-established SfM techniques (see the "Image-Based Point Clouds" and "Platforms" sections). These methods work for sensors based on mosaic filters, e.g., Cubert cameras. In the case of time sequential HS scanning, such as the Senop HSI, precise georeferencing of the nonaligned spectral bands can be carried out by using 3D band matching procedures [208] or implementing a suitable dynamic sensor model in bundle block adjustment [209], [210].

The most common HS imagers are push broom scanners that are highly sensitive to flight dynamics. Their georeferencing is based on either precise GNSS/IMU systems [180], [197] or utilizing an integrated approach founded on a lower-quality GNSS/IMU and 2D camera [196], [198]. Push broom scanners can also be integrated with lidar to enable accurate georeferencing [199]. Point spectrometers are the most challenging to georeference. The location and size/shape of the spectral footprint of each measured spectra are different and determined by the position, orientation, FOV, integration time of the spectroradiometer, flying height and speed of the UAV, and surface topography [203].

RADAR

UAV radar is being developed based on low-cost, small, lightweight, and low-power sensors, and it is expected to be used for close-range Earth observations with high revisit frequencies and immediate responses. Research into UAV radar is focused on system development [211]. Fitting all the necessary equipment into lightweight, commercial UAVs with relatively small payloads is a challenge since radar systems are typically power and space demanding. Few works have been targeted at tree and forest applications.

SENSORS AND PLATFORMS

Radar operates in the microwave wavelength to measure ranges. It observes target areas during day and night, under a wide range of weather conditions, and with wide swaths and long ranges. It operates on different wavelengths. Short wavelengths, e.g., the C and X bands, measure solid targets, e.g., buildings, at high accuracy. Longer wavelengths, such as the P and L bands, are useful when vegetation is present. Low-frequency ultrawideband (UWB) millimeter radar has good penetration capacity and offers potential for imaging building interiors. Previous demonstrations of UAV SAR include the P, L, and C bands [212] for civil and deformation monitoring applications; X band [213] for calculating the scattering characteristics of complex targets; P and C bands for estimating the terrain height of a eucalyptus forest [214]; UWB [215] for snow coverage scanning; and W band [216] to minimize the size and weight of the hardware, among others, and different or full polarization combinations, e.g., horizontal and vertical backscatters.

The onboard sensors typically include transmitting and receiving antennas, a signal generation and recording unit, a navigation system, and a control unit. Frequency-modulated continuous-wave signals are common in current systems. The antennas may be large in comparison to the UAVs, especially for radar systems operating at longer wavelengths, e.g., the L and P bands, which may negatively impact the aircrafts' aerodynamic properties. Rotary-wing platforms suit large antennas better because of their low platform speed. The reported resolutions vary significantly. The resolution was approximately, 1.5 m using the X band [217], 30 cm using the C band [218], and 3 m using the P band [214] in the slant range, and it was 0.5 and 5 m in single and multilook images, respectively, using the P band [214] in the azimuth direction. A planer resolution of better than 2 m obtained using the C and P bands was reported [214].

Rotary-wing UAV platforms have great feasibility for agile maneuvering. However, they have a much less stable flight path in comparison with fixed-wing platforms. Their vibrations can be reduced by using a gimbal but cannot be eliminated. Meanwhile, navigation systems introduce position errors. It has been shown that a low-cost, small IMU was nonviable for UAV positioning [217]. Centimeter-level positioning requires an RTK GNSS and higher-grade IMU. Few studies reported quantitative results with accurate field references.

DATA ACQUISITION

SAR systems combine measurements from different positions along a platform's flight path to form a focused image, given precise relative measurement positions, thus achieving high resolution at a long range without a sizeable physical aperture. UAV flight trajectories significantly impact SAR data quality. Accurate positioning, constant velocity, and stable trajectories are ideal for UAV radar operations. Repeat, single, parallel, and cross-pass flight paths are used in different applications. Instead of one onboard antenna, a pair of physically separated antennas provides low-cost and fast interferometry data acquisition in a single flight. In the multiantenna configurations, each antenna can transmit and receive its own signals, or one transmits a signal while all antennas receive. Flights can be in a vertical directions and circular shapes to derive tomographic information.

Platform instability and positioning errors degrade the quality of UAV SAR data during synthetic aperture time. These disturbances reduce the maximum aperture length and introduce defocusing, especially for large apertures. To compensate for defocusing, 3D motion errors in SAR data need to be modeled and corrected. Interferometric SAR (InSAR) uses a baseline between two antenna positions to derive phase differences, e.g., for topographic mapping. Large baselines result in great sensitivity to variations in height. Interferometric maps were found to be extremely difficult to obtain since perfectly parallel and aligned passes are hard to achieve with UAV platforms [217]. Differential InSAR (DInSAR) uses two interferometric data streams from different passes separated by a short baseline for deformation measurements. Platform instability and positioning errors similarly hinder DInSAR accuracy. Tomographic SAR can obtain volume information about scatters, e.g., for vegetated areas and ground topography estimations. Due to air turbulence, it is typically challenging to derive vertical, evenly allocated baselines in fixed-wing UAVs. In multirotor UAVs, vertical flight was found to be stable, and the trajectory did not suffer from important deviations from the normal track [217].

Depending on the application, side and downward measurements are used. Side-looking measurements typically cover relatively large areas. Downward measurements can be used to generate terrain and vegetation

profiles. The penetration rate of UAV radar is limited at this moment. It was found that street tree canopies and bare ground can be observed in the downward-looking UAV radar range profile [219].

PERFORMANCE

Point cloud data collected in ULS and MS imageries over the same plot and tree are provided in Figure 9. The ULS data were collected on 26 April 2019 during a leaf-on condition. A low-cost laser sensor, i.e., a Nano M8, was used, with ±50° off-nadir scan angles, a 420-Hz pulse rate, and a 20-Hz frame rate. The flight was 70 m above the ground, the speed was 5 m/s, and the side overlap was 75%. The average point density was 285 points/m^2. The UAV imagery data were collected on 26 April 2019 and 19 March 2020, representing the leaf-off and leaf-on seasons. The leaf-off data were gathered using a Sony Alpha 7RII camera with a 24-mm lens. The flight height was 120 m, and the GSD was 2.2 cm. The point cloud was generated with half-resolution images, resulting in 913 points/m^2. The leaf-on data were assembled using a Sony A6000 camera with an 18-mm lens. The flight altitude was 120 m, and the GSDs were 2.5 cm at ground level and 2 cm at the top canopy height of 33 m. The point cloud was generated with half-resolution images, resulting in 1,095.86 points/m^2. In general, ULS has a better chance to record the forest vertical structure. UAV imagery data nicely record the canopy surface structure in the leaf-on season and the ground in the leaf-off season if it is visible. If the camera is oriented in the nadir direction or the GSD is large, UAV imagery is probably not

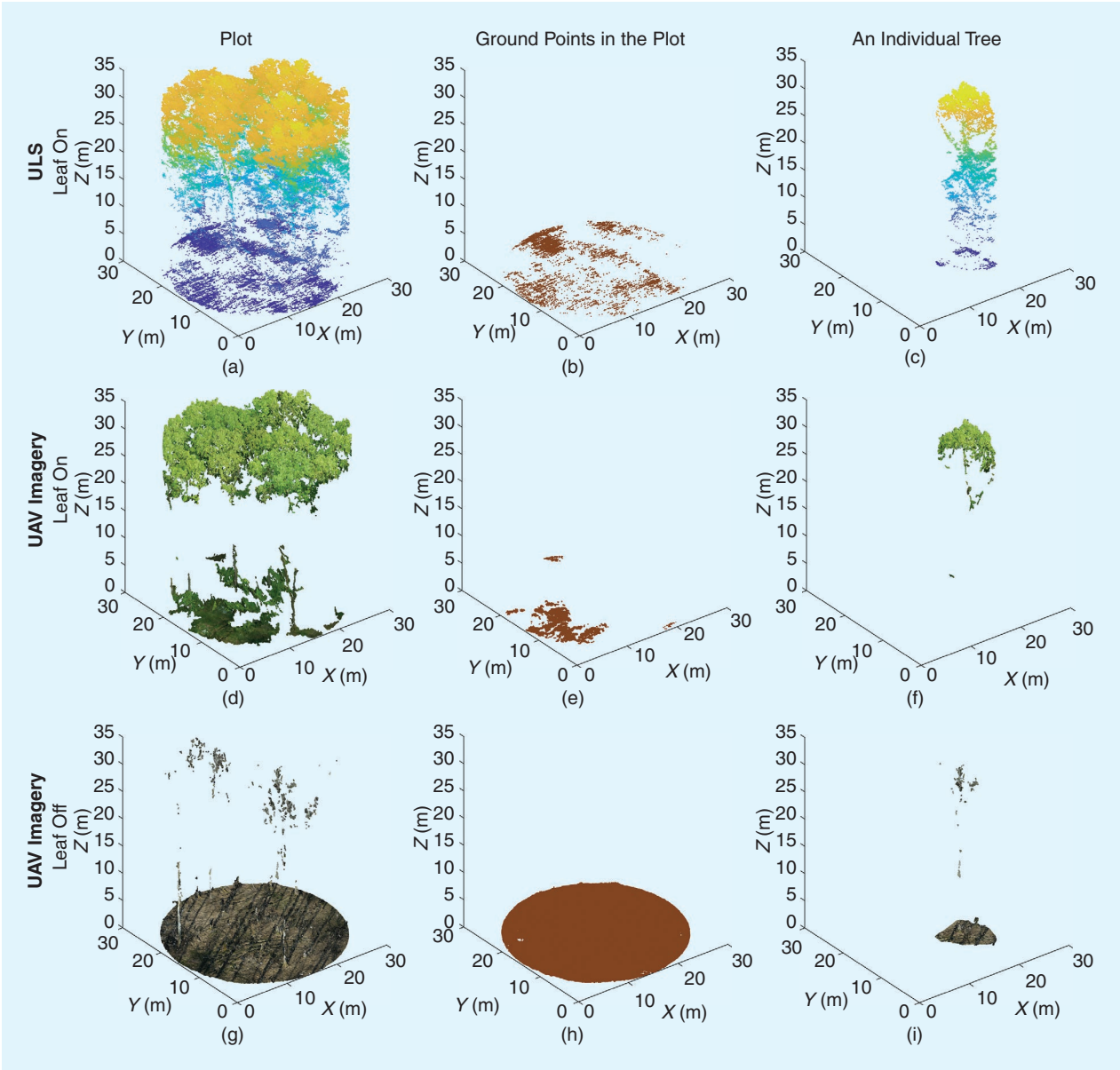

FIGURE 9. The same plot and tree in ULS and UAV imagery point clouds. (a)–(c) The ULS data in the leaf-on season. (d)–(f) The UAV imagery point clouds in the leaf-on season. (h)–(j) The UAV imagery point clouds in the leaf-off season.

suitable for studying undercanopy individual trees, as there is too little information in the generated point cloud.

Benchmarking studies recently reported some surprising findings and updated our understanding of forest observations through close-range remote sensing. Tree height observations from a conventional field inventory, TLS, and ULS in a boreal forest were compared [24]. The test was based on 1,174 trees from 18 plots (32×32 m) with four crown classes and three plot complexity categories. The terrestrial and ULS data were from high-end professional systems. In general, the ULS tree height estimates were shown to be robust across all stand conditions. Due to the difficulty of identifying treetops, the highest uncertainty in the ULS-based tree heights was from trees in the intermediate crown class. The conventional field measurement overestimated the heights of tall trees, especially in the codominant crown class. High uncertainties also existed in the field-measured heights for small trees in the intermediate and suppressed crown classes in dense stands. TLS is reliable for measuring trees shorter than 15–20 m.

In another work, the reliability of conventional tree height estimates in a managed, even-aged, deciduous, lowland forest was studied [25]. Tree height observations from a conventional field inventory and three low-cost, close-range remote sensing solutions, i.e., PLS_{hh}, UAV imagery, and ULS, were compared based on the observation of 130 trees. Tree height estimates were analyzed with respect to the crown class, tree height, sensor, and tree species. Field measurements were more sensitive to the crown class than the tree height, whereas remote sensing data sets displayed robustness to crown classes. Field measurements were found to underestimate the tree height for trees taller than 21 m. Tree species become an influential factor on the tree height only when they change tree geometry and tree and crown structure. On the other hand, a low-cost sensor may not have enough penetration ability, which causes missed treetops beneath the main vegetation layer.

The authors of [47] compared the accuracy of tree height estimation from a low-cost ULS, UAV/airborne/gyrocopter imagery, and conventional Vertex measurement, using 15 felled trees in six 50-year-old Douglas fir plots. The ULS data had a 1,690- and 2,118-points/m^2 point density in 2017 and 2018, respectively. ULS achieved the most accurate tree height estimates (RMSE = 0.36 m; RMSE percentage = 1.05%) and lowest bias (the mean error was 0.13 m), especially compared to the vertex observations (RMSE = 1.02 m; mean error = −0.66 m).

In [147], the authors compared the performance of ULS with conventional field observations and two terrestrial methods: TLS and MLS/PLS. The test was carried out in 22 plots with three forest complexity categories. Manual measurement from the ULS point cloud was also performed to detect trees and measure the DBH and tree height as a reference. Forest and tree attributes, i.e., the tree positions, DBH, tree height, stem volume, stem curve, and total tree biomass, were benchmarked among ULS, TLS, and MLS/PLS using the same automatic processing method. The RMSE percentage of the DBH, tree height, stem curve, biomass, and total tree volume across three densities when the automatic method was used were 16–28, 9–27, 28–55, 60–220, and 35–175%, respectively. The highest accuracy was achieved within the least stem-dense plots, and it was the lowest within the densest plots.

When manual measurement was used, the accuracy of DBH estimates from ULS was comparable to MLS (RMSE percentage of 15–30%) but twice as much as the RMSE percentage of TLS. At the same time, tree height estimates had higher accuracy than MLS and TLS, especially for medium- and high-density plots. ULS was previously assumed to have higher accuracy in stem curve estimates in comparison with terrestrial-based technologies, especially for upper parts of trunks, due to the above-canopy perspective. On the contrary, the accuracy was modest due to the lack of points from the middle section of trunks, which led to less accurate stem curve estimations. The ULS-based PHC stem curve estimate was, in general, higher than that of MLS but lower than that of TLS.

DISCUSSION AND OUTLOOK

Field observation is an inevitable part of forest investigations. Conventional field inventories are labor-intensive, time-consuming, and expensive. They are limited to small areas and have a low temporal resolution. Small sample sizes may lack representatives. Thus, errors in field observations propagate to a large area through airborne and satellite remote sensing. Foresters and researchers are constantly looking for efficient solutions for acquiring reliable forest attributes and conditions.

Significant attention has been paid to close-range remote sensing solutions in recent decades. Research and progress demonstrated promising potential, brought new knowledge and possibilities, and raised questions that need to be answered before close-range remote sensing can be practically applied. Meanwhile, developments also challenge knowledge about the applicability, performance, and potential of existing methods for forest observations. This section discusses the challenges that close-range remote sensing faces, especially data quality, which directly impacts the performance of forest attribute estimation. Trends and opportunities for applying close-range remote sensing in forest observations are further explored.

CHALLENGES

The quality of the input data, e.g., the completeness and accuracy, fundamentally determines the quantity and reliability of the information that can be derived. Sophisticated processing methods can calibrate, compensate, and correct errors and inaccuracies inherent in raw data, but they introduce additional uncertainties and can barely increase the amount of information recorded in the raw data. On the other hand, the data collection protocol impacts hardware performance and data quality. A fundamental problem

is how to collect data that meet the needs of particular applications.

COMPLETENESS AND ACCURACY

The completeness of recorded data refers to the degree to which all the necessary information is recorded. It may be close to but mostly never reaches 100%. The completeness of forest remote sensing data is overwhelmingly low due to the high level of forest complexity, restricted performance of the applied sensors and protocols, and practical limitations in data acquisition. In a recent benchmarking study between high-quality UAV and terrestrial point clouds, it was found that, on a plot-level (a fixed size of 32×32 m), 96.7, 92.7, and 75.3% of individual trees could be recorded in easy (~700 stems/hectare), medium (~900 stems/hectare), and difficult boreal stands (~2, 200 stems/hectare), respectively, when using five-scan TLS. The individual trees recorded by ULS were 87.2, 69.1, and 55.3%, respectively, in the corresponding plots. Notably, 25–50% of trees in difficult stands were not sufficiently recorded in UAV and terrestrial laser data [16].

Geometric inconsistencies are ubiquitous due to wind, measurement inaccuracy, and registration errors [147]. Wind changes the topography of trees and forests. Such changes can hardly be eliminated, especially when time lags exist between consecutive observations, such as in the scanning-based mechanism. Winds introduce ghost objects, where identical items are recorded at different spatial locations in data from different viewpoints and at varying points of time [80], [220]. A common recommendation is to collect data in windless conditions, which, however, reduces the number of possible measurement days. The impacts of wind on tree attribute estimations have not been sufficiently investigated.

Sensor specifications determine measurement accuracy. In laser-based systems, the magnitude of the beam divergence and range measurement accuracy directly govern the reliability of point measurements. Contemporary commercial laser sensors typically have less than 1 mrad of beam divergence and a few millimeters of range accuracy at 20 m. The angular resolution, PRF, and FOV regulate the sampling space between points within and between scan lines, which determines the ability to identify small targets and penetrate forest canopies. In image-based systems, influence factors include the pixel size and dynamic range of the image sensor, distortion of the image sensor and lens, and width of the spectral band. The accuracy of the equipment itself has significant influences on data accuracy. Namely, a high-end sensor typically has greater accuracy [175].

It is worth noting that high-end and low-cost sensors can produce data sets with very different qualities. For example, low-cost laser sensors typically have large beam divergence and low ranging accuracy, e.g., 3–5 mrad and 1–3 cm in PLS_{hh} systems, which may limit their applications to a few cases that do not require high accuracy. Low-cost sensors usually cannot resolve multiple echoes from a transmitted signal, which is often an element in high-end scanners to delineate canopy properties, such as branch structure.

The data acquisition protocol influences the data quality when the same sensors and sensor parameters are applied. In static terrestrial systems, the acquisition parameters are mainly the observations' number, positions, and viewing geometries. In mobile systems, they include the trajectory and platform speed. Higher platform speeds increase the point spacing in scanning systems and decrease the overlap rate in imaging systems. A high overlap rate between trajectories and consequent observations increases the point density, leading to better canopy penetration, though not guaranteed. When the hardware and data acquisition protocols are comparable, geometric accuracies vary among systems. In general, static and laser-based systems have higher geometric accuracies in comparison with mobile, aerial, and image-based counterparts.

TLS has the highest geometry accuracy among all systems at the plot level. Its high-quality data well suit applications requiring accurate observations [222]–[224] that can be used to develop and calibrate algometric models [225]–[227]. Mobile and imagery systems are comparable with TLS in easy forest conditions [147]. All mobile systems in the air and on the ground face the same challenge of accurate registration between trajectories [111], [147]. Even though aerial systems suffer less from positioning errors, dynamic errors are not at a neglectable level [147]. Image matching has become mature. The remaining challenge is the dense vegetation near the forest floor, which may introduce significant changes between consequent images and fail the matching process.

It is also worth remarking that hardware performance continuously improves. Sensor evolution has triggered profound changes and is expected to push the research and application frontier forward. The improvement process can be seen in data quality changes. Challenges associated with the low completeness and low accuracy of data, which seem hard to solve, may become much less severe and even disappear in only a few years. For example, early generations of PLS_{hh} suffered from an insufficient measurement range, e.g., around 20 m, and caused bias in tree height estimates [116]. A recent PLS_{hh} instrument (the ZEB Horizon) integrates an improved ranging sensor that has a measurement range up to 100 m. It has been shown to reliably measure the height of deciduous trees [25]. It can be anticipated that further mobile system development will be directed to hardware improvement and the integration of different sensors (e.g., IMUs, lidars, cameras, and the GNSS), leading to enhanced efficiency and applicability.

DATA ACQUISITION PROTOCOL

The data acquisition design directly impacts point cloud quality, which has often been neglected. The terrestrial image-based point cloud has one of the most complicated data acquisition procedures among different data sources. Image acquisition is the most crucial part of the whole process

chain. However, it can fail in many ways. A single mismatch between two images may partially or entirely undermine plot-wise data acquisition. Many factors influence the accuracy of the final point clouds. Yet, these influences have not been analyzed, and knowledge of their impacts is missing. Two fundamental challenges in this area are 1) to improve the stability of image matching through sensor integration, data acquisition methods, and matching algorithms, to name a few, and 2) establish a user-friendly protocol for data acquisition, which will be successful in most cases and easy to follow for foresters who have little professional knowledge of image processing and data acquisition. A few studies of the measuring protocol exist, e.g., [95] and [99], but far from enough.

In the future, researchers are encouraged to report data acquisition in more detail, especially cases where the generation of image-based point clouds failed, to help the community learn from mistakes. Examples can be seen in studies, e.g., [99], where image matching from combined inside/outside paths partly failed; [90], where six out of 25 plots were successful; and [98], where three out of seven approaches to data acquisition failed and the tree detection rate varied significantly among the four methods that did work. The same idea applies equally to other static and mobile platforms. The data collection protocol's practical influences have been discussed in only a few studies of TLS (see the "Laser Scanning" section), and they have rarely been investigated for mobile approaches.

REGISTRATION AND RADIOMETRIC CALIBRATION

Geometric inconsistency needs to be solved before thematic information extraction, which applies to all platforms and data sources. The forest environment is heavily disturbed by noise, wind, and occlusion, and it has a limited number of features suitable to be used as matching targets. Forest canopies also heavily disturb positioning signals, which leads to errors in the trajectories of the terrestrial mobile system and, consequently, in the data. Thus, automated registration in forested areas is a challenging task.

For mobile systems, SLAM types of algorithms can eliminate inconsistencies between trajectories [103], [109], [119], [228], [230], [232]. While trajectory correction results are sufficient for navigation purposes, it is unclear what their impacts are on mapping and thematic information extraction. It should be noted that the requirements for navigation and information extraction are at different levels, where the latter typically requires much higher registration accuracy. Current mobile systems provide comparable thematic information extraction results only in easy forest conditions [111].

Compared with terrestrial mobile laser systems, drone-based systems appear to have fewer geometric inconsistencies by overlapping trajectories if measurements from all trajectories are merged since the GNSS IMU solution is more reliable when there are good satellite visibilities above the forest canopy. However, inherent inconsistencies within individual trajectories, i.e., distortion, introduce geometric inconsistencies that are hard to remove [147]. Multiscan TLS faces a similar registration challenge, and solutions are being developed [72]–[75], [233], [235], where the resulting merged point cloud has not reached a similar level of accuracy as the point cloud built by using artificial reference targets and manual registration.

Geometric registration requires more careful studies, especially considering the extensive research on fine-scale objects, such as branches. Notably, registration solutions should be tested in varying forest conditions to evaluate their performance. Methods that work for one test plot are not guaranteed to work in other forest conditions, and thus algorithms suited for specific conditions are needed. The forest sector will see a boom in the application of close-range remote sensing when hardware-independent registration solutions become practical and satisfy the requirements set in forest field inventories. Radiometric calibration is a crucial step in the spectrometer data processing chain to transfer image radiance to reflectance, thus enabling quantitative analyses. In passive imaging, the radiometry is subject to a number of factors resulting from the sensor, illumination, atmosphere, and object. The calibration of active sensors is challenging, and no practical solution is available, as discussed in the "Laser Scanning" section.

OPPORTUNITIES

The landscape of close-range remote sensing and its applications changes rapidly. Challenges exist in improving data quality to faithfully digitize objects and in establishing data acquisition best practices according to sensor/system properties to support information extraction and applications. Meanwhile, hardware and software developments bring new solutions and possibilities. Some difficulties that cannot be solved due to measurement challenges may disappear shortly after new systems are introduced, and knowledge that has widely and long been accepted may be challenged.

MEASURABLE PARAMETERS

While the completeness of the derived information is still limited, especially in complicated forest conditions, the data extracted from close-range remote sensing is reliable [16], [24], [25], [31], [177]. Important tree attributes that were previously not measurable in conventional field inventories have been proved to be practically measurable at high accuracy. This means that close-range remote sensing has the potential to improve operational efficiency and the amount of information derived from field observations.

At the plot level, these newly available attributes include the stem curve, crown shape, tree height, branch position/orientation, and tree count and location, which are measurable in a very limited number of sample plots or not practically measurable in conventional field inventories due to the time-consuming procedure. For example, collecting tree counts and locations is particularly challenging in

young plots with high stem density, e.g., several thousands of stems per hectare. The characterization of young seedling stands by using UAV image-based point clouds and HS imagery was reported in [236]. The authors found that the proposed random forest-based estimation had the potential to replace conventional laborious field inventory methods for reliably characterizing seedling stands, even though the tree density and tree height were underestimated by 7–21%.

Tree height estimations from close-range remote sensing were evaluated using a comparison method without destructive references in boreal and broadleaved forests in [24] and [25], respectively. ULS, TLS, and conventional field measures were evaluated in coniferous forests, whereas ULS, PLS_{hh}, UAV imagery, and conventional field measures were assessed in broadleaved forests. Both studies found that remote sensing methods were more consistent if conventional field measures were not included in the comparison. Errors varied depending on the data source, forest complexity, tree crown class, and forest type.

Individual trees can be modeled in high detail, e.g., at LoD 2 [237] and 3 [238]–[242]. Point clouds collected from terrestrial platforms may have limited spatial coverage of tree structures inside the canopy above the live canopy base, even high-resolution TLS point clouds [80]. Applying more observations, using time-of-flight sensors with multiecho returns, and reducing the distance between a target and the measurement locations are approaches to solve this problem. The associated higher cost, however, requires careful planning.

Tree models with great detail provides a series of useful branch architecture parameters, such as the number of branches, branch diameter, and branch insertion angle, which can be used to establish and update allometric biomass and wood quality equations [80], [237]. These branch architecture parameters have great potential for studies of biophysical processes and metabolic theories in ecology [243] because branch architecture is the dominant factor affecting the size and spatial distribution of tree elements, e.g., leaves; the exchange of matter and energy between a tree and the ambient environment; and the tree photosynthesis process, and so on.

Canopy features and tree height may serve as effective explanatory variables in estimating forest attributes, such as biomass, age, and productivity [16]. ULS data are well suited for studying canopies at a higher LoD than what is presently achievable. The aerial point of view and potential to mitigate occlusion effects caused by tree canopies make ULS a powerful platform to study canopy features, even though its geometric accuracy has not reached a satisfactory level for more detailed stem/branch studies.

Many studies confirmed that a wide range of vegetation indices correlated well with leaf pigments and water statuses, e.g., leaf chlorophyll, nitrogen, carotenoids, leaf water content, sun-induced chlorophyll fluorescence, and so on. Applying MS and RGB cameras to estimate forest structure [244] and biomass [160] has achieved limited success. Both of those studies indicated that MS data did not provide added value in comparison to RGB camera-based data. The authors of [245] studied the biodiversity of boreal forests, and their results showed that HS and photogrammetric data could be used, especially for studying structural diversity. In [246], the authors used RGB, MS, and TIR sensors for the phenotyping of forest genetic trials. They concluded that the combination of spectral indices and canopy temperature accounted for about 60% of the population variability in the stem volume of *Pinus halepensis*. Since these findings are based only on a few specific studies, further research is required to obtain general conclusions.

In general, the door for deriving more tree and forest attributes through close-range remote sensing has been opened. The reliability of the feature estimations largely determines their application potentials. At this moment, challenges exist in deriving critical tree and forest attributes as well as in the application of such techniques in different forest conditions. One example is the applicability of the latest technologies in tropical areas. Since the top canopy of all the trees is merged, the fundamental processing of geometrically locating and reconstructing individual trees from ULS becomes more difficult than in boreal areas. Further research needs to answer questions about proper sensors and data acquisition protocols for challenging tropical conditions.

HARDWARE AND SOFTWARE

Hardware and software development supports the advance of close-range remote sensing for forests. Among the advances in hardware, the capacity for capturing MS information from active sensors has been one of the most significant developments in the past decade, which is expected to solve many challenges that cannot be addressed using spatial features only. Currently, the utilization of MS–LS is still at a very early stage in forest research. Before MS–LS can be practically used, a number of challenges have to be resolved. One is to decide the best wavelengths and their number and the required special resolution for particular applications. Technically, fewer wavelengths make instrument design more straightforward, and it becomes more feasible to produce high-quality point clouds in terms of the spatial resolution, point collection frequency, and scanning range. A higher number of wavelengths requires specific consideration in the optic design and compromises the point cloud quality. Therefore, sensor properties should be carefully designed depending on use cases.

The second challenge is the lack of applicable calibration solutions, especially for the incidence angle and range effect. Methods have been developed for correcting the incidence angle and range effect on lidar intensity. The lidar equation was found to be available for distance correction under the premise that the target–sensor distance was greater than 10–15 m for the FARO LS880 and Leica HDS 6100 scanners since both instruments were equipped with a brightness reducer for near distances. The most effective method for near distance correction was applying a reference table.

For incidence angle correction, an empirical function was developed [137]. However, the relationship between range and intensity changes when the target is smaller than the laser footprint since some of the reflected laser intensity is lost due to multiple scattering [176]. A priori information about the illuminated footprint is required unless it could be assumed that the target width and density can be approximated from other properties, such as tree forms and environmental conditions. However, the stability of intensity features with varied scanner–target distances and incident angles need to be examined.

Studies of the intensity responses of the stems and canopies of various tree species should be conducted to take advantage of the increasing availability of MS active sensors and to take a step toward automated methods for the collection of field data. Perfectly collimated laser beams with the same beam diameter at the output and beam divergence could solve the challenges of varying intensity–distance relationships with small targets. When the amount of multiple scattering is similar for each wavelength, a normalized index of the wavelengths should remain stable, although the distance will vary. Rigorous calibration models should also be developed for all shapes and forms of trees.

Applications of HS systems in the field are very limited at this moment. Safety issues are the main concern that arises from the utilization of a supercontinuum laser source, due to the high power of the laser, which causes immediate damage to the eye when exposed. The eye safety issue should be tackled before commercial manufacturers are interested in bringing HS and LS to the market. The weight, e.g., 15 kg, also limits field operability, especially in rugged terrain, whereas single-wavelength commercial TLSs weigh 5 kg or less. In addition, the generally larger beam divergences in HS TLS systems compared to single-wavelength systems result in wider laser footprints that may cause errors at longer distances, due to edge effects from targets. In addition to hardware development in controlled environments, more research should be done in the field to provide practical instructions for using MS and HS LS. The advantages of the additional spectral information provided by an HS system need to be jointly considered with economic feasibility.

The development of data science has significantly pushed forward the development of close-range remote sensing. The most impressive progress is probably the dense matching that achieved a breakthrough in the early 2000s and today is been routinely used in various terrestrial and aerial imagery observations through commercial software. Yet, there are still many unsolved challenges that require new algorithms and software. Geometrical inconsistency in the data is currently the most significant limiting factor for mobile applications. As long as geometrical inconsistency exists, mobile mapping is suitable for a few applications that require less accurate data. The robustness of the algorithms in deriving forest and tree attributes in complicated forest conditions is always at center stage and is the critical factor in practical applications.

CROWDSOURCING

The popularity and success of crowdsourcing data acquisition have their roots in low-cost sensors, massive data storage, convenient communications, and active volunteer participation. Commonly, crowdsourcing refers to data acquisition by volunteers who are not trained in particular disciplines, under a condition without a clear goal. It reverses the traditional top-down flow of information, in which data are acquired after setting a clear goal [221]. With the popularity and simple operation of personal data collection devices, such as smartphones and cameras, ordinary citizens can collect large data sets anywhere and anytime. Currently, such consumer-level devices have achieved measurement accuracy comparable to professional instruments, which ensures the availability of crowdsourcing data [99]. Thus, forest data can be collected via crowdsourcing by any people who visit forests regularly or irregularly and centralized processing. Crowdsourced forest data have been used to calculate plot-level and individual tree-level attributes.

Many applications that use smartphone images to measure plot- and individual tree-level attributes are being tested. NASA released a smartphone tool in 2019 as part of its Global Learning and Observations to Benefit the Environment Observer program. The app enables a smartphone user to record tree heights by using only a smartphone camera. The idea is to compare crowdsourced tree height estimates with satellite-based estimates and help understand how carbon moves through ecosystems. The app does not require the exact distance measured with a laser ranging device. Instead, it requests users to roughly measure the distance from the photo-taking location to a tree by counting steps from one to the other to obtain scale information.

Trestima is an app that measures a species-specific basal area as well as the diameter and height of a median tree from sample plots. It follows the principles of stand-wise field inventories, where a relascope is used to measure the basal area from multiple locations within each stand [229]. For determining species-specific basal areas, users take several images at different locations with a clear view around a forest stand. The basal area is estimated from individual photos and as an average across several images through three steps: 1) tree detection, 2) species identification, and 3) tree inclusion in the basal area count, following angle count sampling principles. For determining tree diameters and heights, users take images of a few sample trees per species. The measurements are based on the smartphone's camera properties and machine vision, which users can manually edit if necessary. All images are uploaded and stored by the app, including the location and time, and automatically processed. Species-specific results are available in real time in either the smartphone app or a web browser [231].

The feasibility and reliability of those apps are under investigation. The authors of [234] evaluated Trestima by using 2,169 measured trees from sample plots (32×32 m). The study found that all imaging setups with the app included bias in basal area measurements. The biases varied from 11.4 to 18.4% depending on the number and locations of the images taken per sample plot. The RMSEs in the basal area ranged from 19.7 to 29.3%, respectively. Increasing the number of captured images to four per plot only marginally improved the results. The RMSEs of the diameter and height estimates varied from 5.2 to 11.6% and 10 to 13.6%, respectively, depending on the tree species. So far, the reliability of such an app has not been widely evaluated. The acquisition of forest data through crowdsourcing is at a very early stage but deserves more attention. Challenges from data storage, analysis, accumulation, quality checks, and privacy should be further analyzed.

CONCLUSION

This article reviewed the status and progress of close-range remote sensing in forest observations from the system and data acquisition points of view. In general, the system and data acquisition stay at the beginning of the interpretation pipeline, jointly determining the quality of the collected data. Consequently, they have profound influences on the following processing and applications, e.g., the amount, reliability, and applicability of the thematic information extracted.

Among all sensors and platforms, TLS leads the recent fast progress and has the potential to become the next generation's main operational tool in applications requiring high accuracy. Terrestrial image-based point clouds provide a low-cost alternative to TLS, using a wide variety of imaging sensors and covering professional and nonprofessional users. The technology requires the lowest investment and empowers a vast number of potential users, which is appreciated in applications where professional and costly sensors are lacking and when many participants, including citizens, are involved. Terrestrial mobile platforms significantly increase data acquisition efficiency. The GNSS can be used as an informative indicator to measure some physical properties of forests. Personal sensors, handheld or wearable, have the highest mobility among all terrestrial systems. UAVs are free from ground obstacles. Thus, they outperform terrestrial systems in the sense of data collection speed and provide spatial and temporal high-resolution observations.

Although having shown promising results, the preceding solutions still face their challenges. To be practically employed in forest applications, robust registration and calibration solutions are required to solve spatial inconsistency and spectral uncertainties. Data acquisition protocols, preferably user friendly, are currently absent for most systems and are urgently needed to support data collection with high completeness and accuracy. The recent developments bring many new possibilities for forest observations. The number of measurable parameters is increasing and has the potential to solve the problem of lacking reliable forest and tree estimations and open doors to new applications, e.g., allometric model development and calibration. Hardware is under constant improvement and challenges the current knowledge of the applicability, performance, and potentials of existing methods for forest mensuration all the time. A new trend in the data acquisition, i.e., crowdsourcing, together with improved sensor performance and computational power, may have a profound influence on forest observations since crowdsourcing has the potential to vastly increase the number of field observations in spatial and temporal domains and because the bottleneck in calibrating airborne and satellite-borne observation is a lack of field references. This new possibility deserves attention for future research, especially to establish quality control protocols.

Tremendous diversity exists in the reported results, e.g., accuracies and reliabilities, in the literature, due to the varying forest conditions, sensors, and methods involved in individual studies. State of the art and potential close-range remote sensing solutions have only recently been clarified through benchmarking studies. In the future, studies are recommended to be carried out with sufficient test data to provide statistically reliable conclusions, e.g., regarding the amount, variation, and difficulty-level of test data. Similar work carried out in different geographical locations is welcomed to reveal or demonstrate the applicability of results outside of areas in a particular study. The applicability of the proposed methods and reached conclusions in other forest conditions can be far different.

ACKNOWLEDGMENTS

Xinlian Liang and Antero Kukko are the joint first authors. Yunsheng Wang is the corresponding author. The authors would like to acknowledge financial support from the the Natural Science Fund of China (grants 32171789, 32211530031), Wuhan University (grant WHUZZJJ202220), Academy of Finland (grants 334060, 334829, 334830, 344755, 337656, 331708, 327861, 330422, 315079), Ministry of Agriculture of Finland (VN/3482/2021), Operational Programme Research, Development and Education (grant CZ.02.1.01/0.0/0.0/16_019/0000803), Scientific Grant Agency of the Ministry of Education, Science, Research, and Sport of the Slovak Republic and Slovak Academy of Sciences (1/0335/20), and the Croatian Science Foundation, funded by the European Union from the European Social Fund, Young Researchers' Career Development Project—Training of Doctoral Students.

AUTHOR INFORMATION

Xinlian Liang (xinlian.liang@whu.edu.cn) is with the State Key Laboratory of Information Engineering in Surveying, Mapping and Remote Sensing, Wuhan University, 430070 Wuhan, China.

Antero Kukko (antero.kukko@nls.fi) is with the Department of Remote Sensing and Photogrammetry, Finnish

Geospatial Research Institute (National Land Survey of Finland), Masala, 02431, Finland.

Ivan Balenović (ivanb@sumins.hr) is with the Division for Forest Management and Forestry Economics, Croatian Forest Research Institute, Zagreb, 10450, Croatia.

Ninni Saarinen (ninni.saarinen@uef.fi) is with the School of Forest Sciences, University of Eastern Finland, Joensuu, 80101, Finland.

Samuli Junttila (samuli.junttila@uef.fi) is with the School of Forest Sciences, University of Eastern Finland, Joensuu, 80101, Finland.

Ville Kankare (ville.kankare@uef.fi) is with the School of Forest Sciences, University of Eastern Finland, Joensuu, 80101, Finland.

Markus Holopainen (markus.holopainen@helsinki.fi) is with the Department of Forest Sciences, University of Helsinki, Helsinki, 00014, Finland.

Martin Mokroš (mokros@fld.czu.cz) is with the Faculty of Forestry and Wood Sciences, Czech University of Life Sciences Prague, Prague, 16500, Czech Republic.

Peter Surový (surovy@fld.czu.cz) is with the Faculty of Forestry and Wood Sciences, Czech University of Life Sciences Prague, Prague, 16500, Czech Republic.

Harri Kaartinen (harri.kaartinen@nls.fi) is with the Department of Remote Sensing and Photogrammetry, Finnish Geospatial Research Institute (National Land Survey of Finland), Masala, 02431, Finland.

Luka Jurjević (lukaj@sumins.hr) is with the Division for Forest Management and Forestry Economics, Croatian Forest Research Institute, Zagreb, 10450, Croatia.

Eija Honkavaara (eija.honkavaara@nls.fi) is with the Department of Remote Sensing and Photogrammetry, Finnish Geospatial Research Institute (National Land Survey of Finland), Masala, 02431, Finland.

Roope Näsi (roope.nasi@nls.fi) is with the Department of Remote Sensing and Photogrammetry, Finnish Geospatial Research Institute (National Land Survey of Finland), Masala, 02431, Finland.

Jingbin Liu (ljb04@163.com) is with the State Key Laboratory of Information Engineering in Surveying, Mapping and Remote Sensing, Wuhan University, 430070 Wuhan, China.

Markus Hollaus (markus.hollaus@geo.tuwien.ac.at) is with the Department of Geodesy and Geoinformation, TU Wien, Vienna, 1040, Austria.

Jiaojiao Tian (jiaojiao.tian@dlr.de) is with the Remote Sensing Technology Institute, German Aerospace Center, Wessling, 82234, Germany.

Xiaowei Yu (xiaowei.yu@nls.fi) is with the Department of Remote Sensing and Photogrammetry, Finnish Geospatial Research Institute (National Land Survey of Finland), Masala, 02431, Finland.

Jie Pan (panjie_njfu@126.com) is with the College of Forestry, Nanjing Forestry University, Nanjing, 210037, China.

Shangshu Cai (shangshu_cai@whu.edu.cn) is with the State Key Laboratory of Information Engineering in Surveying, Mapping and Remote Sensing, Wuhan University, 430070 Wuhan, China.

Juho-Pekka Virtanen (juho.virtanen@nls.fi) is with the Department of Remote Sensing and Photogrammetry, Finnish Geospatial Research Institute (National Land Survey of Finland), Masala, 02431, Finland.

Yunsheng Wang (yunsheng.wang@nls.fi) is with the Department of Remote Sensing and Photogrammetry, Finnish Geospatial Research Institute (National Land Survey of Finland), Masala, 02431, Finland.

Juha Hyyppä (juha.coelasr@gmail.com) is with the Department of Remote Sensing and Photogrammetry, Finnish Geospatial Research Institute (National Land Survey of Finland), Masala, 02431, Finland.

REFERENCES

[1] B. E. Schutz, H. J. Zwally, C. A. Shuman, D. Hancock, and J. P. DiMarzio, "Overview of the ICESat mission," *Geophys. Res. Lett.*, vol. 32, no. 21, p. L21S01, 2005, doi: 10.1029/2005GL024009.

[2] D. S. Boyd and F. m. Danson, "Satellite remote sensing of forest resources: Three decades of research development," *Prog. Phys. Geography, Earth Environ.*, vol. 29, no. 1, pp. 1–26, Mar. 2005, doi: 10.1191/0309133305pp432ra.

[3] M. A. Wulder, J. G. Masek, W. B. Cohen, T. R. Loveland, and C. E. Woodcock, "Opening the archive: How free data has enabled the science and monitoring promise of Landsat," *Remote Sens. Environ.*, vol. 122, pp. 2–10, Jul. 2012, doi: 10.1016/j.rse.2012.01.010.

[4] R. Torres et al., "GMES Sentinel-1 mission," *Remote Sens. Environ.*, vol. 120, pp. 9–24, May 2012, doi: 10.1016/j.rse.2011.05.028.

[5] M. Drusch et al., "Sentinel-2: ESA's optical high-resolution mission for GMES operational services," *Remote Sens. Environ.*, vol. 120, pp. 25–36, May 2012, doi: 10.1016/j.rse.2011.11.026.

[6] B. Cook et al., "NASA Goddard's LiDAR, hyperspectral and thermal (G-LiHT) airborne imager," *Remote Sens.*, vol. 5, no. 8, pp. 4045–4066, Aug. 2013, doi: 10.3390/rs5084045.

[7] J. Li and D. Roy, "A global analysis of Sentinel-2A, Sentinel-2B and Landsat-8 data revisit intervals and implications for terrestrial monitoring," *Remote Sens.*, vol. 9, no. 9, p. 902, Aug. 2017, doi: 10.3390/rs9090902.

[8] E. Næsset, "Predicting forest stand characteristics with airborne scanning laser using a practical two-stage procedure and field data," *Remote Sens. Environ.*, vol. 80, no. 1, pp. 88–99, Apr. 2002, doi: 10.1016/S0034-4257(01)00290-5.

[9] K. Lim, P. Treitz, m. Wulder, B. St-Onge, and m. Flood, "LiDAR remote sensing of forest structure," *Prog. Phys. Geography, Earth Environ.*, vol. 27, no. 1, pp. 88–106, Mar. 2003, doi: 10.1191/0309133303pp360ra.

[10] E. Næsset et al., "Laser scanning of forest resources: The nordic experience," *Scand. J. Forest Res.*, vol. 19, no. 6, pp. 482–499, Dec. 2004, doi: 10.1080/02827580410019553.

[11] J. C. White, N. C. Coops, m. A. Wulder, m. Vastaranta, T. Hilker, and P. Tompalski, "Remote sensing technologies for enhancing forest inventories: A review," *Can. J. Remote Sens.*, vol. 42, no. 5, pp. 619–641, Sep. 2016, doi: 10.1080/07038992.2016.1207484.

[12] J. Hyyppa and m. Inkinen, "Detecting and estimating attributes for single trees using laser scanner," *Photogrammetric J. Finland*, vol. 16, pp. 27–42, Jan. 1999.

[13] H. Hirschmuller and D. Scharstein, "Evaluation of cost functions for stereo matching," in *Proc. IEEE Conf. Comput. Vision Pattern Recognit.*, Minneapolis, MN, USA, Jun. 2007, pp. 1–8, doi: 10.1109/CVPR.2007.383248.

[14] H. Hirschmuller, "Stereo processing by semiglobal matching and mutual information," *IEEE Trans. Pattern Anal. Mach. Intell.*, vol. 30, no. 2, pp. 328–341, Feb. 2008, doi: 10.1109/TPAMI.2007.1166.

[15] E. Honkavaara et al., "Digital airborne photogrammetry—A new tool for quantitative remote sensing?—A state-of-the-art review on radiometric aspects of digital photogrammetric images," *Remote Sens.*, vol. 1, no. 3, pp. 577–605, Sep. 2009, doi: 10.3390/rs1030577.

[16] Y. Wang et al., "In situ biomass estimation at tree and plot levels: What did data record and what did algorithms derive from terrestrial and aerial point clouds in boreal forest," *Remote Sens. Environ.*, vol. 232, p. 111,309, Oct. 2019, doi: 10.1016/j.rse.2019.111309.

[17] A. van Laar and A. Akça, *Forest Mensuration*. Dordrecht: Springer Netherlands, 2007, vol. 13.

[18] J. A. Kershaw, m. J. Ducey, T. W. Beers, and B. Husch, *Forest Mensuration*. Chichester, U.K.: Wiley, 2016.

[19] K. Stereńczak et al., "Factors influencing the accuracy of ground-based tree-height measurements for major European tree species," *J. Environ. Manage.*, vol. 231, pp. 1284–1292, Feb. 2019, doi: 10.1016/j.jenvman.2018.09.100.

[20] V. Luoma et al., "Assessing precision in conventional field measurements of individual tree attributes," *Forests*, vol. 8, no. 2, p. 38, Feb. 2017, doi: 10.3390/f8020038.

[21] A. Persson, J. Holmgren, and U. Soderman, "Detecting and measuring individual trees using an airborne laser scanner," *Photogrammetric Eng. Remote Sens.*, vol. 68, no. 9, pp. 925–932, 2002.

[22] C. Hopkinson, L. Chasmer, and R. J. Hall, "The uncertainty in conifer plantation growth prediction from multi-temporal lidar datasets," *Remote Sens. Environ.*, vol. 112, no. 3, pp. 1168–1180, Mar. 2008, doi: 10.1016/j.rse.2007.07.020.

[23] J. Hyyppä, H. Hyyppä, D. Leckie, F. Gougeon, X. Yu, and m. Maltamo, "Review of methods of small-footprint airborne laser scanning for extracting forest inventory data in boreal forests," *Int. J. Remote Sens.*, vol. 29, no. 5, pp. 1339–1366, Mar. 2008, doi: 10.1080/01431160701736489.

[24] Y. Wang et al., "Is field-measured tree height as reliable as believed – A comparison study of tree height estimates from field measurement, airborne laser scanning and terrestrial laser scanning in a boreal forest," *ISPRS J. Photogrammetry Remote Sens.*, vol. 147, pp. 132–145, Jan. 2019, doi: 10.1016/j.isprsjprs.2018.11.008.

[25] L. Jurjević, X. Liang, m. Gašparović, and I. Balenović, "Is field-measured tree height as reliable as believed – Part II, a comparison study of tree height estimates from conventional field measurement and low-cost close-range remote sensing in a deciduous forest," *ISPRS J. Photogrammetry Remote Sens.*, vol. 169, pp. 227–241, Nov. 2020, doi: 10.1016/j.isprsjprs.2020.09.014.

[26] R. L. McConnell, K. C. Elliot, S. H. Blizzard, and K. H. Koster, "Electronic measurement of tree-row-volume," in Proc. Nat. Conf. Agricultural Electron. Appl., 1984.

[27] X. Liang et al., "Terrestrial laser scanning in forest inventories," *ISPRS J. Photogrammetry Remote Sens.*, vol. 115, pp. 63–77, May 2016, doi: 10.1016/j.isprsjprs.2016.01.006.

[28] H. Kaartinen et al., "An international comparison of individual tree detection and extraction using airborne laser scanning," *Remote Sens.*, vol. 4, no. 4, pp. 950–974, Mar. 2012, doi: 10.3390/rs4040950.

[29] J. Vauhkonen et al., "Comparative testing of single-tree detection algorithms under different types of forest," *Forestry*, vol. 85, no. 1, pp. 27–40, Jan. 2012, doi: 10.1093/forestry/cpr051.

[30] Y. Wang et al., "International benchmarking of the individual tree detection methods for modeling 3-D canopy structure for silviculture and forest ecology using airborne laser scanning," *IEEE Trans. Geosci. Remote Sens.*, vol. 54, no. 9, pp. 5011–5027, Sep. 2016, doi: 10.1109/TGRS.2016.2543225.

[31] X. Liang et al., "International benchmarking of terrestrial laser scanning approaches for forest inventories," *ISPRS J. Photogrammetry Remote Sens.*, vol. 144, pp. 137–179, Oct. 2018, doi: 10.1016/j.isprsjprs.2018.06.021.

[32] M. Hollaus, m. Mokroš, and Y. Wang, "International benchmarking of terrestrial image-based point clouds for forestry," *Geophys. Res. Abstr.*, vol. 21, p. 1, 2019.

[33] J.-M. Binot, D. Pothier, and J. Lebel, "Comparison of relative accuracy and time requirement between the caliper, the diameter tape and an electronic tree measuring fork," *Forestry Chronicle*, vol. 71, no. 2, pp. 197–200, Apr. 1995, doi: 10.5558/tfc71197-2.

[34] P. Tompalski, N. C. Coops, J. C. White, and m. A. Wulder, "Simulating the impacts of error in species and height upon tree volume derived from airborne laser scanning data," *Forest Ecol. Manage.*, vol. 327, pp. 167–177, Sep. 2014, doi: 10.1016/j.foreco.2014.05.011.

[35] T. R. Feldpausch et al., "Tree height integrated into pantropical forest biomass estimates," *Biogeosciences*, vol. 9, no. 8, pp. 3381–3403, Aug. 2012, doi: 10.5194/bg-9-3381-2012.

[36] E. Kearsley et al., "Conventional tree height–diameter relationships significantly overestimate aboveground carbon stocks in the Central Congo Basin," *Nature Commun.*, vol. 4, no. 1, p. 2269, Oct. 2013, doi: 10.1038/ncomms3269.

[37] B. Tallant and m. Pelkki, "A comparison of four forest inventory tools in southeast Arkansas," in *Competitiveness of Southern Forest Products Markets in a Global Economy: Trends and Predictions. Proceedings of the Southern Forest Economics Workshop*. Gainesville, FL, USA: Univ. of Florida, 2004, pp. 23–34.

[38] D. C. Bragg, "Accurately measuring the height of (real) forest trees," *J. Forestry*, vol. 112, no. 1, pp. 51–54, Jan. 2014, doi: 10.5849/jof.13-065.

[39] E. Sibona et al., "Direct measurement of tree height provides different results on the assessment of LiDAR accuracy," *Forests*, vol. 8, no. 1, p. 7, Dec. 2016, doi: 10.3390/f8010007.

[40] S. Krause, T. G. m. Sanders, J.-P. Mund, and K. Greve, "UAV-based photogrammetric tree height measurement for intensive forest monitoring," *Remote Sens.*, vol. 11, no. 7, p. 758, Mar. 2019, doi: 10.3390/rs11070758.

[41] M. Larjavaara and H. C. Muller-Landau, "Measuring tree height: A quantitative comparison of two common field meth-

ods in a moist tropical forest," *Methods Ecol. Evol.*, vol. 4, no. 9, pp. 793–801, Sep. 2013, doi: 10.1111/2041-210X.12071.

[42] A. N. Goodwin, "Measuring tall tree heights from the ground," *Tasforests*, vol. 15, pp. 85–98, 2004.

[43] L. A. Moran and R. A. Williams, "Field note—Comparison of three dendrometers in measuring diameter at breast height field note," *Northern J. Appl. Forestry*, vol. 19, no. 1, pp. 28–33, Mar. 2002, doi: 10.1093/njaf/19.1.28.

[44] F. Guillemette and m.-C. Lambert, "Relative effects of dendrometers on the estimation of diameter at breast height, stand basal area and stand volume in uneven-aged northern hardwoods," *Forestry Chronicle*, vol. 85, no. 3, pp. 446–452, Jun. 2009, doi: 10.5558/tfc85446-3.

[45] S. Liu, W. Bitterlich, C. J. Cieszewski, and m. J. Zasada, "Comparing the use of three dendrometers for measuring diameters at breast height," *Southern J. Appl. Forestry*, vol. 35, no. 3, pp. 136–141, Aug. 2011, doi: 10.1093/sjaf/35.3.136.

[46] D. C. Bragg, "The sine method as a more accurate height predictor for hardwoods," U.S. Dept. of Agriculture, Forest Service, Southern Research Station, e-Gen. Tech. Rep. SRS–101, 2007, pp. 23–33.

[47] S. Ganz, Y. Käber, and P. Adler, "Measuring tree height with remote sensing—A comparison of photogrammetric and LiDAR data with different field measurements," *Forests*, vol. 10, no. 8, p. 694, Aug. 2019, doi: 10.3390/f10080694.

[48] S. Durrieu, C. Vega, m. Bouvier, F. Gosselin, J.-P. Renaud, and L. Saint-André, *Optical Remote Sensing of Tree and Stand Heights*. New York, NY, USA: Taylor & Francis, 2015.

[49] M. Božić, J. Čavlović, N. Lukić, K. Teslak, and D. Kos, "Efficiency of ultrasonic vertex iii hypsometer compared to the most commonly used hypsometers in Croatian forestry," *Croatian J. Forest Eng., J. Theory Appl. Forestry Eng.*, vol. 26, no. 2, pp. 91–99, 2005.

[50] D. R. Larsen, D. W. Hann, and S. C. Stearns-Smith, "Accuracy and precision of the tangent method of measuring tree height," *Western J. Appl. Forestry*, vol. 2, no. 1, pp. 26–28, Jan. 1987, doi: 10.1093/wjaf/2.1.26.

[51] J. Korning and K. Thomsen, "A new method for measuring tree height in tropical rain forest," *J. Vegetation Sci.*, vol. 5, no. 1, pp. 139–140, Feb. 1994, doi: 10.2307/3235647.

[52] R. C. Goodman, O. L. Phillips, and T. R. Baker, "The importance of crown dimensions to improve tropical tree biomass estimates," *Ecol. Appl.*, vol. 24, no. 4, pp. 680–698, Jun. 2014, doi: 10.1890/13-0070.1.

[53] F. Kitahara, N. Mizoue, and S. Yoshida, "Effects of training for inexperienced surveyors on data quality of tree diameter and height measurements," *Silva Fennica*, vol. 44, no. 4, pp. 657–667, 2010, doi: 10.14214/sf.133.

[54] V. Kankare et al., "Outlook for the single-tree-level forest inventory in nordic countries," in *The Rise of Big Spatial Data*, I. Ivan, A. Singleton, J. Horák, and T. Inspektor, Eds. Cham: Springer International Publishing, 2017, pp. 183–195.

[55] P. Wilkes et al., "Data acquisition considerations for terrestrial laser scanning of forest plots," *Remote Sens. Environ.*, vol. 196, pp. 140–153, Jul. 2017, doi: 10.1016/j.rse.2017.04.030.

[56] M. Disney, A. Burt, K. Calders, C. Schaaf, and A. Stovall, "Innovations in ground and airborne technologies as reference and for training and validation: Terrestrial laser scanning (TLS)," *Surv. Geophys.*, vol. 40, no. 4, pp. 937–958, Jul. 2019, doi: 10.1007/s10712-019-09527-x.

[57] A. Elsherif, R. Gaulton, and J. Mills, "Estimation of vegetation water content at leaf and canopy level using dual-wavelength commercial terrestrial laser scanners," *Interface Focus*, vol. 8, no. 2, p. 20,170,041, Apr. 2018, doi: 10.1098/rsfs.2017.0041.

[58] S. Junttila et al., "The potential of dual-wavelength terrestrial lidar in early detection of Ips typographus (L.) infestation – Leaf water content as a proxy," *Remote Sens. Environ.*, vol. 231, p. 111264, Sep. 2019, doi: 10.1016/j.rse.2019.111264.

[59] E. S. Douglas et al., "DWEL: A dual-wavelength echidna lidar for ground-based forest scanning," in *Proc. IEEE Int. Geosci. Remote Sens. Symp.*, Munich, Germany, Jul. 2012, pp. 4998–5001, doi: 10.1109/IGARSS.2012.6352489.

[60] F. m. Danson et al., "Developing a dual-wavelength full-waveform terrestrial laser scanner to characterize forest canopy structure," *Agricultural Forest Meteorol.*, vols. 198–199, pp. 7–14, Nov. 2014, doi: 10.1016/j.agrformet.2014.07.007.

[61] S. Junttila et al., "Measuring leaf water content with dual-wavelength intensity data from terrestrial laser scanners," *Remote Sens.*, vol. 9, no. 1, p. 8, Dec. 2016, doi: 10.3390/rs9010008.

[62] S. Junttila et al., "Can leaf water content be estimated using multispectral terrestrial laser scanning? A case study with Norway spruce seedlings," *Front. Plant Sci.*, vol. 9, p. 299, Mar. 2018, doi: 10.3389/fpls.2018.00299.

[63] T. Hakala, J. Suomalainen, S. Kaasalainen, and Y. Chen, "Full waveform hyperspectral LiDAR for terrestrial laser scanning," *Opt. Express*, vol. 20, no. 7, p. 7119, Mar. 2012, doi: 10.1364/OE.20.007119.

[64] S. Junttila, S. Kaasalainen, m. Vastaranta, T. Hakala, O. Nevalainen, and m. Holopainen, "Investigating bi-temporal hyperspectral lidar measurements from declined trees—Experiences from laboratory test," *Remote Sens.*, vol. 7, no. 10, pp. 13,863–13,877, Oct. 2015, doi: 10.3390/rs71013863.

[65] E. Puttonen et al., "Artificial target detection with a hyperspectral LiDAR over 26-h measurement," *Opt. Eng.*, vol. 54, no. 1, p. 13,105, Jan. 2015, doi: 10.1117/1.OE.54.1.013105.

[66] T. Malkamäki, S. Kaasalainen, and J. Ilinca, "Portable hyperspectral lidar utilizing 5 GHz multichannel full waveform digitization," *Opt. Exp.*, vol. 27, no. 8, p. A468, Apr. 2019, doi: 10.1364/OE.27.00A468.

[67] D. Li et al., "Monitoring litchi canopy foliar phosphorus content using hyperspectral data," *Comput. Electron. Agriculture*, vol. 154, pp. 176–186, Nov. 2018, doi: 10.1016/j.compag.2018.09.007.

[68] Z. Wang et al., "A hyperspectral LiDAR with eight channels covering from VIS to SWIR," in *Proc. IEEE Int. Geosci. Remote Sens. Symp. (IGARSS 2018)*, Valencia, Jul. 2018, pp. 4293–4296, doi: 10.1109/IGARSS.2018.8517741.

[69] Y. Chen et al., "A 10-nm spectral resolution hyperspectral LiDAR system based on an acousto-optic tunable filter," *Sensors*, vol. 19, no. 7, p. 1620, Apr. 2019, doi: 10.3390/s19071620.

[70] W. Li, Z. Niu, G. Sun, S. Gao, and m. Wu, "Deriving backscatter reflective factors from 32-channel full-waveform LiDAR data for the estimation of leaf biochemical contents," *Opt. Express*, vol. 24, no. 5, p. 4771, Mar. 2016, doi: 10.1364/OE.24.004771.

[71] X. Liang, P. Litkey, J. Hyyppa, H. Kaartinen, m. Vastaranta, and m. Holopainen, "Automatic stem mapping using single-scan terrestrial laser scanning," *IEEE Trans. Geosci. Remote Sens.*, vol. 50, no. 2, pp. 661–670, Feb. 2012, doi: 10.1109/TGRS.2011.2161613.

[72] D. Kelbe, J. van Aardt, P. Romanczyk, m. van Leeuwen, and K. Cawse-Nicholson, "Marker-free registration of forest terrestrial laser scanner data pairs with embedded confidence metrics," *IEEE Trans. Geosci. Remote Sens.*, vol. 54, no. 7, pp. 4314–4330, Jul. 2016, doi: 10.1109/TGRS.2016.2539219.

[73] J. Liu et al., "Automated matching of multiple terrestrial laser scans for stem mapping without the use of artificial references," *Int. J. Appl. Earth Observ. Geoinf.*, vol. 56, pp. 13–23, Apr. 2017, doi: 10.1016/j.jag.2016.11.003.

[74] J.-F. Tremblay and m. Béland, "Towards operational marker-free registration of terrestrial lidar data in forests," *ISPRS J. Photogrammetry Remote Sens.*, vol. 146, pp. 430–435, Dec. 2018, doi: 10.1016/j.isprsjprs.2018.10.011.

[75] W. Dai et al., "Fast registration of forest terrestrial laser scans using key points detected from crowns and stems," *Int. J. Digital Earth*, vol. 13, no. 12, pp. 1–19, May 2020, doi: 10.1080/17538947.2020.1764118.

[76] N. Saarinen et al., "Feasibility of terrestrial laser scanning for collecting stem volume information from single trees," *ISPRS J. Photogrammetry Remote Sens.*, vol. 123, pp. 140–158, Jan. 2017, doi: 10.1016/j.isprsjprs.2016.11.012.

[77] N. Saarinen et al., "Assessing the effects of sample size on parametrizing a taper curve equation and the resultant stem-volume estimates," *Forests*, vol. 10, no. 10, p. 848, Sep. 2019, doi: 10.3390/f10100848.

[78] C. Gollob, T. Ritter, C. Wassermann, and A. Nothdurft, "Influence of scanner position and plot size on the accuracy of tree detection and diameter estimation using terrestrial laser scanning on forest inventory plots," *Remote Sens.*, vol. 11, no. 13, p. 1602, Jul. 2019, doi: 10.3390/rs11131602.

[79] T. Yrttimaa et al., "Investigating the feasibility of multi-scan terrestrial laser scanning to characterize tree communities in southern boreal forests," *Remote Sens.*, vol. 11, no. 12, pp. 1423, Jun. 2019, doi: 10.3390/rs11121423.

[80] J. Pyörälä et al., "Assessing branching structure for biomass and wood quality estimation using terrestrial laser scanning point clouds," *Can. J. Remote Sens.*, vol. 44, no. 5, pp. 462–475, Sep. 2018, doi: 10.1080/07038992.2018.1557040.

[81] S. Bauwens, A. Fayolle, S. Gourlet-Fleury, L. m. Ndjele, C. Mengal, and P. Lejeune, "Terrestrial photogrammetry: A non-destructive method for modelling irregularly shaped tropical tree trunks," *Methods Ecol. Evol.*, vol. 8, no. 4, pp. 460–471, Apr. 2017, doi: 10.1111/2041-210X.12670.

[82] M. Mokroš et al., "High precision individual tree diameter and perimeter estimation from close-range photogrammetry," *Forests*, vol. 9, no. 11, p. 696, Nov. 2018, doi: 10.3390/f9110696.

[83] Agisoft LLC, *Agisoft Metashape User Manual: Professional Edition*, Agisoft LLC, St. Petersburg, Russia, 2019.

[84] T. Sieberth, R. Wackrow, and J. H. Chandler, "Motion blur disturbs – The influence of motion-blurred images in photogrammetry," *Photogrammetric Rec.*, vol. 29, no. 148, pp. 434–453, Dec. 2014, doi: 10.1111/phor.12082.

[85] T. Luhmann, C. Fraser, and H.-G. Maas, "Sensor modelling and camera calibration for close-range photogrammetry," *ISPRS J. Photogrammetry Remote Sens.*, vol. 115, pp. 37–46, May 2016, doi: 10.1016/j.isprsjprs.2015.10.006.

[86] J. Hyyppä, J.-P. Virtanen, A. Jaakkola, X. Yu, H. Hyyppä, and X. Liang, "Feasibility of Google Tango and Kinect for crowdsourcing forestry information," *Forests*, vol. 9, no. 1, p. 6, Dec. 2017, doi: 10.3390/f9010006.

[87] J. Tomaštík, Š. Saloň, D. Tunák, F. Chudý, and m. Kardoš, "Tango in forests – An initial experience of the use of the new Google technology in connection with forest inventory tasks," *Comput. Electron. Agriculture*, vol. 141, pp. 109–117, Sep. 2017, doi: 10.1016/j.compag.2017.07.015.

[88] Y. Fan, Z. Feng, A. Mannan, T. Khan, C. Shen, and S. Saeed, "Estimating tree position, diameter at breast height, and tree height in real-time using a mobile phone with RGB-D SLAM," *Remote Sens.*, vol. 10, no. 11, p. 1845, Nov. 2018, doi: 10.3390/rs10111845.

[89] J. McGlade, L. Wallace, B. Hally, A. White, K. Reinke, and S. Jones, "An early exploration of the use of the Microsoft Azure Kinect for estimation of urban tree diameter at breast height," *Remote Sens. Lett.*, vol. 11, no. 11, pp. 963–972, Nov. 2020, doi: 10.1080/2150704X.2020.1802528.

[90] M. Forsman, N. Börlin, and J. Holmgren, "Estimation of tree stem attributes using terrestrial photogrammetry with a camera rig," *Forests*, vol. 7, no. 12, p. 61, Mar. 2016, doi: 10.3390/f7030061.

[91] M. Mokroš et al., "Novel low-cost mobile mapping systems for forest inventories as terrestrial laser scanning alternatives," *Int. J. Appl. Earth Observ. Geoinf.*, vol. 104, p. 102,512, Dec. 2021, doi: 10.1016/j.jag.2021.102512.

[92] C. Mulverhill, N. C. Coops, P. Tompalski, and C. W. Bater, "Digital terrestrial photogrammetry to enhance field-based forest inventory across stand conditions," *Can. J. Remote Sens.*, vol. 46, no. 5, pp. 622–639, Sep. 2020, doi: 10.1080/07038992.2020.1831376.

[93] A. Berveglieri, A. Tommaselli, X. Liang, and E. Honkavaara, "Photogrammetric measurement of tree stems from vertical fisheye images," *Scandinavian J. Forest Res.*, vol. 32, no. 8, pp. 737–747, Nov. 2017, doi: 10.1080/02827581.2016.1273381.

[94] A. Berveglieri, A. Tommaselli, X. Liang, and E. Honkavaara, "Vertical optical scanning with panoramic vision for tree trunk reconstruction," *Sensors*, vol. 17, no. 12, p. 2791, Dec. 2017, doi: 10.3390/s17122791.

[95] L. Piermattei et al., "Terrestrial structure from motion photogrammetry for deriving forest inventory data," *Remote Sens.*, vol. 11, no. 8, p. 950, Apr. 2019, doi: 10.3390/rs11080950.

[96] T. Mikita, P. Janata, and P. Surový, "Forest stand inventory based on combined aerial and terrestrial close-range photogrammetry," *Forests*, vol. 7, no. 12, p. 165, Jul. 2016, doi: 10.3390/f7080165.

[97] M. Campos et al., "A backpack-mounted omnidirectional camera with off-the-shelf navigation sensors for mobile terrestrial mapping: development and forest application," *Sensors*, vol. 18, no. 3, p. 827, Mar. 2018, doi: 10.3390/s18030827.

[98] M. Mokroš et al., "Evaluation of close-range photogrammetry image collection methods for estimating tree diameters," *IJGI*, vol. 7, no. 3, p. 93, Mar. 2018, doi: 10.3390/ijgi7030093.

[99] X. Liang et al., "Forest data collection using terrestrial image-based point clouds from a handheld camera compared to ter-

restrial and personal laser scanning," *IEEE Trans. Geosci. Remote Sens.*, vol. 53, no. 9, pp. 5117–5132, Sep. 2015, doi: 10.1109/TGRS.2015.2417316.

[100] X. Liang et al., "The use of a hand-held camera for individual tree 3D mapping in forest sample plots," *Remote Sens.*, vol. 6, no. 7, pp. 6587–6603, Jul. 2014, doi: 10.3390/rs6076587.

[101] C. Mulverhill, N. C. Coops, P. Tompalski, C. W. Bater, and A. R. Dick, "The utility of terrestrial photogrammetry for assessment of tree volume and taper in boreal mixedwood forests," *Ann. Forest Sci.*, vol. 76, no. 3, p. 83, Sep. 2019, doi: 10.1007/s13595-019-0852-9.

[102] J. Liu et al., "Extraction of sample plot parameters from 3D point cloud reconstruction based on combined RTK and CCD continuous photography," *Remote Sens.*, vol. 10, no. 8, pp. 1299, Aug. 2018, doi: 10.3390/rs10081299.

[103] M. Pierzchała, P. Giguère, and R. Astrup, "Mapping forests using an unmanned ground vehicle with 3D LiDAR and graph-SLAM," *Comput. Electron. Agriculture*, vol. 145, pp. 217–225, Feb. 2018, doi: 10.1016/j.compag.2017.12.034.

[104] N. El-Sheimy, "An overview of mobile mapping systems," in Proc. FIG Working Week, 2005, pp. 16–21.

[105] G. Petrie, "An introduction to the technology: Mobile mapping systems," *Geoinformatics*, vol. 13, no. 1, p. 32, 2010.

[106] I. Puente, H. González-Jorge, J. Martínez-Sánchez, and P. Arias, "Review of mobile mapping and surveying technologies," *Measurement*, vol. 46, no. 7, pp. 2127–2145, Aug. 2013, doi: 10.1016/j.measurement.2013.03.006.

[107] N. Haala, m. Peter, J. Kremer, and G. Hunter, "Mobile LiDAR mapping for 3D point cloud collection in urban areas—A performance test," *Int. Arch. Photogrammetry Remote Sens. Spatial Inf. Sci.*, vol. 37, pp. 1119–1127, Jul. 2008.

[108] H. Kaartinen et al., "Accuracy of kinematic positioning using global satellite navigation systems under forest canopies," *Forests*, vol. 6, no. 12, pp. 3218–3236, Sep. 2015, doi: 10.3390/f6093218.

[109] A. Kukko, R. Kaijaluoto, H. Kaartinen, V. V. Lehtola, A. Jaakkola, and J. Hyyppä, "Graph SLAM correction for single scanner MLS forest data under boreal forest canopy," *ISPRS J. Photogrammetry Remote Sens.*, vol. 132, pp. 199–209, Oct. 2017, doi: 10.1016/j.isprsjprs.2017.09.006.

[110] A. Kukko and H. Kaartinen, "Multiplatform mobile laser scanning," in *Laser Scanning: An Emerging Technol. Structural Eng.* Boca Raton, FL, USA: CRC Press, 2019, vol. 14, p. 19.

[111] X. Liang et al., "In-situ measurements from mobile platforms: An emerging approach to address the old challenges associated with forest inventories," *ISPRS J. Photogrammetry Remote Sens.*, vol. 143, pp. 97–107, Sep. 2018, doi: 10.1016/j.isprsjprs.2018.04.019.

[112] A. Kukko, H. Kaartinen, J. Hyyppä, and Y. Chen, "Multiplatform mobile laser scanning: Usability and Performance," *Sensors*, vol. 12, no. 9, pp. 11712–11733, Aug. 2012, doi: 10.3390/s120911712.

[113] X. Liang et al., "Possibilities of a personal laser scanning system for forest mapping and ecosystem services," *Sensors*, vol. 14, no. 1, pp. 1228–1248, Jan. 2014, doi: 10.3390/s140101228.

[114] S. Chen, H. Liu, Z. Feng, C. Shen, and P. Chen, "Applicability of personal laser scanning in forestry inventory," *PLoS ONE*, vol. 14, no. 2, p. e0211392, Feb. 2019, doi: 10.1371/journal.pone.0211392.

[115] J. Ryding, E. Williams, m. Smith, and m. Eichhorn, "Assessing handheld mobile laser scanners for forest surveys," *Remote Sens.*, vol. 7, no. 1, pp. 1095–1111, Jan. 2015, doi: 10.3390/rs70101095.

[116] C. Cabo, S. Del Pozo, P. Rodríguez-Gonzálvez, C. Ordóñez, and D. González-Aguilera, "Comparing terrestrial laser scanning (TLS) and wearable laser scanning (WLS) for individual tree modeling at plot level," *Remote Sens.*, vol. 10, no. 4, p. 540, Apr. 2018, doi: 10.3390/rs10040540.

[117] F. Giannetti et al., "Integrating terrestrial and airborne laser scanning for the assessment of single-tree attributes in Mediterranean forest stands," *Eur. J. Remote Sens.*, vol. 51, no. 1, pp. 795–807, Jan. 2018, doi: 10.1080/22797254.2018.1482733.

[118] B. Del Perugia, F. Giannetti, G. Chirici, and D. Travaglini, "Influence of scan density on the estimation of single-tree attributes by hand-held mobile laser scanning," *Forests*, vol. 10, no. 3, p. 277, Mar. 2019, doi: 10.3390/f10030277.

[119] E. Hyyppä et al., "Accurate derivation of stem curve and volume using backpack mobile laser scanning," *ISPRS J. Photogrammetry Remote Sens.*, vol. 161, pp. 246–262, Mar. 2020, doi: 10.1016/j.isprsjprs.2020.01.018.

[120] S. Bauwens, H. Bartholomeus, K. Calders, and P. Lejeune, "Forest inventory with terrestrial LiDAR: A comparison of static and hand-held mobile laser scanning," *Forests*, vol. 7, no. 12, p. 127, Jun. 2016, doi: 10.3390/f7060127.

[121] N. A. Clark, R. H. Wynne, D. L. Schmoldt, and m. Winn, "An assessment of the utility of a non-metric digital camera for measuring standing trees," *Comput. Electron. Agriculture*, vol. 28, no. 2, pp. 151–169, Aug. 2000, doi: 10.1016/S0168-1699(00)00125-3.

[122] T. Melkas, m. Vastaranta, m. Holopainen, R. Hill, J. Rosette, and J. Suárez, "Accuracy and efficiency of the laser-camera," in *Proc. SilviLaser*, 2008, pp. 315–324.

[123] M. Vastaranta, T. Melkas, m. Holopainen, H. Kaartinen, J. Hyyppae, and H. Hyyppae, "Laser-based field measurements in tree-level forest data acquisition," *Photogrammetric J. Finland*, vol. 21, no. 2, pp. 51–61, 2009.

[124] J. Juujarvi, J. Heikkonen, S. S. Brandt, and J. Lampinen, "Digital-image-based tree measurement for forest inventory," in Proc. *Intell. Robots Comput. Vis. XVII: Algorithms, Techniques, and Active Vision*, 1998, pp. 114–123.

[125] A. I. Hapca, F. Mothe, and J.-M. Leban, "A digital photographic method for 3D reconstruction of standing tree shape," *Ann. Forest Sci.*, vol. 64, no. 6, pp. 631–637, Jan. 2007, doi: 10.1051/forest:2007041.

[126] A. R. Dick, J. A. Kershaw, and D. A. MacLean, "Spatial tree mapping using photography," *Northern J. Appl. Forestry*, vol. 27, no. 2, pp. 68–74, 2010, doi: 10.1093/njaf/27.2.68.

[127] G. C. Evans and D. E. Coombe, "Hemisperical and woodland canopy photography and the light climate," *J. Ecol.*, vol. 47, no. 1, p. 103, Mar. 1959, doi: 10.2307/2257250.

[128] F. Chianucci and A. Cutini, "Estimation of canopy properties in deciduous forests with digital hemispherical and cover photography," *Agricultural Forest Meteorol.*, vol. 168, pp. 130–139, Jan. 2013, doi: 10.1016/j.agrformet.2012.09.002.

[129] G. Ligot, P. Balandier, B. Courbaud, and H. Claessens, "Forest radiative transfer models: Which approach for which application?" *Can. J. For. Res.*, vol. 44, no. 5, pp. 391–403, May 2014, doi: 10.1139/cjfr-2013-0494.

[130] M. C. Anderson, "Stand structure and light penetration. II. A theoretical analysis," *J. Appl. Ecol.*, vol. 3, no. 1, p. 41, May 1966, doi: 10.2307/2401665.

[131] I. Jonckheere et al., "Review of methods for in situ leaf area index determination," *Agricultural Forest Meteorol.*, vol. 121, nos. 1–2, pp. 19–35, Jan. 2004, doi: 10.1016/j.agrformet.2003.08.027.

[132] J. m. Chen, T. A. Black, and R. S. Adams, "Evaluation of hemispherical photography for determining plant area index and geometry of a forest stand," *Agricultural Forest Meteorol.*, vol. 56, nos. 1–2, pp. 129–143, Jul. 1991, doi: 10.1016/0168-1923(91)90108-3.

[133] S. Bianchi, C. Cahalan, S. Hale, and J. m. Gibbons, "Rapid assessment of forest canopy and light regime using smartphone hemispherical photography," *Ecol. Evol.*, vol. 7, no. 24, pp. 10,556–10,566, Dec. 2017, doi: 10.1002/ece3.3567.

[134] A. F. H. Goetz, "Three decades of hyperspectral remote sensing of the Earth: A personal view," *Remote Sens. Environ.*, vol. 113, pp. S5–S16, Sep. 2009, doi: 10.1016/j.rse.2007.12.014.

[135] A. F. H. Goetz, G. Vane, J. E. Solomon, and B. N. Rock, "Imaging spectrometry for earth remote sensing," *Science*, vol. 228, no. 4704, pp. 1147–1153, 1985, doi: 10.1126/science.228.4704.1147.

[136] A. F. H. Goetz, "Portable field reflectance spectrometer. Appendix E in application of ERTS images and image processing to regional geologic problems and geologic mapping in Northern Arizona," Jet Propulsion Lab., Pasadena, CA, USA, Tech. Rep. 32-1597, 1975, p. 32–1597.

[137] S. Kaasalainen, A. Jaakkola, m. Kaasalainen, A. Krooks, and A. Kukko, "Analysis of incidence angle and distance effects on terrestrial laser scanner intensity: Search for correction methods," *Remote Sens.*, vol. 3, no. 10, pp. 2207–2221, Oct. 2011, doi: 10.3390/rs3102207.

[138] J. Markwell, J. C. Osterman, and J. L. Mitchell, "Calibration of the Minolta SPAD-502 leaf chlorophyll meter," *Photosynthesis Res.*, vol. 46, no. 3, pp. 467–472, 1995, doi: 10.1007/BF00032301.

[139] F. E. Fassnacht et al., "Review of studies on tree species classification from remotely sensed data," *Remote Sens. Environ.*, vol. 186, pp. 64–87, Dec. 2016, doi: 10.1016/j.rse.2016.08.013.

[140] Y. Shi et al., "Tree species classification using plant functional traits from LiDAR and hyperspectral data," *Int. J. Appl. Earth Observ. Geoinf.*, vol. 73, pp. 207–219, Dec. 2018, doi: 10.1016/j.jag.2018.06.018.

[141] J. Liu et al., "A novel GNSS technique for predicting boreal forest attributes at low cost," *IEEE Trans. Geosci. Remote Sens.*, vol. 55, no. 9, pp. 4855–4867, Sep. 2017, doi: 10.1109/TGRS.2017.2650944.

[142] A. Alonso Arroyo et al., "Dual-polarization GNSS-R interference pattern technique for soil moisture mapping," *IEEE J. Sel. Top. Appl. Earth Observ. Remote Sens.*, vol. 7, no. 5, pp. 1533–1544, May 2014, doi: 10.1109/JSTARS.2014.2320792.

[143] P. Sigrist, P. Coppin, and m. Hermy, "Impact of forest canopy on quality and accuracy of GPS measurements," *Int. J. Remote Sens.*, vol. 20, no. 18, pp. 3595–3610, Jan. 1999, doi: 10.1080/014311699211228.

[144] "Radio propagation effects on next-generation fixed-service terrestrial telecommunication systems," COST235, 1996.

[145] Y. S. Meng, Y. H. Lee, and B. C. Ng, "Empirical near ground path loss modeling in a forest at VHF and UHF bands," *IEEE Trans. Antennas Propag.*, vol. 57, no. 5, pp. 1461–1468, May 2009, doi: 10.1109/TAP.2009.2016703.

[146] I. Colomina and P. Molina, "Unmanned aerial systems for photogrammetry and remote sensing: A review," *ISPRS J. Photogrammetry Remote Sens.*, vol. 92, pp. 79–97, Jun. 2014, doi: 10.1016/j.isprsjprs.2014.02.013.

[147] X. Liang et al., "Forest in situ observations using unmanned aerial vehicle as an alternative of terrestrial measurements," *For. Ecosyst.*, vol. 6, no. 1, p. 20, Dec. 2019, doi: 10.1186/s40663-019-0173-3.

[148] S. Candiago, F. Remondino, m. De Giglio, m. Dubbini, and m. Gattelli, "Evaluating multispectral images and vegetation indices for precision farming applications from UAV images," *Remote Sens.*, vol. 7, no. 4, pp. 4026–4047, Apr. 2015, doi: 10.3390/rs70404026.

[149] A. Simic Milas, m. Romanko, P. Reil, T. Abeysinghe, and A. Marambe, "The importance of leaf area index in mapping chlorophyll content of corn under different agricultural treatments using UAV images," *Int. J. Remote Sens.*, vol. 39, nos. 15–16, pp. 5415–5431, Aug. 2018, doi: 10.1080/01431161.2018.1455244.

[150] J. Kim, S. Kim, C. Ju, and H. I. Son, "Unmanned aerial vehicles in agriculture: A review of perspective of platform, control, and applications," *IEEE Access*, vol. 7, pp. 105,100–105,115, 2019, doi: 10.1109/ACCESS.2019.2932119.

[151] S. P. Bemis et al., "Ground-based and UAV-based photogrammetry: A multi-scale, high-resolution mapping tool for structural geology and paleoseismology," *J. Struct. Geol.*, vol. 69, pp. 163–178, Dec. 2014, doi: 10.1016/j.jsg.2014.10.007.

[152] C. Gomez and H. Purdie, "UAV- based photogrammetry and geocomputing for hazards and disaster risk monitoring – A review," *Geoenviron Disasters*, vol. 3, no. 1, p. 23, Dec. 2016, doi: 10.1186/s40677-016-0060-y.

[153] E. Salamí, C. Barrado, and E. Pastor, "UAV flight experiments applied to the remote sensing of vegetated areas," *Remote Sens.*, vol. 6, no. 11, pp. 11,051–11,081, Nov. 2014, doi: 10.3390/rs61111051.

[154] T. R. H. Goodbody, N. C. Coops, P. L. Marshall, P. Tompalski, and P. Crawford, "Unmanned aerial systems for precision forest inventory purposes: A review and case study," *Forestry Chronicle*, vol. 93, no. 1, pp. 71–81, Jan. 2017, doi: 10.5558/tfc2017-012.

[155] M. Mokroš et al., "Early stage forest windthrow estimation based on unmanned aircraft system imagery," *Forests*, vol. 8, no. 9, p. 306, Aug. 2017, doi: 10.3390/f8090306.

[156] I. Balenović, L. Jurjević, A. Simic Milas, A. Gašparović, D. Ivanković, and A. Seletković, "Testing the applicability of the official Croatian DTM for normalization of UAV-based DSMs and plot-level tree height estimations in lowland forests," *Croat. J. For. Eng.*, vol. 40, no. 1, pp. 163–174, 2019.

[157] N. Guimarães, L. Pádua, P. Marques, N. Silva, E. Peres, and J. J. Sousa, "Forestry remote sensing from unmanned aerial vehicles: A review focusing on the data, processing and potentialities," *Remote Sens.*, vol. 12, no. 6, p. 1046, Mar. 2020, doi: 10.3390/rs12061046.

[158] A. S. Saeed, A. B. Younes, C. Cai, and G. Cai, "A survey of hybrid unmanned aerial vehicles," *Progress Aerosp. Sci.*, vol. 98, pp. 91–105, Apr. 2018, doi: 10.1016/j.paerosci.2018.03.007.

[159] C. Webster, m. Westoby, N. Rutter, and T. Jonas, "Three-dimensional thermal characterization of forest canopies using UAV photogrammetry," *Remote Sens. Environ.*, vol. 209, pp. 835–847, May 2018, doi: 10.1016/j.rse.2017.09.033.

[160] V. González-Jaramillo, A. Fries, and J. Bendix, "AGB estimation in a tropical mountain forest (TMF) by means of RGB and multispectral images using an unmanned aerial vehicle (UAV)," *Remote Sens.*, vol. 11, no. 12, p. 1413, Jun. 2019, doi: 10.3390/rs11121413.

[161] A. Jaakkola et al., "Autonomous collection of forest field reference—The outlook and a first step with UAV laser scanning," *Remote Sens.*, vol. 9, no. 8, p. 785, Jul. 2017, doi: 10.3390/rs9080785.

[162] R. A. Chisholm, J. Cui, S. K. Y. Lum, and B. m. Chen, "UAV LiDAR for below-canopy forest surveys," *J. Unmanned Veh. Sys.*, vol. 1, no. 1, pp. 61–68, Dec. 2013, doi: 10.1139/juvs-2013-0017.

[163] S. Dionisio-Ortega, L. O. Rojas-Perez, J. Martinez-Carranza, and I. Cruz-Vega, "A deep learning approach towards autonomous flight in forest environments," in *Proc. Int. Conf. Electron., Commun. Comput. (CONIELECOMP)*, Feb. 2018, pp. 139–144, doi: 10.1109/CONIELECOMP.2018.8327189.

[164] B. G. Maciel-Pearson, P. Carbonneau, and T. P. Breckon, "Extending deep neural network trail navigation for unmanned aerial vehicle operation within the forest canopy," in *Towards Autonom. Robot. Syst.*, 2018, pp. 147–158, doi: 10.1007/978-3-319-96728-8_13.

[165] E. Hyyppä et al., "Under-canopy UAV laser scanning for accurate forest field measurements," *ISPRS J. Photogrammetry Remote Sens.*, vol. 164, pp. 41–60, Jun. 2020, doi: 10.1016/j.isprsjprs.2020.03.021.

[166] Y. Wang et al., "Seamless integration of above- and under-canopy unmanned aerial vehicle laser scanning for forest investigation," *For. Ecosyst.*, vol. 8, no. 1, p. 10, Dec. 2021, doi: 10.1186/s40663-021-00290-3.

[167] S. Krisanski, B. Del Perugia, m. S. Taskhiri, and P. Turner, "Below-canopy UAS photogrammetry for stem measurement in radiata pine plantation," *Remote Sens. Agriculture, Ecosyst., Hydrol. XX*, vol. 10783, p. 1,078,309, 2018.

[168] K. Kuželka and P. Surový, "Mapping forest structure using UAS inside flight capabilities," *Sensors*, vol. 18, no. 7, p. 2245, Jul. 2018, doi: 10.3390/s18072245.

[169] J. P. Dandois and E. C. Ellis, "Remote sensing of vegetation structure using computer vision," *Remote Sens.*, vol. 2, no. 4, pp. 1157–1176, Apr. 2010, doi: 10.3390/rs2041157.

[170] J. Tomaštík, m. Mokroš, Š. Saloň, F. Chudý, and D. Tunák, "Accuracy of photogrammetric UAV-based point clouds under conditions of partially-open forest canopy," *Forests*, vol. 8, no. 5, p. 151, Apr. 2017, doi: 10.3390/f8050151.

[171] J. Tomaštík, m. Mokroš, P. Surový, A. Grznárová, and J. Merganič, "UAV RTK/PPK method—An optimal solution for mapping inaccessible forested areas?" *Remote Sens.*, vol. 11, no. 6, p. 721, Mar. 2019, doi: 10.3390/rs11060721.

[172] A. Jaakkola et al., "A low-cost multi-sensoral mobile mapping system and its feasibility for tree measurements," *ISPRS J. Photogrammetry Remote Sens.*, vol. 65, no. 6, pp. 514–522, Nov. 2010, doi: 10.1016/j.isprsjprs.2010.08.002.

[173] L. Wallace, A. Lucieer, C. Watson, and D. Turner, "Development of a UAV-LiDAR system with application to forest inventory," *Remote Sens.*, vol. 4, no. 6, pp. 1519–1543, May 2012, doi: 10.3390/rs4061519.

[174] L. Wallace, A. Lucieer, and C. S. Watson, "Evaluating tree detection and segmentation routines on very high resolution UAV LiDAR data," *IEEE Trans. Geosci. Remote Sens.*, vol. 52, no. 12, pp. 7619–7628, Dec. 2014, doi: 10.1109/TGRS.2014.2315649.

[175] M. Bruggisser, m. Hollaus, J. Otepka, and N. Pfeifer, "Influence of ULS acquisition characteristics on tree stem parameter estimation," *ISPRS J. Photogrammetry Remote Sens.*, vol. 168, pp. 28–40, Oct. 2020, doi: 10.1016/j.isprsjprs.2020.08.002.

[176] I. Korpela, "Acquisition and evaluation of radiometrically comparable multi-footprint airborne LiDAR data for forest remote sensing," *Remote Sens. Environ.*, vol. 194, pp. 414–423, Jun. 2017, doi: 10.1016/j.rse.2016.10.052.

[177] J. Li, B. Yang, Y. Cong, L. Cao, X. Fu, and Z. Dong, "3D forest mapping using a low-cost UAV laser scanning system: Investigation and comparison," *Remote Sens.*, vol. 11, no. 6, p. 717, Mar. 2019, doi: 10.3390/rs11060717.

[178] L. Wallace, A. Lucieer, Z. Malenovský, D. Turner, and P. Vopénka, "Assessment of forest structure using two UAV techniques: A comparison of airborne laser scanning and structure from motion (SfM) point clouds," *Forests*, vol. 7, no. 12, p. 62, Mar. 2016, doi: 10.3390/f7030062.

[179] C. Torresan et al., "Forestry applications of UAVs in Europe: A review," *Int. J. Remote Sens.*, vol. 38, nos. 8–10, pp. 2427–2447, May 2017, doi: 10.1080/01431161.2016.1252477.

[180] H. Aasen, E. Honkavaara, A. Lucieer, and P. Zarco-Tejada, "Quantitative remote sensing at ultra-high resolution with UAV spectroscopy: A review of sensor technology, measurement procedures, and data correction workflows," *Remote Sens.*, vol. 10, no. 7, p. 1091, Jul. 2018, doi: 10.3390/rs10071091.

[181] J. Vautherin, et al. "Photogrammetric accuracy and modeling of rolling shutter cameras," *ISPRS Ann. Photogrammetric Remote Sens. Spatial Inf. Sci.*, vol. III-3, pp. 139–146, Jun. 2016, doi: 10.5194/isprsannals-III-3-139-2016.

[182] Y. Zhou, m. Daakir, E. Rupnik, and m. Pierrot-Deseilligny, "A two-step approach for the correction of rolling shutter distortion in UAV photogrammetry," *ISPRS J. Photogrammetry Remote Sens.*, vol. 160, pp. 51–66, Feb. 2020, doi: 10.1016/j.isprsjprs.2019.11.020.

[183] B. Stark, B. Smith, and Y. Chen, "Survey of thermal infrared remote sensing for unmanned aerial systems," in *Proc. Int. Conf. Unmanned Aircraft Syst. (ICUAS)*, Orlando, FL, USA, May 2014, pp. 1294–1299, doi: 10.1109/ICUAS.2014.6842387.

[184] R. Ludovisi, F. Tauro, R. Salvati, S. Khoury, G. m. Scarascia, and A. Harfouche, "UAV-based thermal imaging for high-throughput field phenotyping of black poplar response to drought," *Front. Plant Sci.*, vol. 8, p. 1681, Sep. 2017, doi: 10.3389/fpls.2017.01681.

[185] E. Seifert et al., "Influence of drone altitude, image overlap, and optical sensor resolution on multi-view reconstruction of

forest images," *Remote Sens.*, vol. 11, no. 10, p. 1252, May 2019, doi: 10.3390/rs11101252.

[186] J. O'Connor, m. J. Smith, and m. R. James, "Cameras and settings for aerial surveys in the geosciences: Optimising image data," *Prog. Phys. Geography, Earth Environ.*, vol. 41, no. 3, pp. 325–344, Jun. 2017, doi: 10.1177/0309133317703092.

[187] J. Dandois, m. Olano, and E. Ellis, "Optimal altitude, overlap, and weather conditions for computer vision UAV estimates of forest structure," *Remote Sens.*, vol. 7, no. 10, pp. 13,895–13,920, Oct. 2015, doi: 10.3390/rs71013895.

[188] J. Frey, K. Kovach, S. Stemmler, and B. Koch, "UAV photogrammetry of forests as a vulnerable process. A sensitivity analysis for a structure from motion RGB-image pipeline," *Remote Sens.*, vol. 10, no. 6, p. 912, Jun. 2018, doi: 10.3390/rs10060912.

[189] W. Ni et al., "Mapping three-dimensional structures of forest canopy using UAV stereo imagery: Evaluating impacts of forward overlaps and image resolutions with LiDAR data as reference," *IEEE J. Sel. Top. Appl. Earth Observ. Remote Sens.*, vol. 11, no. 10, pp. 3578–3589, Oct. 2018, doi: 10.1109/JSTARS.2018.2867945.

[190] J.-P. Jhan, J.-Y. Rau, and C.-Y. Huang, "Band-to-band registration and ortho-rectification of multilens/multispectral imagery: A case study of MiniMCA-12 acquired by a fixed-wing UAS," *ISPRS J. Photogrammetry Remote Sens.*, vol. 114, pp. 66–77, Apr. 2016, doi: 10.1016/j.isprsjprs.2016.01.008.

[191] J. Iglhaut, C. Cabo, S. Puliti, L. Piermattei, J. O'Connor, and J. Rosette, "Structure from motion photogrammetry in forestry: A review," *Curr. Forestry Rep.*, vol. 5, no. 3, pp. 155–168, Sep. 2019, doi: 10.1007/s40725-019-00094-3.

[192] E. Baltsavias, A. Gruen, H. Eisenbeiss, L. Zhang, and L. T. Waser, "High-quality image matching and automated generation of 3D tree models," *Int. J. Remote Sens.*, vol. 29, no. 5, pp. 1243–1259, Mar. 2008, doi: 10.1080/01431160701736513.

[193] S. Puliti, H. Ørka, T. Gobakken, and E. Næsset, "Inventory of small forest areas using an unmanned aerial system," *Remote Sens.*, vol. 7, no. 8, pp. 9632–9654, Jul. 2015, doi: 10.3390/rs70809632.

[194] T. Ota, m. Ogawa, N. Mizoue, K. Fukumoto, and S. Yoshida, "Forest structure estimation from a UAV-based photogrammetric point cloud in managed temperate coniferous forests," *Forests*, vol. 8, no. 9, p. 343, Sep. 2017, doi: 10.3390/f8090343.

[195] P. J. Zarco-Tejada, V. González-Dugo, and J. A. J. Berni, "Fluorescence, temperature and narrow-band indices acquired from a UAV platform for water stress detection using a micro-hyperspectral imager and a thermal camera," *Remote Sens. Environ.*, vol. 117, pp. 322–337, Feb. 2012, doi: 10.1016/j.rse.2011.10.007.

[196] A. Burkart, S. Cogliati, A. Schickling, and U. Rascher, "A novel UAV-based ultra-light weight spectrometer for field spectroscopy," *IEEE Sensors J.*, vol. 14, no. 1, pp. 62–67, Jan. 2014, doi: 10.1109/JSEN.2013.2279720.

[197] A. Lucieer, Z. Malenovský, T. Veness, and L. Wallace, "HyperUAS-imaging spectroscopy from a multirotor unmanned aircraft system: HyperUAS-imaging spectroscopy from a multirotor unmanned," *J. Field Robot.*, vol. 31, no. 4, pp. 571–590, Jul. 2014, doi: 10.1002/rob.21508.

[198] J. Suomalainen et al., "A lightweight hyperspectral mapping system and photogrammetric processing chain for unmanned aerial vehicles," *Remote Sens.*, vol. 6, no. 11, pp. 11,013–11,030, Nov. 2014, doi: 10.3390/rs61111013.

[199] Q. Lin, H. Huang, J. Wang, K. Huang, and Y. Liu, "Detection of pine shoot beetle (PSB) stress on pine forests at individual tree level using UAV-based hyperspectral imagery and lidar," *Remote Sens.*, vol. 11, no. 21, p. 2540, Oct. 2019, doi: 10.3390/rs11212540.

[200] N. Zhang, X. Zhang, G. Yang, C. Zhu, L. Huo, and H. Feng, "Assessment of defoliation during the Dendrolimus tabulaeformis Tsai et Liu disaster outbreak using UAV-based hyperspectral images," *Remote Sens. Environ.*, vol. 217, pp. 323–339, Nov. 2018, doi: 10.1016/j.rse.2018.08.024.

[201] E. Honkavaara et al., "Processing and assessment of spectrometric, stereoscopic imagery collected using a lightweight UAV spectral camera for precision agriculture," *Remote Sens.*, vol. 5, no. 10, pp. 5006–5039, Oct. 2013, doi: 10.3390/rs5105006.

[202] R. A. Oliveira, A. m. G. Tommaselli, and E. Honkavaara, "Generating a hyperspectral digital surface model using a hyperspectral 2D frame camera," *ISPRS J. Photogrammetry Remote Sens.*, vol. 147, pp. 345–360, Jan. 2019, doi: 10.1016/j.isprsjprs.2018.11.025.

[203] D. Gautam, A. Lucieer, J. Bendig, and Z. Malenovsky, "Footprint determination of a spectroradiometer mounted on an unmanned aircraft system," *IEEE Trans. Geosci. Remote Sens.*, vol. 58, no. 5, pp. 3085–3096, May 2020, doi: 10.1109/TGRS.2019.2947703.

[204] R. Minařík, J. Langhammer, and J. Hanuš, "Radiometric and atmospheric corrections of multispectral μMCA camera for UAV spectroscopy," *Remote Sens.*, vol. 11, no. 20, p. 2428, Oct. 2019, doi: 10.3390/rs11202428.

[205] T. Hakala et al., "Direct reflectance measurements from drones: Sensor absolute radiometric calibration and system tests for forest reflectance characterization," *Sensors*, vol. 18, no. 5, p. 1417, May 2018, doi: 10.3390/s18051417.

[206] J. Suomalainen et al., "A novel tilt correction technique for irradiance sensors and spectrometers on-board unmanned aerial vehicles," *Remote Sens.*, vol. 10, no. 12, p. 2068, Dec. 2018, doi: 10.3390/rs10122068.

[207] E. Honkavaara and E. Khoramshahi, "Radiometric correction of close-range spectral image blocks captured using an unmanned aerial vehicle with a radiometric block adjustment," *Remote Sens.*, vol. 10, no. 2, p. 256, Feb. 2018, doi: 10.3390/rs10020256.

[208] E. Honkavaara, T. Rosnell, R. Oliveira, and A. Tommaselli, "Band registration of tuneable frame format hyperspectral UAV imagers in complex scenes," *ISPRS J. Photogrammetry Remote Sens.*, vol. 134, pp. 96–109, Dec. 2017, doi: 10.1016/j.isprsjprs.2017.10.014.

[209] A. Berveglieri, A. m. G. Tommaselli, L. D. Santos, and E. Honkavaara, "Bundle adjustment of a time-sequential spectral camera using polynomial models," *IEEE Trans. Geosci. Remote Sens.*, vol. 57, no. 11, pp. 9252–9263, Nov. 2019, doi: 10.1109/TGRS.2019.2925783.

[210] A. m. G. Tommaselli, L. D. Santos, R. A. de Oliveira, A. Berveglieri, N. N. Imai, and E. Honkavaara, "Refining the interior orientation of a hyperspectral frame camera with preliminary

bands co-registration," *IEEE J. Sel. Top. Appl. Earth Observ. Remote Sens.*, vol. 12, no. 7, pp. 2097–2106, Jul. 2019, doi: 10.1109/JSTARS.2019.2911547.

[211] P. Hugler, F. Roos, m. Schartel, m. Geiger, and C. Waldschmidt, "Radar taking off: New capabilities for UAVs," *IEEE Microw.*, vol. 19, no. 7, pp. 43–53, Nov. 2018, doi: 10.1109/MMM.2018.2862558.

[212] L. Moreira et al., "A drone-borne multiband DInSAR: Results and applications," in *Proc. IEEE Radar Conf. (RadarConf)*, Boston, MA, USA, Apr. 2019, pp. 1–6, doi: 10.1109/RADAR.2019.8835653.

[213] J. Yan, J. Guo, Q. Lu, K. Wang, and X. Liu, "X-band mini SAR radar on eight-rotor mini-UAV," in *Proc. IEEE Int. Geosci. Remote Sens. Symp. (IGARSS)*, Beijing, China, Jul. 2016, pp. 6702–6705, doi: 10.1109/IGARSS.2016.7730750.

[214] L. Moreira et al., "Drone-borne P-band single-pass InSAR," in *Proc. IEEE Radar Conf. (RadarConf20)*, Florence, Italy, Sep. 2020, pp. 1–6, doi: 10.1109/RadarConf2043947.2020.9266502.

[215] R. O. R. Jenssen, m. Eckerstorfer, and S. Jacobsen, "Drone-mounted ultrawideband radar for retrieval of snowpack properties," *IEEE Trans. Instrum. Meas.*, vol. 69, no. 1, pp. 221–230, Jan. 2020, doi: 10.1109/TIM.2019.2893043.

[216] S. Kim et al., "Multichannel W-band SAR system on a multirotor UAV platform with real-time data transmission capabilities," *IEEE Access*, vol. 8, pp. 144,413–144,431, Aug. 2020, doi: 10.1109/ACCESS.2020.3014700.

[217] M. Lort, A. Aguasca, C. Lopez-Martinez, and T. m. Marin, "Initial evaluation of SAR capabilities in UAV multicopter platforms," *IEEE J. Sel. Top. Appl. Earth Observ. Remote Sens.*, vol. 11, no. 1, pp. 127–140, Jan. 2018, doi: 10.1109/JSTARS.2017.2752418.

[218] D. Gromek et al., "C-band SAR radar trials using UAV platform: Experimental results of SAR system integration on a UAV carrier," in *Proc. 17th Int. Radar Symp. (IRS)*, Krakow, Poland, May 2016, pp. 1–5, doi: 10.1109/IRS.2016.7497305.

[219] C. J. Li and H. Ling, "High-resolution, downward-looking radar imaging using a small consumer drone," in *Proc. IEEE Int. Symp. Antennas Propag. (APSURSI)*, Fajardo, PR, USA, Jun. 2016, pp. 2037–2038, doi: 10.1109/APS.2016.7696725.

[220] M. T. Vaaja, J.-P. Virtanen, m. Kurkela, V. Lehtola, J. Hyyppä, and H. Hyyppä, "The effect of wind on tree stem parameter estimation using terrestrial laser scanning," *ISPRS Ann. Photogrammetry, Remote Sens. Spatial Inf. Sci.*, vol. III-8, pp. 117–122, Jun. 2016, doi: 10.5194/isprsannals-III-8-117-2016.

[221] S. Fritz et al., "Geo-wiki.org: The use of crowdsourcing to improve global land cover," *Remote Sens.*, vol. 1, no. 3, pp. 345–354, Aug. 2009, doi: 10.3390/rs1030345.

[222] X. Yu, X. Liang, J. Hyyppä, V. Kankare, m. Vastaranta, and m. Holopainen, "Stem biomass estimation based on stem reconstruction from terrestrial laser scanning point clouds," *Remote Sens. Lett.*, vol. 4, no. 4, pp. 344–353, Apr. 2013, doi: 10.1080/2150704X.2012.734931.

[223] X. Liang, V. Kankare, Y. Xiaowei, J. Hyyppa, and m. Holopainen, "Automated stem curve measurement using terrestrial laser scanning," *IEEE Trans. Geosci. Remote Sens.*, vol. 52, no. 3, pp. 1739–1748, Mar. 2014, doi: 10.1109/TGRS.2013.2253783.

[224] K. Calders et al., "Nondestructive estimates of above-ground biomass using terrestrial laser scanning," *Methods Ecol. Evol.*, vol. 6, no. 2, pp. 198–208, Feb. 2015, doi: 10.1111/2041-210X.12301.

[225] Y. Sun, X. Liang, Z. Liang, C. Welham, and W. Li, "Deriving merchantable volume in poplar through a localized tapering function from non-destructive terrestrial laser scanning," *Forests*, vol. 7, no. 12, p. 87, Apr. 2016, doi: 10.3390/f7040087.

[226] J. Gonzalez de Tanago et al., "Estimation of above-ground biomass of large tropical trees with terrestrial LiDAR," *Methods Ecol. Evol.*, vol. 9, no. 2, pp. 223–234, Feb. 2018, doi: 10.1111/2041-210X.12904.

[227] A. Lau et al., "Tree biomass equations from terrestrial LiDAR: A case study in Guyana," *Forests*, vol. 10, no. 6, p. 527, Jun. 2019, doi: 10.3390/f10060527.

[228] C. Qian et al., "An integrated GNSS/INS/LiDAR-SLAM positioning method for highly accurate forest stem mapping," *Remote Sens.*, vol. 9, no. 1, p. 3, Dec. 2016, doi: 10.3390/rs9010003.

[229] W. Bitterlich, *The Relascope Idea: Relative Measurements in Forestry*. London: Commonwealth Agricultural Bureau, 1984.

[230] J. Shao et al., "SLAM-aided forest plot mapping combining terrestrial and mobile laser scanning," *ISPRS J. Photogrammetry Remote Sens.*, vol. 163, pp. 214–230, May 2020, doi: 10.1016/j.isprsjprs.2020.03.008.

[231] Trestima Forest. Accessed: Mar. 19, 2020. [Online]. Available: https://www.trestima.com/en

[232] I. Balenović, X. Liang, L. Jurjević, J. Hyyppä, A. Seletković, and A. Kukko, "Hand-held personal laser scanning: Current status and perspectives for forest inventory application," *Croat. J. For. Eng.*, vol. 42, no. 1, pp. 163–174, 2021, doi: 10.5552/crojfe.2021.858.

[233] W. Ni, G. Sun, Z. Guo, and H. Huang, "A method for the registration of multiview range images acquired in forest areas using a terrestrial laser scanner," *Int. J. Remote Sens.*, vol. 32, no. 24, pp. 9769–9787, 2011, doi: 10.1080/01431161.2011.578597.

[234] M. Vastaranta, E. Latorre, V. Luoma, N. Saarinen, m. Holopainen, and J. Hyyppä, "Evaluation of a smartphone app for forest sample plot measurements," *Forests*, vol. 6, no. 12, pp. 1179–1194, Apr. 2015, doi: 10.3390/f6041179.

[235] W. Zhang, Y. Chen, H. Wang, m. Chen, X. Wang, and G. Yan, "Efficient registration of terrestrial LiDAR scans using a coarse-to-fine strategy for forestry applications," *Agricultural Forest Meteorol.*, vol. 225, pp. 8–23, Sep. 2016, doi: 10.1016/j.agrformet.2016.05.005.

[236] M. Imangholiloo et al., "Characterizing seedling stands using leaf-off and leaf-on photogrammetric point clouds and hyperspectral imagery acquired from unmanned aerial vehicle," *Forests*, vol. 10, no. 5, p. 415, May 2019, doi: 10.3390/f10050415.

[237] J. Pyörälä et al., "Quantitative assessment of scots pine (Pinus sylvestris L.) whorl structure in a forest environment using terrestrial laser scanning," *IEEE J. Sel. Top. Appl. Earth Observ. Remote Sens.*, vol. 11, no. 10, pp. 3598–3607, Oct. 2018, doi: 10.1109/JSTARS.2018.2819598.

[238] J.-F. Côté, R. A. Fournier, G. W. Frazer, and K. Olaf Niemann, "A fine-scale architectural model of trees to enhance LiDAR-derived measurements of forest canopy structure," *Agricultural*

Forest Meteorol., vols. 166–167, pp. 72–85, Dec. 2012, doi: 10.1016/j.agrformet.2012.06.007.

[239] P. Raumonen et al., "Fast Automatic precision tree models from terrestrial laser scanner data," *Remote Sens.*, vol. 5, no. 2, pp. 491–520, Jan. 2013, doi: 10.3390/rs5020491.

[240] J. Hackenberg, C. Morhart, J. Sheppard, H. Spiecker, and m. Disney, "Highly accurate tree models derived from terrestrial laser scan data: A method description," *Forests*, vol. 5, no. 5, pp. 1069–1105, May 2014, doi: 10.3390/f5051069.

[241] M. Dassot, m. Fournier, and C. Deleuze, "Assessing the scaling of the tree branch diameters frequency distribution with terrestrial laser scanning: Methodological framework and issues," *Ann. Forest Sci.*, vol. 76, no. 3, p. 66, Sep. 2019, doi: 10.1007/s13595-019-0854-7.

[242] Y. Li et al., "Retrieval of tree branch architecture attributes from terrestrial laser scan data using a Laplacian algorithm," *Agricultural Forest Meteorol.*, vol. 284, p. 107,874, Apr. 2020, doi: 10.1016/j.agrformet.2019.107874.

[243] Y. Su et al., "Large-scale geographical variations and climatic controls on crown architecture traits," *J. Geophys. Res. Biogeosci.*, vol. 125, no. 2, Feb. 2020, doi: 10.1029/2019JG005306.

[244] X. Shen, L. Cao, B. Yang, Z. Xu, and G. Wang, "Estimation of forest structural attributes using spectral indices and point clouds from UAS-based multispectral and RGB imageries," *Remote Sens.*, vol. 11, no. 7, p. 800, Apr. 2019, doi: 10.3390/rs11070800.

[245] N. Saarinen et al., "Assessing biodiversity in boreal forests with UAV-based photogrammetric point clouds and hyperspectral imaging," *Remote Sens.*, vol. 10, no. 2, p. 338, Feb. 2018, doi: 10.3390/rs10020338.

[246] F. Santini, S. C. Kefauver, V. Resco de Dios, J. L. Araus, and J. Voltas, "Using unmanned aerial vehicle-based multispectral, RGB and thermal imagery for phenotyping of forest genetic trials: A case study in Pinus halepensis," *Ann. Appl. Biol.*, vol. 174, no. 2, pp. 262–276, Mar. 2019, doi: 10.1111/aab.12484.

GRS